Aus der
Klinik für Orthopädie und Unfallchirurgie
Klinik der Universität München
Direktor: Prof. Dr. Wolfgang Böcker

Characterisation of a skeletal muscle-specific myostatin over-expressing mouse model

Dissertation
Zur Erlangung des Doktorgrades der Medizin
an der Medizinischen Fakultät
der Ludwig-Maximilians-Universität zu München

vorgelegt von
Maximilian Joachim Strenzke

aus
Schorndorf

Jahr
2024

Mit Genehmigung der Medizinischen Fakultät
der Universität München

Berichterstatter:	Prof. Dr. Wolfgang Böcker
Mitberichterstatter:	Prof. Dr. Wolfgang Müller-Felber
	Prof. Dr. Eric Heese
Mitbetreuung durch den promovierten Mitarbeiter:	Dr. Maximilian Michael Saller
Dekan:	Prof. Dr. med. Thomas Gudermann
Tag der mündlichen Prüfung:	17.10.2024

For my beloved wife.

Abstract

Sarcopenia displays a progressive loss of muscle mass and performance, which extends above the level of physiological ageing processes. In ageing societies, this condition becomes increasingly significant. While patients may notice a strong impact on self-reliance, the socio-economic burden presents itself through rising costs for health care and increasing commitment of manpower. Unfortunately, no pharmacological treatments are yet available to prevent or treat this condition effectively.

To conduct further research on sarcopenia a reliable mouse model should be established. Myostatin (MSTN) or GDF-8, a member of transforming growth and differentiation factor (TGF) family, is a strong inhibitor of skeletal muscle mass. Physiologically, MSTN reduces skeletal muscle mass adapted to physical exercise. The absence of functional MSTN in animals with a natural loss-of-function mutation or in artificial models leads to a tremendous increase in muscle mass. The opposite (sarcopenic) phenotype could be hypothesised to result from *Mstn* gain-of-function. This makes MSTN a promising candidate for genetic modification to simulate sarcopenic conditions. Due to the strong monogenetic impact on morphology, the aim of this thesis was to analyse possible effects of *Mstn* over-expression on skeletal muscles. Hence a *Mstn* over-expressing mouse line was created and thoroughly analysed. Interestingly, the results showed no significant influence on overall bodyweight. However, a significant decrease in skeletal muscle weight of lower limb muscles could be found in homozygous *Mstn* over-expressing male mice. No significant changes in fibre area or fibre type composition were found, but a small tendency towards smaller myofibres in homozygous *Mstn* over-expressing male mice. In addition, no significant impact on grip strength was detected. Next generation sequencing (NGS) of *Mstn* over-expressing mice muscle revealed a pattern of up- and down-regulated genes that indicates a homeostatic regulatory function of MSTN.

In addition, the results of this work will provide the basis for further genetic modifications of the *Mstn* over-expressing mouse line toward an inducible gene modification to expand research opportunities by controlling the onset of over-expression.

Zusammenfassung

Sarkopenie beschreibt einen fortschreitenden Verlust an Muskelmasse und Leistungsfähigkeit, der über die physiologischen Alterungsprozesse hinausgeht. In alternden Gesellschaften gewinnt dieser Zustand zunehmend an Bedeutung. Während Patienten starke Einschränkungen ihrer Selbstständigkeit feststellen können, zeigt sich die sozioökonomische Belastung durch steigende Kosten für die Gesundheitsversorgung und eine zunehmende Beanspruchung von Arbeitskräften. Leider gibt es noch keinen pharmakologischen Therapieansatz, der diesem Zustand wirksam vorbeugen oder ihn behandeln könnte.

Für die weitere Erforschung der Sarkopenie sollte ein zuverlässiges Mausmodell etabliert werden. Myostatin (MSTN) oder GDF-8, ein Mitglied der Familie der transforming growth and differentiation factor (TGF), ist ein starker Inhibitor der Skelettmuskelmasse. Physiologisch reduziert es die Skelettmuskelmasse angepasst an den funktionellen Bedarf.

Das Fehlen von MSTN sowohl bei Tieren mit einer natürlichen Loss-of-Function Mutation als auch in künstlichen Tiermodellen führt zu einer enormen Zunahme der Muskelmasse. Es liegt auf der Hand, dass der gegenteilige (sarkopene) Phänotyp durch eine Überexpression von *Mstn* hervorgerufen werden könnte. Dies macht MSTN zu einem vielversprechenden Kandidaten für eine genetische Modifikation, um Sarkopenie zu simulieren. Aufgrund der starken monogenetischen Auswirkung auf die Morphologie war es das Ziel dieser Arbeit, die möglichen Auswirkungen einer Überexpression von *Mstn* auf die Skelettmuskulatur zu analysieren. Daher wurde eine *Mstn*-überexprimierende Mauslinie erstellt und gründlich analysiert. Interessanterweise zeigten die Ergebnisse keinen signifikanten Einfluss auf das Gesamtkörpergewicht. Allerdings konnte bei homozygoten *Mstn*-überexprimierenden männlichen Mäusen eine signifikante Abnahme des Skelettmuskelgewichts der Hinterbeinmuskulatur festgestellt werden. Es konnte kein signifikanter Einfluss auf die Größe der Muskelfasern oder der Fasertypzusammensetzung nachgewiesen werden, jedoch zeigte sich eine leichte Tendenz hin zu kleineren Muskelfasern in *Mstn*-überexprimierenden männlichen Mäusen. Ferner zeigte sich keine Einwirkung auf die Griffkraft der Mäuse. Die Analyse mittels Next-Generation-Sequencing (NGS) von Muskeln *Mstn*-überexprimierender Mäuse ergab ein Muster von hoch- und herunterregulierten Genen, welches auf eine homöostatische Regulationsfunktion von MSTN hinweist.

Darüber hinaus sollen die Ergebnisse dieser Arbeit die Grundlage für weitere genetische Modifikationen der *Mstn*-überexprimierenden Mauslinie in Richtung einer induzierbaren Genmodifikation bilden, um die Möglichkeiten der Forschung durch Kontrolle des Beginns der Überexpression zu erweitern.

Contents

1. Introduction

1.1. Skeletal muscle

1.1.1. Anatomy of skeletal muscles

Skeletal muscle is one of the largest organs in the human body. Skeletal muscle mass in the human body makes up around 38% in males and around 31% in females (Janssen *et al.*, 2000). Since it contains a most of the bodies protein content, it also exerts a metabolic function through balance shift of protein synthesis and degradation (Carbone *et al.*, 2012). Hereby, it provides the body with amino acids during catabolic phases, e. g. for gluconeogenesis (Frontera & Ochala, 2015), (Mirzoev, 2020). A widely used classification of muscular tissues distinguishes the three major subtypes of cardiac, smooth and skeletal muscle. All these tissues have in common that they can contract via specific cytoskeletal elements. Briefly, smooth muscle tissue performs non arbitrary, rather slow and long lasting contractions controlled by the autonomic nerve system, while cardiac muscle also performs non arbitrary, but faster, permanently repeating contractions with a high amount of endurance. In contrast to the other two types, skeletal muscle can be controlled intentionally. Contractions can be fast and powerful or long-lasting and enduring. Throughout the body, skeletal muscles appears in various sizes and forms depending on their anatomical environment and requirements. The fine ultrastructure and its close association to skeletal muscle's function becomes clear on microscopic or even molecular scales (see Figure 1.1). A muscle is composed of multiple muscle fascicles, separated by connective tissue, termed perimysium. Fascicles consist of hundreds of muscle fibres, which represent the long, multi-nuclear muscle cells. Myofibres contain up to hundreds of myofibrils, which are mainly built up by repeating units, the sarcomeres, which are basically formed by myosin and actin, in connection with other structural proteins, such as troponin and tropomyosin. Within a sarcomere filaments are arranged in an intertwining pattern. When a neural or ion signal is translated at the neuromuscular junction, sarcomeric filaments over the entire muscle intertwine even further. As a result, the muscle produces contraction force, which is transmitted to the respective tendon, which anchors on the associated bone, causing movement.

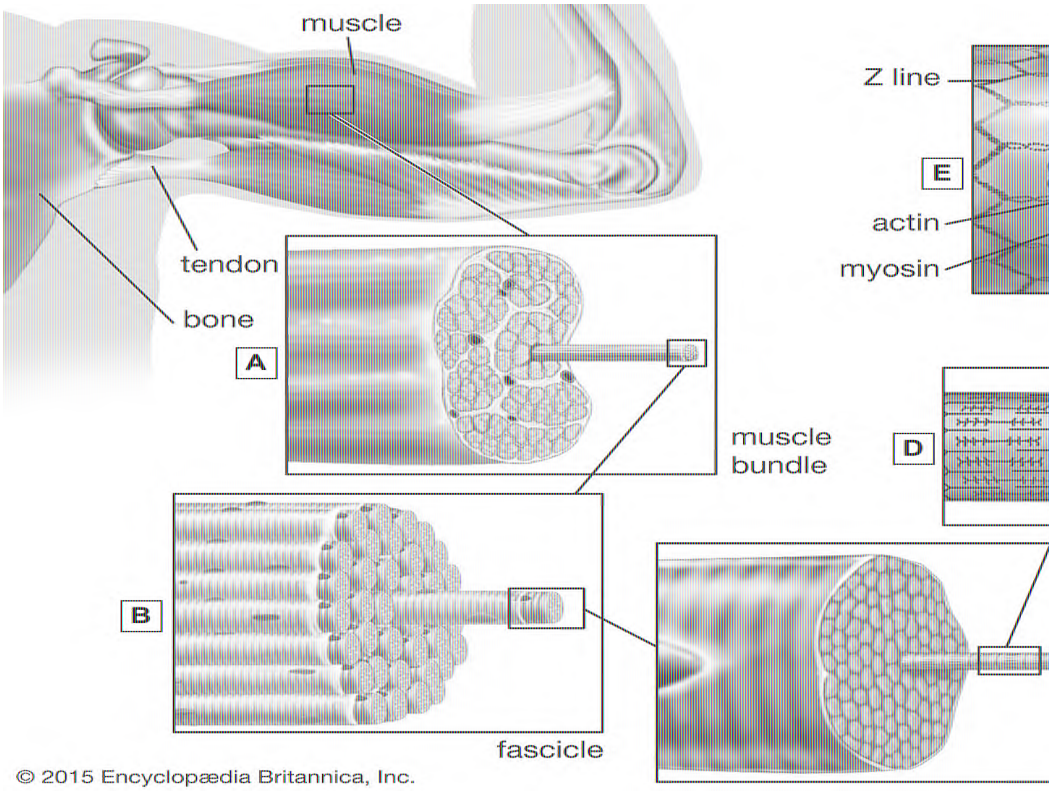

Figure 1.1: Macroscopic and microscopic anatomy of skeletal muscle.
Muscular bellies (musculus biceps brachii shown here) are subdivided into muscular bundles (**A**). These are organised in muscle fascicles (**B**). Muscle fascicles consist of multiple long, cylindrically shaped, multinuclear muscle cells, termed myofibres (**C**). Myofibres again contain up to hundreds of myofibrils (**D**), which are repetitive chains of a scaffold of actin and myosin (**E**). These carry out the contraction movement. Adopted from Encyclopædia Britannica® - https://www.britannica.com/science/skeletal-muscle (last access: 7 December 2022).

A sarcomere ranges from one Z-line to another. Here actin and titin are linked. Titin, the largest known protein in humans, keeps the myosin filaments in place (Linke, 2018). Sarcomeres are the functional unit of muscle fibres and build up the foundation for its ultrastructure. Cell compartments are adapted to sarcomere length and arrangement. A compound of sarcolemmal invaginations, the t-tubuli, side by side with two bulges of sarcoendoplasmic reticulum (SER), follows this sarcomere template and surrounds it in a net-like structure (see Figure 1.2). During contraction Ca^{2+} is released from the SER and binds to troponin C, which reveals the binding sites for myosin heads on actin filaments (Costantin, 1975). The myofibril-adapted architecture of the SER shortens the distances for release of calcium and re-uptake by sarco/endoplasmic reticulum Ca^{2+}-ATPase (SERCA), which accelerates signal transduction. Taken together, skeletal muscle morphology is highly adapted to its unique function, both on a macroscopic and on a microscopic scale.

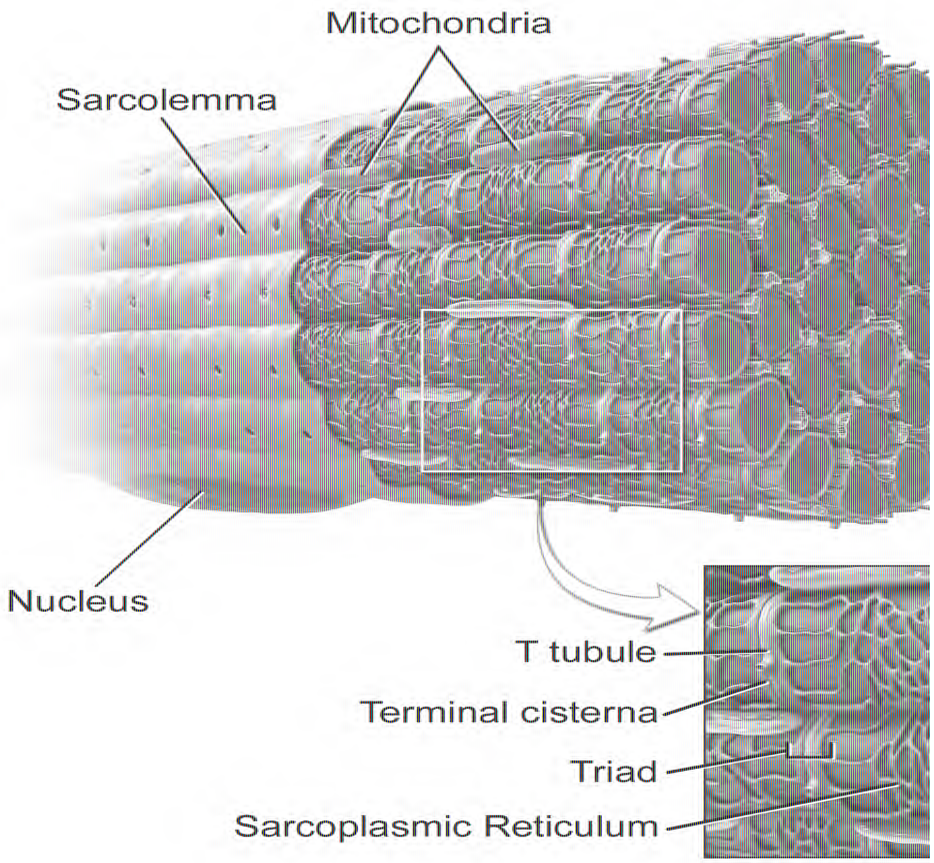

Figure 1.2: Simplified skeletal muscle cell structure.
The figure shows a cross sectioned myofibre and its containing myofibrils. These are surrounded by the cell compartments, which differ from most cell types and are highly adapted to the special structure and function of the myofibre. The endoplasmatic reticulum or sarcoendoplasmatic reticulum (SER) forms extensions along the myofibrils, called terminal cisterna, and comprise the storage for calcium ions. This specialised structure ensures a fast and homogenous release of Ca^{2+} during contraction. Mitochondria lie between the myofibrils and provide ATP. Adopted from (Blausen.com staff (2014). "Medical gallery of Blausen Medical 2014". WikiJournal of Medicine, last access: 7 December 2022); https://creativecommons.org/licenses/by/4.0/.

1.1.2. Skeletal muscle fibre types

Everyday life and sports involve a variety of movements that require different amounts of muscular strength and endurance. The heterogeneity of myofibres within a muscle allows the dynamic utilisation in various forms of motion - from low-intensity postural activity to strong and high-speed contractions, e. g. during sprinting or heavy lifting. In mammals, structural and functional properties enable to classify different skeletal muscle fibre types. A rather simple and outdated classification distinguishes myofibres based on their microscopic appearance in red, slow-twitching (ST), enduring, myoglobin rich myofibres, and white, fast-twitching (FT) and strong myofibres with low myoglobin content (Sica & McComas, 1971). However, advances in molecular biology methods broadened the spectrum towards four major subtypes of myofibres known today. Immunohistochemical staining (IHC) allows to distinguish myofibre types by their expression of myosin heavy chain (MYH) subtypes - type I (MYH 7, slow oxidative), IIA (MYH 2, fast oxidative),

IIX (MYH 1, fast glycolytic) and IIB (MYH 4, very fast glycolytic) (Schiaffino & Reggiani, 2011). To meet specific physiological requirements, each muscle contains a combination of myofibres. In porcine skeletal muscle it was possible to show that MYH composition in a myofibre could be related to other metabolic and anatomic proteins, which together build up a functional profile (Quiroz-Rothe & Rivero, 2004). This study showed that type I (ST) myofibres have lower activity of myosin adenosine 5'-triphosphatase (mATPase) and glycerol-3-phosphate dehydrogenase (GPDH), lower glycogen content and CSA as well as higher activity of oxidative enzymes such as succinate dehydrogenase (SDH). Additionally, ST-fibres show higher vascularisation, higher nuclei density and slow isoforms of sarcoendoplasmic-reticulum-Ca^{2+}-ATPase (SERCA). Endurance training can lead to FT-fibre type switch towards ST-fibre rather than vice versa (Popov, 2018).

1.1.3. Skeletal muscle physiology

The role of skeletal muscle within an organism goes beyond the mere locomotor system. As one of the highest glucose consuming tissues skeletal muscle plays a vital role in blood sugar balance. Especially physical exercise has beneficial effects not only in diabetes mellitus patients (Kumar *et al.*, 2019). Moderate beneficial effects of exercise were found in women presenting with gestational diabetes mellitus (Peters & Brazeau, 2019). The metabolic base rate is around 54 kJ/kg REE/FFM (resting energy expenditure/ fat-free-mass), adipose tissues REE/FFM is around 18.8 kJ/kg for comparison (Heymsfield *et al.*, 2002). Skeletal muscle also provides glucose reserves for phases of higher energy demand, since it holds the major glycogen storage (DeFronzo *et al.*, 1981). ATP is the fundamental energy source and directly required for movements since the dephosphorylation of ATP provides the energy for contraction. Most of the energy produced in myofibres is converted into thermal energy (González-Alonso, 2012). The resting heat production increases significantly during physical exercise and must be emitted via blood stream to the skin.

1.1.4. Skeletal muscle development

Understanding the genetic pathways that regulate the embryonic development of skeletal muscle is crucial since many of the genes are reenacted during adolescence in homeostasis and regeneration (Tajbakhsh, 2009). In early development of vertebrates, three germ layers can be distinguished, which give rise to all tissues of the body. The endoderm forms the inner layer of the gastrointestinal tract, lungs, liver, and pancreas. The ectoderm gives rise to neurons of the brain, epidermis and pigment cells. Whereas, the mesoderm forms connective tissues, cardiac, skeletal ,and smooth muscles, the vascular system, blood cells, dermis, and renal tubules. Hence, most cells that constitute the musculoskeletal system originate from the mesoderm.

Skeletal muscle tissue of the trunk and limbs emerges from pairwise cell aggregations, termed somites (Baker *et al.*, 2006; Hirsinger *et al.*, 2000). Somite formation and differentiation is orchestrated by molecular signals from adjacent tissues (Christ & Ordahl, 1995). WNT1 (wingless type family member 1) signalling from the ectoderm and neural tube leads to *Pax3* and *Pax7* expression in the dorsal cells of the somite (Fan & Tessier-Lavigne, 1994; Kassar-Duchossoy *et al.*, 2005). This region is termed dermomyotome and gives rise to muscle precursor cells (MPCs).

Several factors ensure correct coordination of further myogenesis. *Shh* (sonic hedge hoc) signalling induces expression of the earliest myogenic regulatory factors *Myf5* (myogenic factor 5) and MYOD1 (myoblast determination factor 1) (Gustafsson *et al.*, 2002).

After cellular commitment towards the myogenic lineage, myogenesis continues with migration to the final target sites and fusion of MPCs. Hepatocyte growth factor (HGF), its receptor c-MET (HGFR) and ladybird homeobox 1 (LBX1) are involved in MPC migration into developing limb buds (Kim *et al.*, 2021; Gross *et al.*, 2000). *In vitro* studies could show that Ras homolog family member E (*RhoE)* expression is up-regulated prior to myoblast fusion (Fortier *et al.*, 2008). *RhoE* up-regulates expression of the cell adhesion molecule *M-cadherin*, which mediates myoblast elongation and alignment. In the process of myofibre fusion, integrin-beta1 (ITGB1) acts together with CD9 (Cluster of differentiation 9), in sarcolemma breakdown and reassembly of the sarcomeres (Schwander et al., 2003).

As a results of these complex processes, large, multinucleate, tubular myofibres arise. However, a pool of MPCs remain quiescent and position between the sarcolemma and the basal membrane. These so-called ‘satellite cells’ (SC) are the resident stem cells of skeletal muscle and express (PAX7) paired-box transcriptional factor 7 (Zammit *et al.*, 2004). After activation by extrinsic factors SC down-regulate PAX7 and MYOD1 and become myoblasts, which contribute to muscle regeneration. Simultaneously SC conserve the stem cell pool (Shi & Garry, 2006). In more detail, research on SC-related markers revealed different phases of SC and their descending myoblasts. Quiescent and self-renewing SC ($PAX7^{+}/MYOD1^{-}$), activated, proliferating SC-derived myoblasts ($PAX7^{+}/MYOD1^{+}$) and myoblasts that fuse and differentiate into myotubes ($PAX7^{-}/MYOD1^{+}/Myogenin^{+}$) (Zammit *et al.*, 2006). Even a small number of SC are capable to regenerate an entire myofibre, since only 2 - 6% of nuclei in a myofibre belong to SC (Zammit *et al.*, 2002).

1.2. Sarcopenia

Hunting, fighting or fleeing display just a few examples for complex activities that ensure the survival in higher forms of live. A variety of muscle groups and adjacent tissues contributes to these processes to perform movements or posture. All these intentional movements require a properly interacting locomotor system. In modern societies, a comfortable lifestyle has developed over the last century for most of the population. This process was mainly driven by utilisation of machines that lead to a relief of hard physical labour. To a certain extent, digitalisation even makes leaving the house redundant. Thus, coping with everyday life does set little requirements on physical capacity of an individual nowadays. However, with ageing naturally occurring processes comes to light that present with a progressive loss of muscle mass, strength, and performance. Even if all other organ functions are preserved well in an old age, an impaired musculoskeletal function can threaten health and survival due to increasing risks of both trauma and (resulting) immobility. Disabling musculoskeletal diseases are of constantly growing socioeconomic significance in ageing societies, as seen in most industrialised nations (Beaudart *et al.*, 2018). The impairment of a self-reliant life and co-morbidity require a high commitment of manpower, leading to rising costs for health care systems. Muscle mass and strength reduces naturally during ageing. In sarcopenia, this process is accelerated. Originally, sarcopenia simply described the age-related loss of muscle mass but with the aim of applying the definition of sarcopenia into clinical practice, muscle mass alone neither did correlate with low muscle strength or performance deficits (Newman *et al.*, 2006). In 2019, the European Working Group on Sarcopenia in Older People (EWGSOP2) published an update on their previous review, which showed that impaired muscle strength, sometimes also referred to as dynapenia, which was better in predicting unfavourable outcomes (Cruz-Jentoft *et al.*, 2019). The following section displays the diagnostic algorithm for sarcopenic conditions according to the EWGSOP2.

1.2.1. Diagnostics of sarcopenia

Based on research of recent years three criteria are proposed by the EWGSOP2 to diagnose sarcopenia: low muscle strength, low muscle mass and low physical performance. Presence of sarcopenia is considered possible when one criterion is met. Diagnosis is confirmed by an additional criterion, whereas sarcopenia is classified as severe, if all three criteria are detected. The EWGSOP2 recommends several tests for muscle mass, strength, and performance (Cruz-Jentoft *et al.*, 2019). Muscle mass can be measured using different techniques, such as dual-energy X-ray absorptiometry (DXA) or bioelectrical impedance analysis (BIA). Muscle mass values can be specified i. a. as skeletal muscle mass (SMM) or appendicular skeletal muscle mass (ASM), based on musculature of arms and legs (Cawthon, 2015). Since muscle mass correlates with body size it should be adjusted for height or weight. Modern imaging techniques such as computed tomography (CT) or magnetic resonance imaging (MRI) can be used to measure muscle quality, but an extensive clinical application has not been implemented (Heymsfield *et al.*, 2015; Wang *et al.*, 1996). Muscular performance tests include grip strength and the chair stand test,

which measures the time needed to rise five times from a seated position without using the arms. Possible performance tests are the gait speed test and the Timed-Up and Go test (TUG) (Abellan van Kan *et al.*, 2009; Maggio *et al.*, 2016; Podsiadlo & Richardson, 1991). The results of such diagnostic tests do have different prognostic relevance. Low grip strength was discovered to be a strong indicator for unfavourable outcomes such as prolonged hospitalisation, impaired quality of life and death (Leong *et al.*, 2015). At the same time, grip strength measurement is an uncomplicated method, which can be easily applied in clinical settings. Interestingly, a strong correlation could be found between muscle strength and physical performance with limitations carrying out activities of daily living, quality of life, and health care costs, whereas no significant correlation of muscle mass alone was found (Mijnarends *et al.*, 2018). Moreover, a higher risk of falls was detected in sarcopenic individuals, involving the risk of fractures with even aggravated and prolonged immobility (Yeung *et al.*, 2019; Bischoff-Ferrari *et al.*, 2015). Cut-off-points of diagnostic criteria do have a major impact on the prevalence of sarcopenia, which simply decide whether a physical condition can be considered sarcopenic or not.

1.2.2. Epidemiology of sarcopenia

Many studies on the prevalence of sarcopenia have been carried out across the world reporting various values, depending on heterogeneity of the study group, used diagnostic methods and threshold values. For example, a Japanese study on a community-dwelling elderly population reported a prevalence ranging from 2.5 to 28% in men and 2.3 to 12% in women, with muscle mass measured by DXA. However, when muscle mass was measured by BIA the prevalence was 7 to 98% in men and 20 to 88% in women (Kim *et al.*, 2016). A study on older adults living in nursing homes in the United Kingdom with a mean age of 73 years found a prevalence of sarcopenia to be 4.6% in men and 7.9% in women (Patel *et al.*, 2013). Meanwhile, a Korean study on ambulatory community-dwelling older adults with a mean age of 76 years showed a prevalence of 21% in men and 14% in women, while medical cases meeting all criteria indicating severe sarcopenia were present in 6.4% in men and 3.2% in women (Kim & Won, 2020). In a Spanish study, the prevalence of sarcopenia in general was 26.4% (mean age of 72.6 years), whereas 6% had severe sarcopenia (Blanco-Reina *et al.*, 2022). In a Taiwanese population the prevalence of sarcopenia varied from 2.5% to 6.5% in women and 5.4% to 8.2% in men, or 3.9% to 7.3% overall (Wu *et al.*, 2014). In any case, the global prevalence of sarcopenia is undoubtedly expected to rise in ageing societies across the world.

1.2.3. Pathomechanisms of sarcopenia and skeletal muscle ageing

Pathophysiology of sarcopenia is complex and multifactorial. Basically, processes of increased catabolism and reduced anabolism contribute to the development of loss of muscle mass and strength (Bodine *et al.*, 2001). Aggravating factors include disuse, immobilisation, disease, and malnutrition (see Figure 1.3). Some of these interact, since disease can lead to immobilisation and muscular disuse, as well as several diseases might go along with malnutrition, and vice versa (Bell *et al.*, 2016; Thomas, 2007; Grounds, 2014). With increasing age, morphological changes occur in

skeletal muscle tissue, such as an increase of intra- and intermuscular fat content (Visser *et al.*, 2002). In addition, the quantity and regenerative potential of skeletal muscle stem cells, also known as satellite cells (SC), decreases with age (Brack *et al.*, 2005; Sousa-Victor & Muñoz-Cánoves, 2016). Ageing was found to be associated with increased levels of inflammatory cytokines, such as c-reactive protein (CRP) and interleukin-6 (IL-6) (Krabbe *et al.*, 2004). Inflammatory processes during fever are involved in protein degradation explaining muscle loss (Baracos *et al.*, 1983). Certain habits might come along with ageing that favour the loss of muscle mass. Low physical activity throughout daily life can have multiple reasons such as lowered endurance due to cardiac insufficiency or pain caused by osteoarthritic degeneration. Either way, this results in low muscular training stimuli, which leads to loss of muscle mass and strength and might increase age-related mechanisms (Coker *et al.*, 2015). A study on 70- to 79-year-old men and woman revealed a significantly higher decrease in leg extension strength in proportion to the loss of muscle mass (Goodpaster *et al.*, 2006). Also, low muscle strength, rather than low muscle mass, is associated with poor performance in older people (Visser *et al.*, 2000). Muscle mass and grip strength declines during hospitalisation in older adults (Van Ancum *et al.*, 2017). In young men (mean: 23 years of age), which underwent a 3-week unloading phase, a loss of muscle mass and force was found (Campbell *et al.*, 2013). A similar study on a likewise group of young men (mean: 24 years of age) undergoing one-leg immobilisation following surgery, found concordant results (Snijders *et al.*, 2014). Quadriceps muscle cross sectional area (CSA) reduced by approximately 8%. This study showed no changes in satellite cell content around either type I or type II myofibres. In contrast, a study on adult rats that were exposed to 14 days of hind limb immobilisation showed rapid atrophy of soleus muscle accompanied by reduced amount of satellite cells (Nakanishi *et al.*, 2016). Similar results were found in humans within a group of middle-aged adults around 51 years old after two weeks of bed rest (Arentson-Lantz *et al.*, 2016). Snijders *et al.* (2014) identified a preferential atrophy of type II fibres in young men, concordantly with another study in rats (Babcock *et al.*, 2015). In addition, in healthy older men the same observation was made, which suggests interconnecting mechanisms or behavioural factors involved in ageing and muscle disuse (Proctor *et al.*, 1995). Not only atrophy but also numerical reduction (hypoplasia) of muscle fibres contributes to muscle loss (Lexell *et al.*, 1988). Besides, type II fibre size predominantly decreases with age and therewith muscular oxidative capacity (Proctor *et al.*, 1995). A prospective study on hospitalised older patients could showed a significant impact of nutritional deficits on muscle strength and mass (Pierik *et al.*, 2017). Taken together, ageing goes along with a perceptible decrease in strength and muscle mass, which to a certain extent can be considered physiological. However, the occurrence of various aggravating factors increases the risk of sarcopenic conditions.

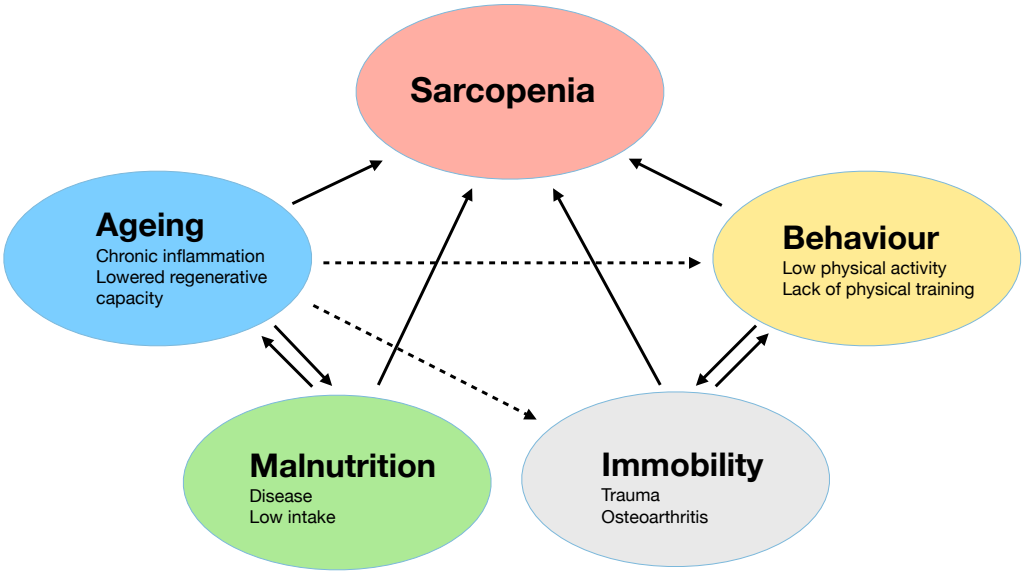

Figure 1.3: Pathomechanisms of sarcopenia.
Several mechanisms are involved in the onset and progression of sarcopenia, which might intertwine or mutually reinforce each other. Ageing might go along with behavioural changes as well as diseases and consequential frailty.

1.2.4. Treatment options for sarcopenia

Due to its rising significance in ageing populations, there is a growing interest in developing interventions to cure or at least reduce the impact of sarcopenia (Grounds, 2014). Unfortunately, no pharmacological treatments are available to prevent or treat this condition with resounding success yet. Currently, the only clinically applied interventions are based on nutrition and physical exercise (Giallauria *et al.*, 2016). For instance, the intake of creatine, which is one of the best investigated supplements, does lead to an increase of muscle mass and strength when combined with resistance training, i. a. by increasing insulin-like growth factor 1 (IGF-1) levels (Burke *et al.*, 2008; Louis *et al.*, 2004). In healthy older men resistance training led to type II fibre hypertrophy and increased muscular vascularisation (Verdijk et al., 2016). In a randomised-controlled study on elderly community-dwelling women, walking speed was increased by exercise and nutritional intervention (Kim H. *et al.*, 2016). The same analysis also showed that a nutritional intervention alone including high protein intake did not improve grip strength. In a study on 28-month-old mice undergoing physical training on a treadmill did enhance the regenerative potential and quantity of satellite cells, when compared to sedentary same-aged mice (Cisterna *et al.*, 2016). A meta-analysis of studies on sarcopenic obesity investigated the effect of resistance training on body weight and body fat percentage (Hsu *et al.*, 2019). Especially, body fat percentage was reduced by resistance exercise or combined workouts. Taken together, physical exercise displays the key component of current therapeutic or preventive concepts in order to regain or maintain muscle mass and strength.

1.3. Myostatin/ GDF8

1.3.1. Discovery of MSTN

Myostatin (also known as growth and differentiation factor 8 or GDF8) is a protein, which belongs to the transforming growth factor (TGF) beta family. Its function was impressively demonstrated by genetic modification through animal knockout models. Homozygous *Mstn*-KO mice (*Mstn*$^{-/-}$) were 30% larger and muscles mass was significantly 2 to 3 times higher (McPherron *et al.*,1997). In Belgian Blue cattle with a naturally occurring loss-of-function mutation of *Mstn*, an enormously muscular phenotype was observed (see Figure 1.4) (McPherron & Lee, 1997). This effect could also be found in other species such as humans (Schuelke *et al.*, 2004) or dogs (Mosher *et al.*, 2007). In *Mstn*$^{-/-}$ mice specific muscle mass of extensor digitorum longus and total muscle cross-sectional area (CSA) increased by more than 60% compared to wildtype (WT) (Mendiaz *et al.*, 2006). Postnatal myostatin gene inactivation was shown to attain a comparable amount of muscle mass hypertrophy as in innate KO models proving that MSTN not only acts during embryogenesis but also in adolescence (Grobet *et al.*, 2003).

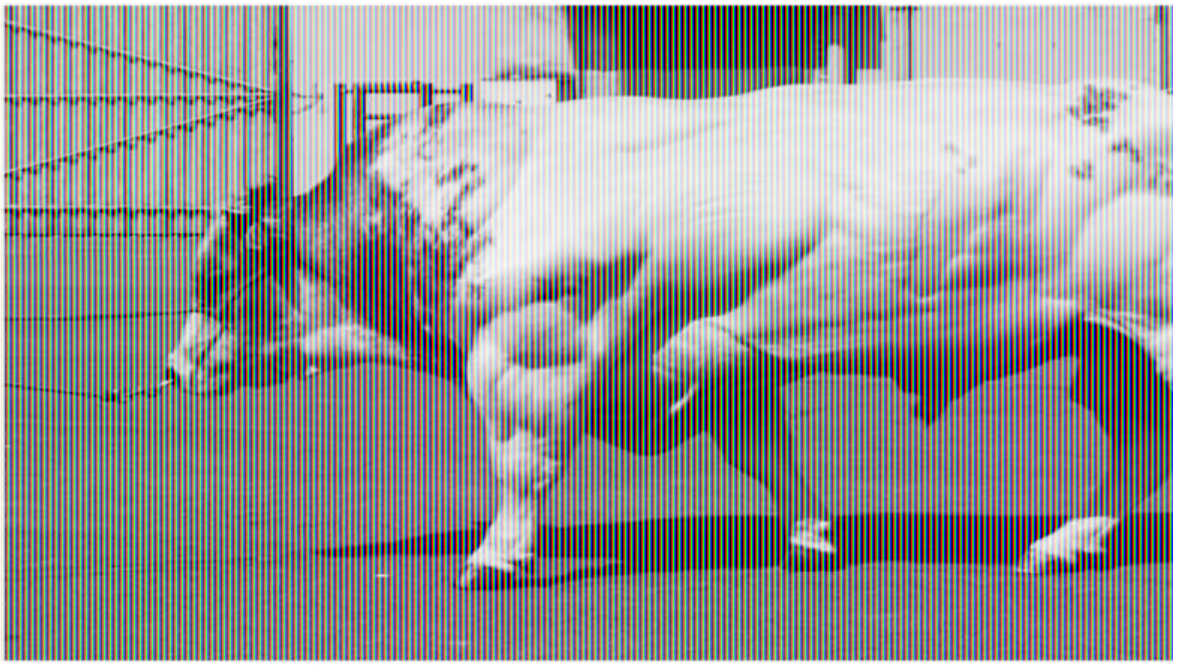

Figure 1.4: Belgian blue cattle carry a defective myostatin gene causing muscular hypertrophy.
In Belgian Blue cattle a mutation within the myostatin gene causes a defective myostatin protein. This results in a dysregulation of skeletal muscle mass that causes massive muscular hypertrophy. Adopted from: Druet *et al.* (2014); https://creativecommons.org/publicdomain/zero/1.0/.

These impressive scientific findings showed that MSTN acts as a potent inhibitor of skeletal muscle mass. Most likely MSTN regulates muscle mass adapted to requirements (Saunders *et al.*, 2006). Inversely, elevated levels of MSTN were found in HIV-infected men, in which it contributes to muscle wasting (Gonzalez-Cadavid *et al.*, 1998). Also, increased levels could be found in older men and women over 60 years old in comparison to younger populations, suggesting its role in

age-related muscle loss (Yarasheski *et al.*, 2002). Male mice over-expressing myostatin showed a 20% reduction of lower hindlimb muscle weight and 18% reduction in quadriceps femoris and gastrocnemius muscle fibre CSA than wild-type male mice (Reisz-Porszasz *et al.*, 2003).

1.3.2. Signalling pathway and regulation of myostatin

The molecular signalling mechanisms of MSTN have been in focus of intense research ever since its discovery (see Figure 1.5). MSTN is a transforming growth factor-β (TGF-β) family member with a specific weight of 26 kDa, which is expressed in myofibres and secreted into the blood stream (Gonzalez-Cadavid *et al.*, 1998). After cleavage of the prodomain of MSTN the mature protein forms homodimers (Yadin *et al.*, 2015), which can bind to activin type II receptors (ACVRII and ACVRIIB). This ligand/ receptor complex recruits activin type I receptors that activate activin receptor-like kinase 4 (ALK4) or 5 (ALK5). Hereby, the canonical intracellular signalling cascade via phosphorylation of SMAD2/3 (Small Mothers Against Decapentaplegic) proteins is initiated (Rebbapragada *et al.*, 2003). SMAD2/3 then translocate into the nucleus, bind to DNA and initiate a specific transcriptional downstream cascade (Massagué & Gomis, 2006). Alternatively, the non-canonical pathway is initiated through mitogen-activated protein kinases (MAPK) such as extracellular signal-regulated kinases (ERKs), c-Jun N-terminal kinases (JNKs), or p38 (Walker *et al.*, 2016).

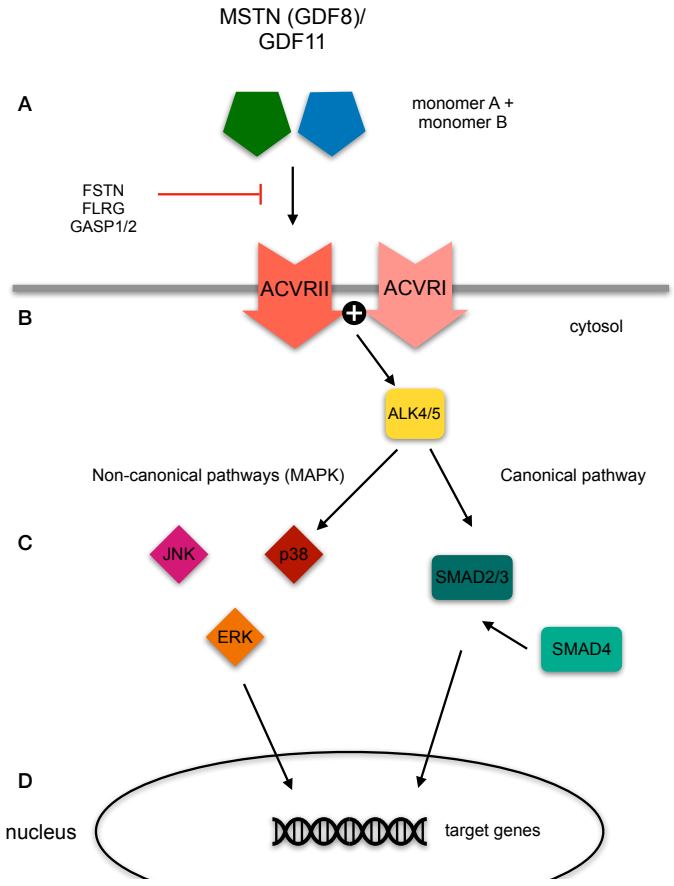

Figure 1.5: Signalling pathway of myostatin and its close related protein GDF-11.
MSTN (GDF-8), as well as the closely related protein GDF11, form homodimers (A). These bind to activin type II receptors. Follistatin (FST), follistatin-related protein 3 (FSTL3), and growth and differentiation factor-

associated serum proteins 1 and 2 (GASP1/2) inhibit ligand/receptor interaction of MSTN/ GDF11 (B). If however, MSTN binds to ACVRII receptors, type I receptors are recruited to form a heteromeric receptor complex, which activates a canonical pathway via activin receptor-like kinase 4 (ALK4) or ALK5 (C). This elicits signalling via phosphorylation of SMAD2 and/or SMAD3, which then translocate into the nucleus and bind to DNA and regulate gene expression (D). Also, SMAD-independent pathway through mitogen-activated protein kinases (MAPK) is activated. Modified after Walker *et al.*, 2016 (last access: 10 November 2022).

Several extracellular inhibitors of MSTN have been identified including follistatin (FST), follistatin-related protein 3 (FSTL3), growth and differentiation factor-associated serum proteins 1 and 2 (GASP1/2) (Zhu *et al.*, 2011; Tsuchida *et al.*, 2004; Kondas *et al.*, 2008). These bind to MSTN, and therewith inhibit MSTN binding to ACVRII receptors. In contrast to FST and FSTL3, which antagonise several TGF-ß proteins, GASP1/2 bind mature forms of MSTN (GDF8) and the similar protein GDF11 more specifically.

1.3.3. Effect of MSTN on skeletal muscle during development and adolescence

Experiments on *Mstn*$^{-/-}$ mice that were treated with a soluble form of ACVRIIB resulted in additional muscle hypertrophy, which suggested that MSTN (GDF8) is not the only potent limiter of muscle mass (Lee *et al.*, 2005). GDF11 was detected as the most promising candidate due to its high sequence homology with GDF8 of around 89% (Souza *et al.*, 2008). However, experiments showed that the absence of GDF11 resulted in skeletal and parenchymatous organ deformations and high perinatal mortality (Suh & Lee, 2020; Baig *et al.*, 2022; Esquela & Lee, 2003). The mortality displays a limiting factor for studying the function of GDF11 in knockout organisms. As an alternative approach, recombinant GDF11 (rGDF11) was used in several studies on mice. Application of rGDF11 showed a protective, or even rejuvenating effect on aged mice by improving muscle structure, strength, and endurance (Sinha *et al.*, 2014). Inconsistent with these findings, another study found no significant effect of rGDF11 (Egerman *et al.*, 2015). In this study on rats GDF11 levels increased with age, whereas MSTN levels decreased. In the same study human skeletal myoblasts were stimulated with either rGDF8, or rGDF11, which inhibited myogenic differentiation. In addition, stimulation with GDF8 and GDF11 resulted in identical transcriptional changes.

In mice *Mstn* is first expressed within somites at E9.5 where it suppresses hyperplasia of skeletal muscle fibres during development (McPherron *et al.*, 1997). GDF11 is expressed in the tail bud at E9.5 and regulates patterning of the axial skeleton (McPherron *et al.*, 1999). *Gdf11*$^{-/-}$ mice have severe morphological changes to the axial skeleton, such as an increased number of vertebrae and ribs. *Gdf11*$^{-/-}$ mice die within a few hours after birth. However, *Gdf11* and *Mstn* double-knockout mice (*Mstn*$^{-/-}$; *Gdf11*$^{-/-}$) show even more extensive alterations of the axial skeleton when compared to *Gdf11*$^{-/-}$ mice, indicating that both proteins share some functions and might be able to compensate dysfunction of the other (McPherron *et al.*, 2009). However, GDF11 and MSTN also have contrary functions. Bone mass is impaired in newborn *Gdf11*$^{-/-}$ mice, while enhanced in newborn *Mstn*$^{-/-}$ mice (Suh *et al.*, 2020). GDF11 enhances osteogenesis during embryonic

development. Moreover, GDF11 inhibits satellite cell (SC) growth in mice (Egerman *et al.*, 2015). The role of SC within the MSTN signalling pathway however was examined using mouse lines with impaired muscle regeneration due to KO of either syndecan4 (*Sdc4*$^{-/-}$) or the paired box transcription factor (*Pax7*$^{-/-}$). Sdc4 is a key receptor in SC for proliferation and differentiation (Cornelison *et al.*, 2004). Pax7 is a specific marker of satellite cells that drives their renewal and determination towards myoblasts (Seale *et al.*, 2000; Oustanina *et al.*, 2004). Interestingly, when *Sdc4*$^{-/-}$ mice were treated with a soluble form of ACVRIIB, skeletal muscle mass increased approximately 50% (Lee *et al.*, 2012). Moreover, when *Sdc4*$^{-/-}$ mice were mated with a *Fst* over-expressing mouse line (F66) muscle mass increased even further to 165% compared to control animals. An increase of 37-52% was observed in *Pax7*$^{-/-}$*,F66* mice. Here, neither proliferation nor fusion of SC to myofibres was affected significantly. These results indicate no significant role of SC in the MSTN signalling pathway.

In contrast, MSTN can induce atrophy in adult myofibres (Sartori *et al.*, 2009; Trendelenburg *et al.*, 2009). Research on trouts revealed that MSTN inhibits proliferation but not differentiation of myoblasts (Seiliez *et al.*, 2012). A study on male rats used gene electrotransfer of a myostatin expression vector into tibialis anterior (TA) muscle (Durieux *et al.*, 2007). Over-expression of *Mstn* lead to a significant decrease in muscle mass of around 10% 7 days and 20% after 14 days after gene transfer. In addition, muscle fibre cross-sectional area (CSA) decreased by 15 and 30%, 7 and 14 days after gene transfer, respectively. Myofibre number was not affected, but a decreased expression of muscle structural genes (myosin heavy chain IIb, troponin I, and desmin) and of myogenic transcription factors (MyoD and myogenin) was found. During murine development, MSTN decreases skeletal muscle fibre hyperplasia as well as hypertrophy in adult muscle (Zimmers *et al.*, 2002). In adolescence myostatin is almost exclusively expressed in muscle tissue (Lee, 2004). An *in vitro* study on myoblasts showed that MSTN is involved in the specification of myofibre types during myogenic differentiation (Wang *et al.*, 2012). *Mstn*$^{-/-}$ myoblasts formed myotubes, which predominantly expressed fast MYH isoforms. Accordingly, myoblasts treated with recombinant MSTN led to up-regulation of slow *Myh7* and down-regulation of fast *Myh4* in newly formed myotubes. *Mstn*-KO (*Mstn*$^{-/-}$) in Belgian Blue cattle, as well as in mice lead to a higher amount of fast IIb fibres (Stavaux *et al.*, 1994; Girgenrath *et al.*, 2005). In heterozygous mutant pigs (*Mstn*$^{+/-}$) a significant increase in muscle mass and higher body weight due to fibre hypertrophy was observed, going along with a change in fibre type distribution, and alteration of myosin heavy chain isoforms, leading to more fast glycolytic fibres (Xing *et al.*, 2017).

Blood levels of GDF8 and GDF11 in mice and humans decrease with age (Loffredo *et al.*, 2013; Olsen *et al.*, 2015). A study on male participants showed that circulating MSTN levels would increase until the age of 57 and decrease from then on (Szulc *et al.*, 2012). The results also reveal a negative correlation of MSTN blood levels and body-mass-index (BMI), total central and peripheral fat mass.

In myoblasts isolated from double-muscled (DM), Japanese shorthorn cattle MSTN increased expression of glucose transporter-4 (GLUT4) compared to normal-muscled (NM), which indicates that a resulting higher insulin sensitivity and thus higher glucose uptake into myoblasts might

contribute to higher muscle mass development in DM cattle (Takahashi *et al.*, 2014). Moreover, physical exercise increases the amount of GLUT4 in sarcolemma (Flores-Opazo *et al.*, 2020). Gene expression of *Mstn* and *Fst* is regulated by resistance training in middle-aged men undergoing 8 weeks of resistance training (Bagheri *et al.*, 2019). Here, *Mstn* was down- and *Fst* up-regulated, when compared to the control group. In mice, expression of *Gdf11* was positively affected in slow-twitch fibres by physical exercise on a treadmill (Lee *et al.*, 2019). Skeletal muscle-specific *Gdf11*-KO in mice (*Gdf11*$^{-/-}$) shows no significant effect on muscle mass, fibre number, or fibre type composition in wildtype as well as in *Mstn-KO* animals (*Mstn*$^{-/-}$). (McPherron *et al.*, 2009). This indicates that GDF11 in contrast to MSTN has no effect on muscle mass.

1.3.4. Myostatin-targeted therapy approaches

The tremendous impact that MSTN inhibition has on skeletal muscle mass makes it perfectly clear that it is of highest interest for therapeutic targeting to treat muscle wasting diseases. Historically, animal models were required to investigate potential therapeutic approaches. Application of MSTN-antagonising propeptide of either MSTN or GDF11 to *mdx* mice, a model organism for Duchenne muscular dystrophy, showed convincing results, as treated mice had an increased muscle mass and strength (Bogdanovich *et al.*, 2005; Jin *et al.*, 2019). A similar effect was observed by *Fst* over-expression in mice (Zhu *et al.*, 2011). In a different study *mdx* mice were mated with a mouse line that expresses a transgene coding for an inhibitor derived from FST (Nakatani *et al.*, 2008). The mice also regained muscle mass and strength. *Mstn*$^{-/-}$ mice showed that regenerative capacities are more preserved in older mice (24 months), when compared to wild type mice after cardiotoxin-induced injury (Wagner *et al.*, 2005).

Application of neutralising antibodies against MSTN increases muscle mass in 22-month old mice (Camporez *et al.*, 2016) and in non-human primates (cynomolgus monkeys) (St Andre *et al.*, 2017). Moreover, application of antibodies against MSTN attenuated skeletal muscle atrophy in 9-month and improved endurance in 19-month old mice (Latres *et al.*, 2015). However, in healthy muscle tissue, MSTN inhibition did not influence strength, but improved performance of mice on a treadmill (Personius *et al.*, 2010), (LeBrasseur *et al.*, 2009). Inhibition of MSTN in mouse models for cancer cachexia preserved skeletal muscle mass and adipose tissue (Benny Klimek *et al.*, 2010). So far, the extent to which MSTN inhibition methods have affected skeletal muscle mass and function appears to be insufficient for proper benefit in muscle wasting diseases (Wagner, 2020). No improvement in muscle strength could be observed in a human clinical trial using a neutralising antibody against MSTN (MYO-029) in adult muscular dystrophy patients (Wagner *et al.*, 2008). However, this study found a 2.4% increase in muscle mass. Several studies have shown resistance training and functional electrical stimulation (FES) to conserve muscle mass and function in older adults (Zampieri *et al.*, 2015; Carraro *et al.*, 2015). Therapy strategies for sarcopenia and other muscle wasting diseases should therefore always consider multifactorial approaches.

2. Aim of study

Proper skeletal muscle function is inevitable for independently coping with tasks of everyday life. The increasing life expectancy and age-related impairment of musculoskeletal performance display one of the biggest challenges for health care systems. Due to demographic shift towards the old-age-cohort in most industrialised nations this socio-economic pressure increases constantly. Accordingly, finding therapeutic solutions to alleviate steadily impairing physical performance in older adults is of growing significance. Myostatin (MSTN/ GDF-8) was found to be a strong inhibitor of skeletal muscle development in several animal KO models or those with targeted inactivation of MSTN. Due to its tremendous impact MSTN displays a promising target of research, with the aim of developing treatments for diseases going along with loss of muscle mass and function, such as sarcopenia. To establish a reliable tool simulating sarcopenic conditions for preclinical application, the aim of this study was:

1. To investigate possible morphological and functional effects of a conditional skeletal muscle-specific *Mstn* over-expression.
2. To evaluate changes in gene expression due to *Mstn* over-expression to find possible targets for further research on therapeutic methods for sarcopenia.

3. Materials and methods

3.1. Ethics statement

The mice were handled and housed according to the federal and institutional guidelines for the care and use of laboratory animals, approved by the Ludwig-Maximilians-University Munich, and the government of Upper Bavaria (TVA 55.2-1-54-2532-16-2016 and TVA 55.2-1-54-2532-15-2016).

3.2. Animal husbandry and housing

Animal housing was conducted under standard animal laboratory conditions with controlled temperature, feeding and water without restraint in individually ventilated cages (IVC, Biozone Global, UK) with an effective area of 530 cm^2. The controlled light cycle involves a 12 h constant bright phase, an 11 h constant dark phase and transition periods of half an hour in between. Female mice were housed at a maximum of five mice per cage, while male mice were housed alone.

3.3. Mouse lines and mating

The following mouse lines were used for the purposes of this thesis: *Rosa26Mstn*$^{fl/+}$ (not published), *Acta1*^{Cre} *(*Miniou *et al.*, 1999*).*
Rosa26Mstn$^{fl/+}$ mice are heterozygous for the *Mstn*-transgene, which was inserted at the Reverse orientation splice acceptor 26 (*Rosa26*) gene locus (Zambrowicz *et al.*, 1997; Friedrich & Soriano, 1991) in previous experimental work. As Figure 3.1 shows the transgene contains a CMV-early-enhancer/β-actin/ß-globin (CAG) promotor (Miyazaki et al., 1989), which provides high expression levels of the transgene, a stop codon, human myostatin (*hMSTN*) gene, and an 'internal ribosomal entry sites - enhanced green fluorescence protein' (*IRES*^{eGFP}) sequence.

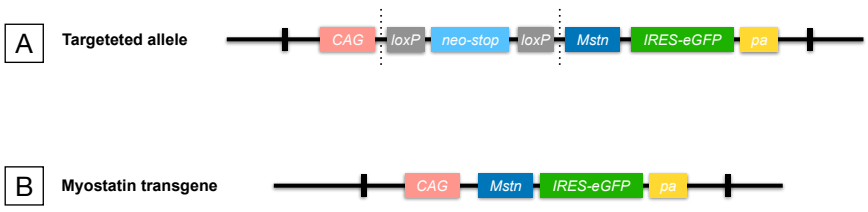

Figure 3.1: Myostatin transgene inserted at the *Rosa26* gene locus.
The figure shows the inserted targeted allele inserted at the *Rosa26* gene locus (**A**). After excision of the *loxP*-flanked stop codon, *Mstn* is expressed under the control of CAG promotor (CMV-early-enhancer/β-actin/ß-globin promotor). Visualisation of success is enabled by co-expression of fluorescing protein *IRES*^{eGFP} (internal ribosomal entry sites - enhanced green fluorescence protein). The *pa* (poly-A tail) stabilises the transcript.

In native conditions, the stop codon inhibits transcription of the myostatin transgene (and *IRES*^{eGFP}). Hence, *Rosa26Mstn*$^{fl/+}$ mice were mated with *Acta1-Cre*$^{+}$ mice (see Figure 3.2), which express the P1 bacteriophage recombinase *Cre* (cyclization recombinase) under the control of the skeletal muscle specific *Acta1* promotor (Hoess *et al.*, 1984; Hamilton & Abremski, 1984; Kos, 2004). *Cre* cuts out DNA between the recognition sites, termed *loxP* (locus of crossing-over of bacteriophage P1 recombinase), which flank the stop codon. As a result, expression of *Cre* leads to deletion of the stop codon, which causes skeletal muscle specific *Mstn* over-expression in *Rosa26Mstn*$^{fl/+}$;*Acta1-Cre*$^{+}$ mice. Additional expression of *IRES-e*^{GFP} (internal ribosomal entry sites - enhanced green fluorescence protein) enables to control successful transgene activation (Bouabe *et al.*, 2008).

Rosa26Mstn$^{fl/+}$;*Acta1-Cre*$^{+}$ mice were breed with homozygous *Rosa26Mstn*$^{fl/fl}$ (*Cre* negative) mice overnight and separated the next morning to give the possibility to trace back the date of conception. Mating success was assumed when females were positively observed for a vaginal plug formation. The offspring had four possible genotypes. Two of those express *Cre*, which is mandatory for the conditional over-expression of *Mstn*. The genotype *Rosa26Mstn*$^{fl/fl}$*;Acta1-Cre*$^{+}$ is henceforth referred to as “homozygous mutant” and the *Rosa26Mstn*$^{fl/+}$*;Acta1-Cre*$^{+}$ as “heterozygous”. Therefore, those mice negative for *Cre* (*Rosa26Mstn*$^{fl/fl}$*;Cre*$^{-}$ and *Rosa26Mstn*$^{fl/+}$*;Cre*$^{-}$) served as controls.

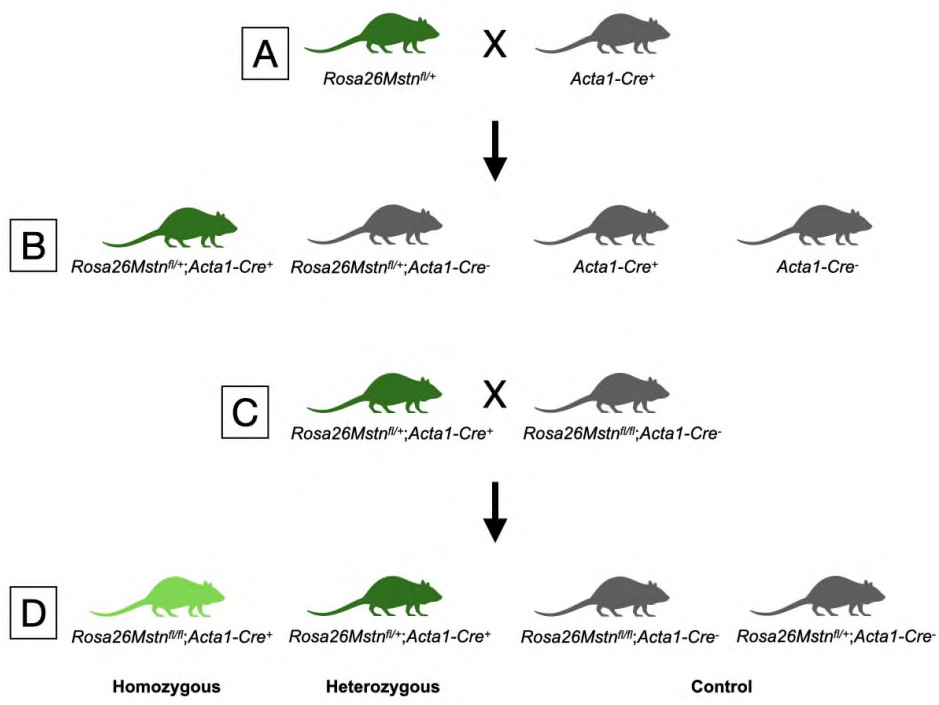

Figure 3.2: Mouse mating.

The figure shows the mating scheme, which was conducted to generate homozygous mutant mice, heterozygous, and control animals. *Rosa26Mstn*$^{fl/+}$ were mated with *Acta1-Cre*$^{+}$ (**A**). Among the offspring are *Rosa26Mstn*$^{fl/+}$*;Acta1-Cre*$^{+}$, which are heterozygous for the *Mstn* transgene and express *Cre* (**B**). Heterozygous were mated with *Rosa26Mstn*$^{fl/fl}$(**C**), whose offspring was *Rosa26Mstn*$^{fl/fl}$*;Acta1-Cre*$^{+}$

(homozygous mutant), *Rosa26Mstn$^{fl/+}$;Acta1-Cre^{+}* (heterozygous) and *Rosa26Mstn$^{fl/fl}$;Cre^{-}* and *Rosa26Mstn$^{fl/+}$;Cre^{-}* (controls).

3.4. Mouse genotyping

Genomic DNA was obtained by digestion of a tail clip in 100 µl of Quick Extract® (Biozym Scientific GmbH, Germany), at 65°C in a thermo shaker for 10 minutes. After raising the temperature to 98°C to inactivate the digestion, the samples were shaken for another 2 minutes and centrifuged, subsequently. PCR reaction mix contained mouse line specific primer pairs (see Table 3.1), desoxynucleotides (dNTPs), PCR Nucleotide Mix (Roche, Switzerland), Taq DNA polymerase (Quiagen, Netherlands), PCR Grade Water (Roche, Switzerland) and buffer 10x CoralLoad PCR Buffer (Quiagen, Netherlands). Preheating at 95 °C for 5 minutes, 35 cycles preheating at 95 ◦C for 5 min, 35 cycles of denaturation (95 ◦C for 30 sec), annealing (primer specific temperature for 60 sec), elongation (72 ◦C for 30 sec), and a final extension step at 72 °C for 10 min. Finally, DNA amplicons were visualised via gel electrophoresis on a 2% agarose gel in 1x TAE buffer with 120 V over 30 minutes. DNA amplicons were stained with ethidium bromide (0.05 µL/mL) to visualise them in fluorescence system.

Genotyping for *R26Mstn* mice required two different primer pairs, which both contained a forward sequence and either a WT specific reverse sequence, or a mutant specific reverse sequence, termed *CAG-rev2* (see Table 3.1). The amplicon in WT is 603 bp, while the amplicon of the *R26Mstn* transgene (mutant) is 450 bp long.

Table 3.1: Primers for genotyping

Gene			Primer Sequence
Cre	fwd		AAC ATG CTT CAT CGT CGG
	rev		TTC GGA TCA TCA GCT ACA CC
Rosa26-Mstn	fwd	WT/MT	AAA GTC GCT CTG AGT TGT TAT
	rev	WT	GGA GCG GGA GAA ATG GAT ATG
	CAG-rev2	MT	GCT ATG AAC TAA TGA CCC CG

fwd - forward; rev - reverse; WT - wild type; MT - mutant

Table 3.2: Instruments and chemicals for mouse genotyping

Instruments	
Thermomixer comfort 1,5 ml	Eppendorf, Germany

Centrifuge 5415 D	Eppendorf, Germany
Peltier Thermal Cycler 200	Bio-Rad, USA
FUSION SL Gel Chemiluminescence Documentation System	Peqlab (VWR), Germany
PerfectBlue Gel System Midi S	Peqlab (VWR), Germany
Peqlab peqPOWER 300	Peqlab (VWR), Germany
Chemicals	
Quick Extract®, Quick Extraction Buffer	Biozym Scientific GmbH, Germany
Taq DNA Polymerase	Thermo Fisher Scientific, USA
PCR Nucleotide Mix	Roche, Switzerland
10x CoralLoad PCR Buffer	Roche, Switzerland
Water PCR Grade	Roche, Switzerland
Gene Ruler 100 bp Plus DNA Ladder	Thermo Fisher Scientific, USA
LE Agarose	Biozym, Germany
Ethidium bromide solution	Sigma-Aldrich, USA
TAE buffer solution:	
- 40mM Tris-Acetat	Carl Roth, Germany
- 1mM EDTA-HCl (pH 8.0)	Sigma-Aldrich, USA

3.5. Body weight measurements and grip strength testing

Body weight measurements were conducted throughout the animals' entire postnatal development until their euthanisation date. During their first two weeks of life, animals weighed every two days and later once every two weeks. Just before euthanisation, a grip strength test was performed using a grip strength metre (Panlab, Spain) with a grid attachment. The mice were held by the tail, put onto the grid, and then pulled with increasing intensity until they lost their grip. This procedure was repeated three times. The grip strength metre displayed the maximum value in gram. For each animal the maximum value was utilised for further analysis.

3.6. Muscle dissection, shock-freezing and cryo-sectioning

The mice were euthanised for muscle dissection at the age of around 3.5 months (100 days) by cervical dislocation. Directly afterwards, the body weight of each mice was measured. Then, animals were skinned, and the thorax was opened. Next, the heart and major blood vessels were

incised and blood samples of approximately 500 µl were collected from the thoracic cave. Subsequently, major lower limb muscles were dissected. These include the tibialis anterior (TA), triceps surae (TS) and quadriceps femoris (QF) muscle. TA and TS were resected along with adjacent proximal and distal tendon. However, QF was cut off at the proximal insertion site as close to the pelvic bone as possible, while distal preparation was carried out taking along the QF tendon. After excision each muscle was weighed. Left hindlimb muscles were shock frozen in liquid nitrogen and stored in -80°C until using them for RNA isolation. The right hindlimb muscles were also dissected and weighed but put in plastic cups covered in Tissue-Tek® O.C.T. Compound, frozen in nitrogen cooled isopentane and stored at -80°C until cryo-sectioning.

For cryo-sectioning the samples were transferred to -20°C two days before sectioning and left over night to provide a less brittle consistence to cut with fewer damage to the sections. The Tissue-Tek®-imbedded muscle samples were then cut in a Cryostar NX50™ (Thermo Scientific, USA). The muscle samples were cross sectioned at a thickness of 12 µm and collected on glass slides. Three slices were collected per slides and stored at -20°C until further use.

Table 3.3 Materials for muscle dissection, weighing and shock-freezing

Materials	
Eppendorf tube	Eppendorf AG, Germany
Parafilm®	Sigma-Aldrich, USA
Tissue-Tek® Cryomolds	Sakura Finetek Germany GmbH, Germany
Tissue-Tek® O.C.T. Compound	Sakura Finetek Germany GmbH, Germany

3.7. Immunohistochemical staining and image acquisition

For immunohistochemical staining, the slides were thawed at room temperature for 15 minutes. Then, they were placed in a plastic cuvette filled with citric buffer (pH: 6.0), which was heated before for around one minute in a microwave at 1000 W, which was stopped as soon as the solution started to boil. After one minute rest, it was reheated again until boiling, which took around 10 seconds. Next, the slides were washed in phosphate buffered saline (PBS). After taking the slides out of PBS, the samples were encircled with a PAP pen (Kisker Biotech, Germany), creating a hydrophobic barrier to reduce the required volumes. Subsequently, 100 µl of 0.1% Triton X-100 in PBS (PBS-T) enriched with 4% mouse Ig Blocking reagent (Vector Laboratories, USA) was applied to the sections and left for one hour at room temperature. After that, the slides were washed in PBS-T, three times for three minutes and PBS-T enriched with 1% bovine serum albumin (BSA) was put onto the slides for one hour at room temperature. Subsequently, the primary antibody solution (1:50 in PBS-T + 1% BSA) was pipetted onto the slides and left overnight at 4°C (Table 3.4).

On the next day, the slides were washed in PBS-T three times, followed by applying the secondary antibody solution (1:250 in PBS-T + 1% BSA) was applied for 45 minutes at 37°C. After the secondary antibody incubation, the sections were washed in PBS for 2 minutes, counterstained with DAPI, and washed in PBS again. Finally, the sections were covered with Fluorshield™ histology mounting medium and carefully covered with glass coverslips.

The stained sections were imaged with an Axio Observer Z1 (Zeiss, Germany) fluorescence microscope. The imaging was conducted via ZEN software (Zen Blue, Version 2.3, Zeiss, Germany), which controls a tile-scanning application. The tiles were manually adapted to feature the samples *in toto*. The image acquisition was carried out in one sequential run through for each fluorescence channel before the next channel would follow. Subsequently, the acquired (original) data were saved separately for each channel until further processing for the quantification procedures. This is described in section 3.11 below.

Table 3.4. Chemicals and antibodies for immunohistochemical staining

Materials	
Triton X-100	Sigma-Aldrich, USA
Phosphate buffered saline (PBS)	Thermo Fisher Scientific, USA
PAP pen	Kicker Biotech, Germany
Mouse Ig Blocking Reagent	Vector Laboratories, USA
Bovine serum albumin (BSA)	Carl Roth, Germany
4’,6-Diamindin-2-phenylindol (DAPI)	Sigma-Aldrich, USA
Fluorshield™ histology mounting medium	Sigma-Aldrich, USA
Primary antibodies	
BA-D5, against MYH 7/ fibre type I (0.46 mg/mL)	DSHB, USA
SC71, against MYH 2/ fibre type IIA (0.48 mg/mL)	DSHB, USA
BF-F3, against MYH 4/ type IIB (0.42 mg/mL)	DSHB, USA
ab11575, against laminin 1 (0.65 mg/mL)	Abcam, UK
Secondary antibodies	
Alexa488-conjugated IgG (2 mg/mL)	Thermo Fisher Scientific, USA
Alexa568-conjugated IgM (2 mg/mL)	Thermo Fisher Scientific, USA
Alexa647-conjugated anti-rabbit (2 mg/mL)	Thermo Fisher Scientific, USA

The primary antibodies were selected to target MyHC isoforms to distinguish myofibre types and laminin to stain the myofibres' basal lamina. Both, anti-MYH7 (BA-D5) and anti-MYH2 (SC-71) are of antibody subtype 'IgG'. Anti-MYH4 (BF-F3) on the other hand is an IgM antibody. Therefore, two sample slides were stained per muscle. One sample was incubated with a combination of antibodies against MYH7 (type I myofibres), MYH4 (IIB myofibres) and laminin. Another sample was incubated with antibodies against MYH2 (type IIA myofibres), MYH4 (IIB myofibres) and laminin.

3.8. Myostatin (GDF-8) ELISA from murine blood samples

The blood samples acquired after euthanisation of the mice as described in section 3.6, were brought to room temperature before starting the assay. Meanwhile, the diluents were prepared as required by the manufacturer (R&D Systems, USA), including the standard stocks, which ranged from 0 to 2000 pg/mL. Afterwards, the diluents were brought onto the 96 well plate and the absorption measurements was performed using a Multiscan™ FC Microplane Photometer (Thermo Fisher Scientific, USA).

3.9. Skeletal muscle RNA sequencing

RNA sequencing was performed using QF muscles, which were dissected from 3.5 months old mice, shock-frozen in liquid nitrogen and stored at -80°C, as described above. The samples were taken out and 1 ml Trizol was added to each tube. In order to provide clear mRNA samples, the major part of cellular RNA, which is ribosomal RNA (rRNA) needs to be depleted, using standardised rRNA depletion kits. RNA was isolated following a standard protocol, RNA quality was measured with a BioAnalyzer (Agilent, USA) and libraries for sequencing were prepared with a SENSE mRNA-Seq Library Prep Kit V2 (Lexogen, Austria). All libraries were sequenced on a HiSeq1500 device (Illumina, USA) with a read length of 50 bp and a sequencing depth of approximately 20 million reads. After demultiplexing, reads were aligned to the murine reference genome (version GRCH38.92) with STAR (Dobin *et al.*, 2013). Differential gene expression analysis was performed using DESeq2 (Love *et al.*, 2014) and an adjusted p-value of less than 0.05 was set to determine significant changed genes between homozygous mutant and wildtype controls.

3.10. Quantification procedures

The evaluation of images gained from experiments was conducted using the Fiji software (Schindelin *et al.*, 2012), Adobe Illustrator and Photoshop. Images of each group were chosen by a random generator.

3.11. MuscleJ analysis

The cross-section images of lower limb muscles were acquired via *ZEN* 2.3 software. Each of the four channels was saved separately since the following image processing and analysis required

separate images per channel. In the next step, the software's stitching function was applied to the original tile images to gain properly merged pictures. These were then exported as uncompressed TIFF data.

Table 3.5 Fluorescence imaging of skeletal muscle cross sections

Cross section image I	**Cross section image II**
DAPI (350nm)	DAPI (350nm)
Type I (488nm)	Type IIA (488nm)
Type IIB (568nm)	Type IIB (568nm)
Laminin (647nm)	Laminin (647nm)

As table 3.5 shows, of every mouse two consecutive cross sections were immunohistochemically stained and visualised in four separate images. Due to the primary antibody combinations they displayed DAPI, laminin, Type IIB fibres, and Type I or Type IIA fibres, respectively. The *TIFF*-file images were processed using ImageJ. The image analysis was carried out with the ImageJ plugin called MuscleJ (Mayeuf-Louchart *et al.*, 2018). This plugin measures total cross-sectional area (CSA), single fibre CSA, detects each fibres nuclei based on location (peripheral or central location within the fibre) and identifies myofibre types, based on immunohistochemical staining of MyHC subtypes. Additionally, it categorises non-stained fibres as type IIX. Resulting data of each cross section were available in the assigned folder as *txt-data* and could simply be transferred into an *Excel*-file for further analysis.

3.11.1. Statistics and data visualisation

The raw data were transferred to Excel (Microsoft Corporation. (2018). *Microsoft Excel*. Retrieved from https://office.microsoft.com/excel). Statistical significance was analysed using RStudio (RStudio Team, version 1.3.1093 (2020). RStudio: Integrated Development Environment for R. RStudio, PBC, Boston, MA URL http://www.rstudio.com/). Quantitative data were acquired by repeating every experimental setup at least three times independently and in duplicates or triplicates. For data processing, analysis and visualisation packages listed in Table 3.6 were utilised.

Table 3.6: Data processing, analysis and visualisation packages used in R

R package name	**Citation**
tidyr (version 1.2.0)	Hadley Wickham (2020). tidyr: Tidy Messy Data. R package version 1.1.2. https://CRAN.R-project.org/package=tidyr

dplyr (version 1.0.1)	Hadley Wickham, Romain François, Lionel Henry and Kirill Müller (2020). dplyr: A Grammar of Data Manipulation. R package version 1.0.2. https://CRAN.R-project.org/package=dplyr
ggplot2 (version 3.3.2)	H. Wickham. ggplot2: Elegant Graphics for Data Analysis. Springer-Verlag New York, 2016.

The data visualisation shows the mean values ± standard deviation. The test for normality was performed by using the Shapiro-Wilk as well as testing for equal variances of the statistical population by using the Levene-test. One-way-ANOVA or Kruskal-Wallis-test was carried out to test for statistical significance. Each figure displaying visualised data states the applied test in the description. In this process a p-value of 0.05 was considered statistically significant.

4. Results

4.1. Behaviour and phenotype

Naturally, it was not possible to assign each mouse to a genotype and track their body weight or physical appearance until earmarks were set after three weeks of age. Apart from that no behavioural abnormalities could be observed during animal husbandry concerning activity, feeding, interaction with littermates, and danger response. During dissection it was noticed that a few (n = 2) homozygous mutant mice had an apparent increase in subcutaneous fat tissue (see Figure 4.1). Nevertheless, this observation was inconsistent since other mutant mice were not affected.

Figure 4.1: Skinned homozygous mutant male mice.
The images show a male homozygous mutant mouse (*Rosa26Mstn$^{fl/fl}$;Acta1-Cre^{+}*) on the left and a male mouse of the control group (*Rosa26Mstn$^{fl/+}$;Acta1-Cre^{-}*) on the right after euthanisation and skinning. In comparison there appears to be a possible increment of subcutaneous fat tissue (red arrows).

4.2. Attenuated weight gain in *Mstn* over-expressing mice but no significant difference in overall body weight

Comparison of homozygous and heterozygous mutants with the control group showed a slightly attenuated weight gain over the 3.5 months of development in both female and male (see Figure 4.2). The difference was more distinct in homozygous mutant mice. In female mice the bodyweight data show a similar tendency with a small attenuation of weight gain in homozygous mutant, when compared to controls. The difference between heterozygous and controls is smaller.

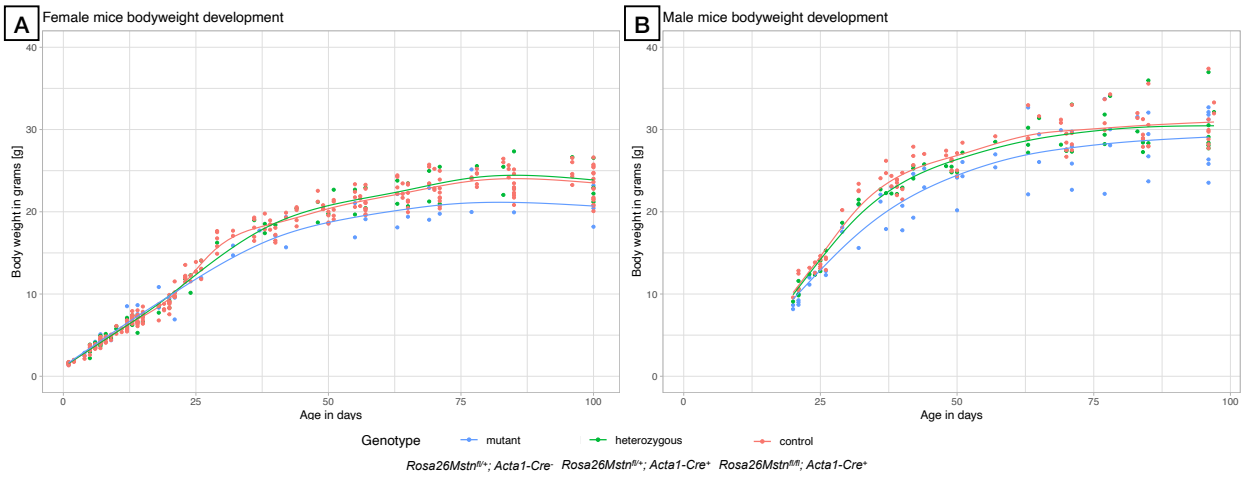

Figure 4.2: Body weight development of female and male mice.
Body weight development was recorded until date of euthanisation at 3.5 months (100 days). Both in female and male a slightly attenuated weight gain in homozygous and heterozygous in comparison to control animals was detected. Female mice: control n = 16; heterozygous n = 4; homozygous mutant n = 3. Male mice: control n = 9; heterozygous n = 8; homozygous mutant n = 7.

Mean bodyweight in female mice at 3.5 months showed no significant difference (see Figure 4.3 A). Homozygous mice were 10% lighter (20.60 ± 2.51 g), while heterozygous were 1.4% heavier (23.22 ± 2.33 g), when compared to controls (22.89 ± 2.24 g). In 3.5 months old male mice no significant difference was found as well (see Figure 4.3, B). Homozygous were 4.4% (29.43 ± 4.11 g) and heterozygous 1.2% lighter (30.41 ± 3.28 g), when compared to controls (30.80 ± 2.72 g).

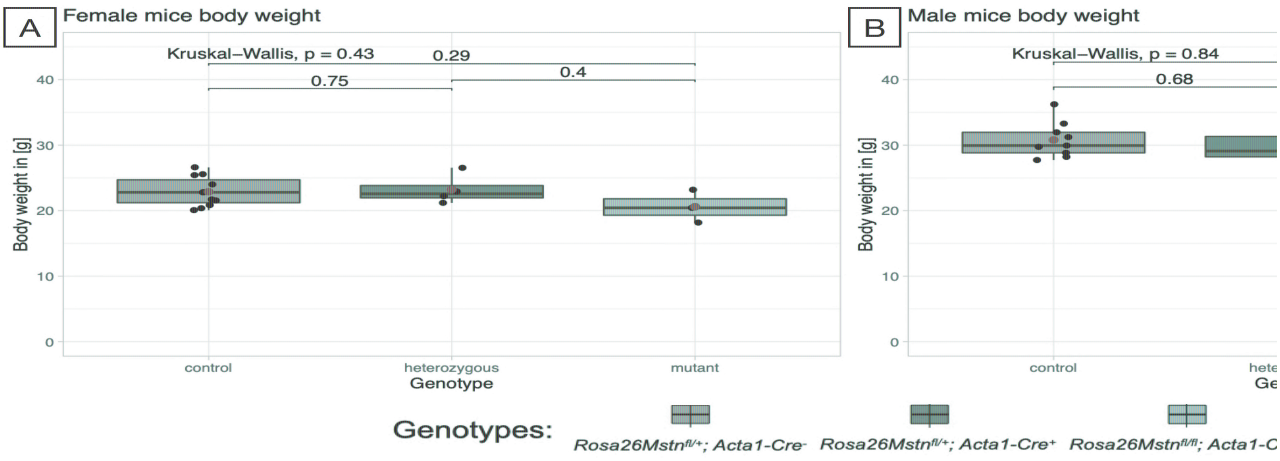

Figure 4.3: Body weight of female and male mice in grams at 3.5 months.
Analysis using the Kruskal-Wallis test revealed no significant difference (p = 0.43) in bodyweight at 3.5 months old female mice (control n = 3, heterozygous n = 4, homozygous mutant n = 10; A). In 3.5 months old male mice analysis showed no significant difference as well (p = 0.68, control n = 9, heterozygous n = 8, homozygous n = 7; B). Data represents the median (black line) & mean (red dot).

4.3. *Mstn* over-expression leads to decreased lower limb muscle weight in 3.5-month-old mice

Mstn over-expression was hypothesised to lead to a decrease in muscle weight. Therefore, lower limb muscles were dissected and weighed. In female homozygous mutant mice, data analysis revealed a significant decrease in muscle weight by 19.2% in QF (p = 0.022), 21.3% in TA (p = 0.038) and 27% in TS (p = 0.011), when compared to heterozygous and controls, whereas no significant difference was detectable between heterozygous and controls (see Figure 4.4). The exact data is listed in the appendix (see Table 7.2).

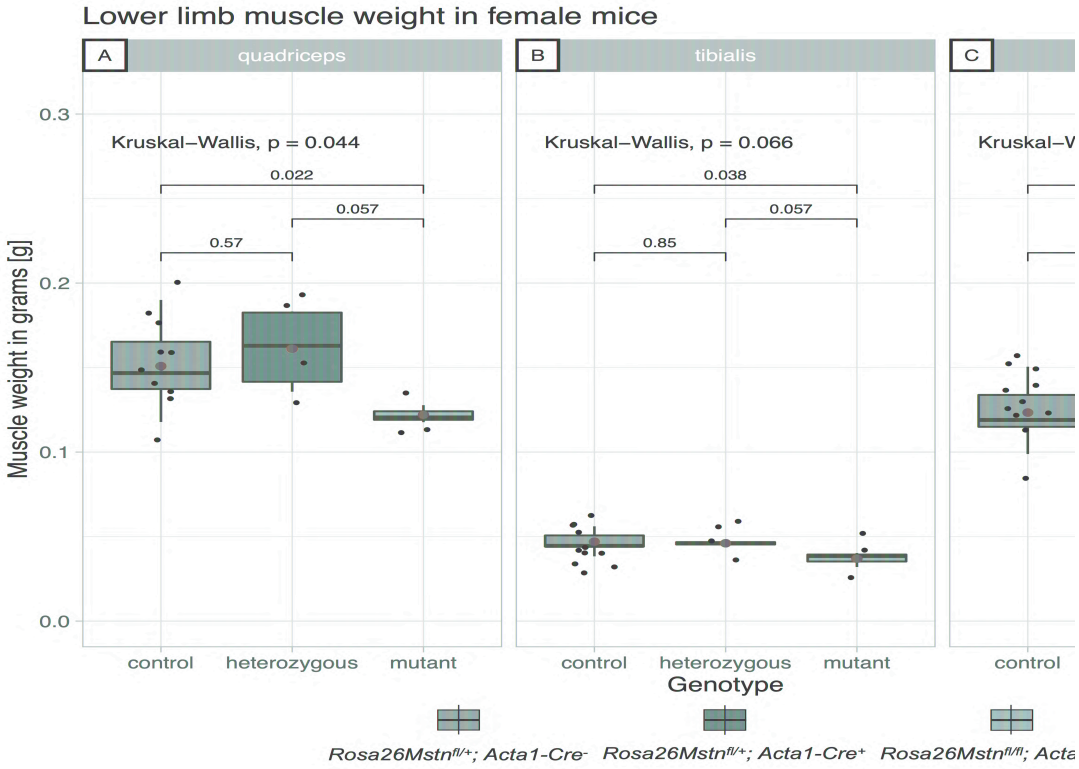

Figure 4.4: Skeletal muscle weight of female mice's lower limb muscles.
Analysis of skeletal muscle weight of 3.5 months old female mice showed a significantly lower relative muscle weight in QF, TA, and TS muscles in homozygous *Mstn* over-expressing mice (n = 3) compared to heterozygous (n = 4) and controls (n = 10). Data represents the median (black line) & mean (red dot).

Male homozygous mice showed a significant decrease in muscle weight by 34.1% in QF (p = 0.029), 37.7% in TA (p = 0.029) and 26.9% in TS (p = 0.029), when compared to heterozygous and controls, whereas no significant difference occurred between heterozygous and controls (see Figure 4.5). Exact data is listed in the appendix (see Table 7.3).

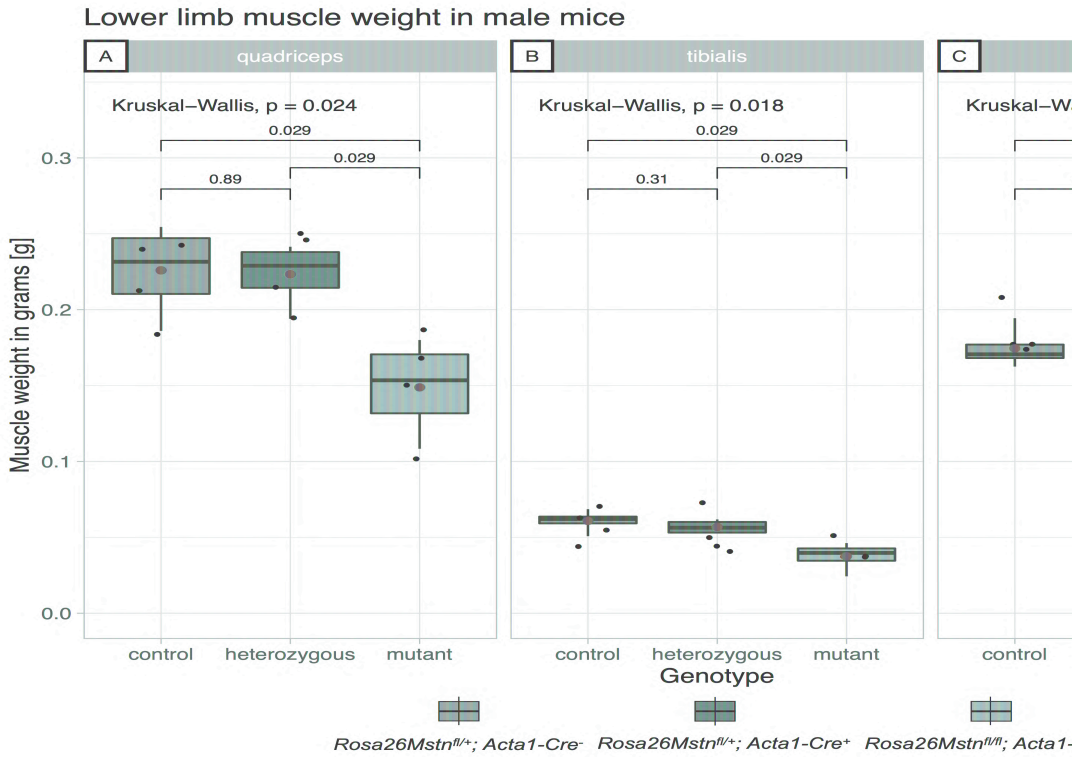

Figure 4.5: Skeletal muscle weight of lower limb muscles in male mice.
Analysis of skeletal muscle weight of 3.5 months old mice showed a significantly lower relative muscle weight in QF, TA and TS muscles in homozygous mutant mice (n = 4), when compared to heterozygous (n = 4) and controls (n = 4). Data represents the median (black line) & mean (red dot).

Bodyweight analysis did not reveal any significant impact by *Mstn* over-expression. Still, body composition might be affected, so that small differences in overall bodyweight could lead to differences in skeletal muscle weight. To eradicate that influence, lower limb muscle weight was analysed in relation to overall bodyweight, referred to as ‘relative muscle weight’. Surprisingly, in female mice analysis showed no significant difference in relative muscle weight between homozygous mutant, heterozygous and controls (see Figure 7.1). In male mice, on the other hand, analysis showed a significant weight reduction of all lower limb muscles in relation to overall bodyweight, when comparing homozygous mutant with either heterozygous or controls (see Figure 7.2). The greatest change of relative muscle weight was seen in QF muscle. Each QF muscle (in relation to total body weight) was 33% lighter in homozygous mutant and 2.3% heavier in heterozygous, in comparison to controls (p = 0.021). The total of lower limb muscles accounted for around 2.1% of bodyweight in homozygous mutant and around 3.0% in heterozygous and controls (Kruskal-Wallis: p = 0.023).

4.4. MSTN blood levels show no significant difference between *Mstn* over-expressing mice and controls

Enzyme-linked immunosorbent assay (ELISA) was used to determine the amount of MSTN circulating within the blood. Analysis revealed no significant difference between the groups (see Figure 4.6). In male mice mean blood concentration of MSTN (GDF-8) was 48.87 ± 7.29 pg/µL in homozygous, 70.71 ± 13.61 pg/µL in heterozygous and 68.11 ± 16.34 pg/µL in controls. In female mice MSTN serum level was 53.98 ± 14.28 pg/µL in homozygous, 50.40 ± 8.09 pg/µL in heterozygous and 37.43 ± 10.51 pg/µL in controls.

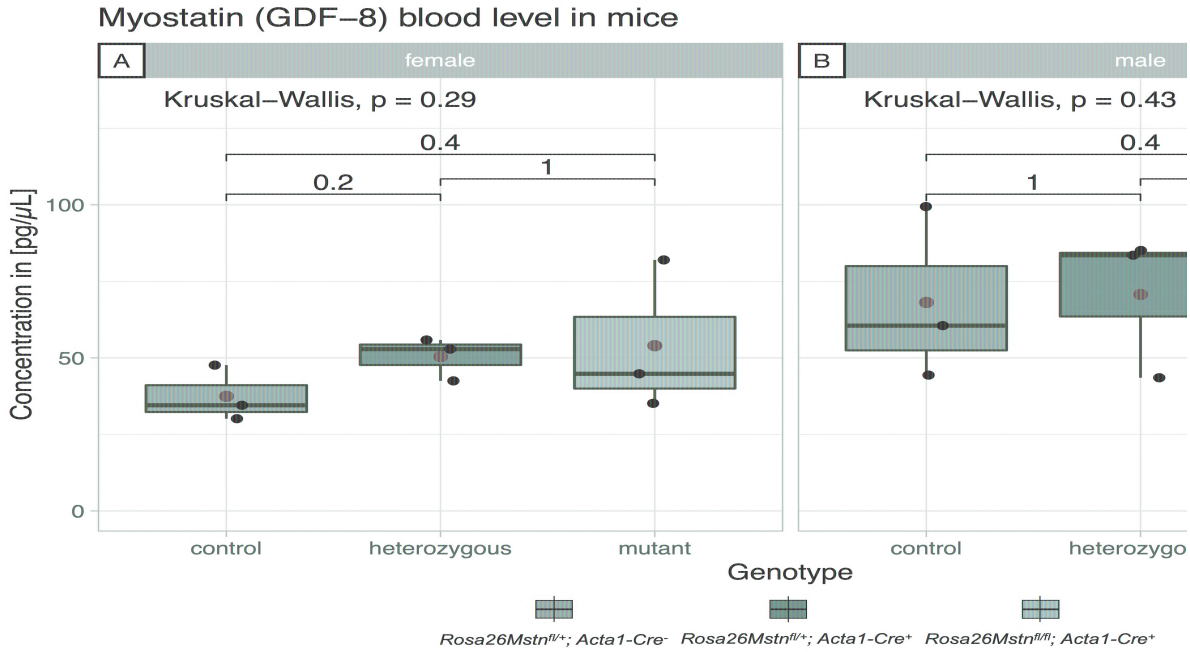

Figure 4.6: Myostatin (GFD-8) ELISA reveals no significant difference.
MSTN (GDF-8)-ELISA of female mice show no significant difference in MSTN blood concentration (p = 0.43). In male mice there was no significant difference as well (p = 0.29). For all genotypes: n = 3. Data represents the median (black line) & mean (red dot).

4.5. No significant changes of myofibre CSA in *Mstn* over-expressing male mice

Both female and male mice showed a significant reduction in lower limb muscle weight (section 4.3). However, muscle weight in relation to bodyweight was not significantly affected in female mice but in male. Since muscle mass is higher in male mice, possible effects of *Mstn* over-expression might be more noticeable. Therefore, only male mice were used for following analyses. Evaluating single myofibre cross sectional area (CSA) revealed a non-significant 11.1% reduction in homozygous mutant TA muscle, when compared to controls. In heterozygous, on the other hand, there was a nearly 6.2% increase, in comparison to controls, but without statistical

significance as well. The same accounts for the 15.3% difference in myofibre size between homozygous and heterozygous male mice (Figure 4.7 and 4.8). Additionally, whole muscle CSA was analysed in TA muscles (see Figure 7.3). In homozygous mutant whole muscle CSA showed a 22%-decrease (3.9 ± 1.8 x 10^6 µm^2), while heterozygous had a 2%-decrease (5.1 ± 1.1 x 10^6 µm^2), when compared to controls (5.0 ± 1.7 x 10^6 µm^2) in controls. Analysis showed that these differences were not significant as well (Kruskal-Wallis test: $p = 0.16$).

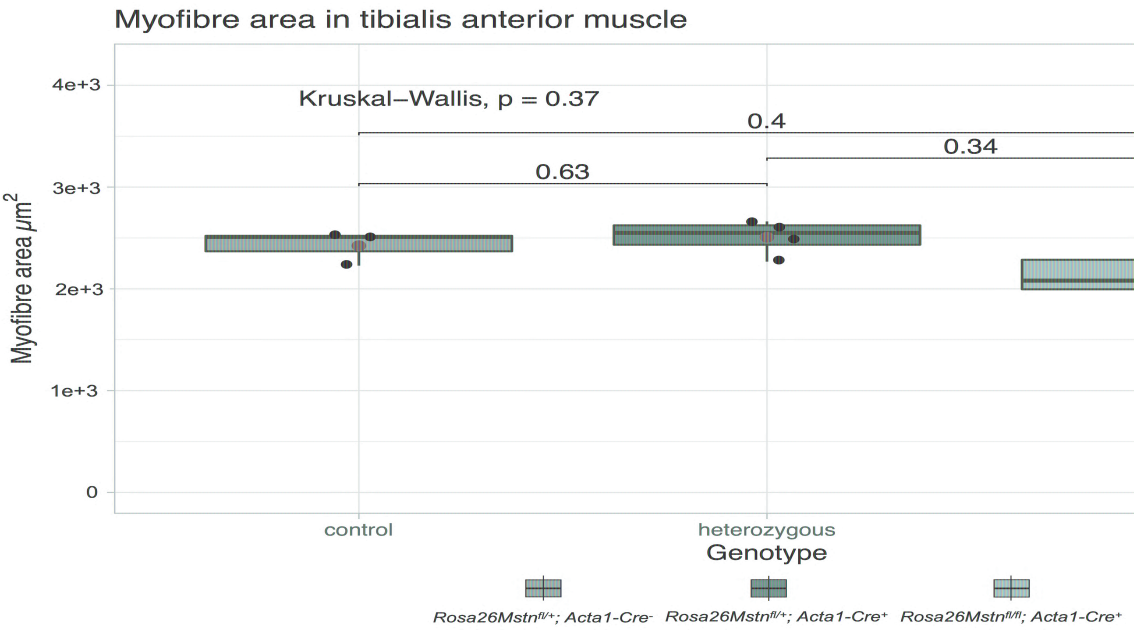

Figure 4.7: Myofibre area of TA muscle in male mice.

The figure shows the mean myofibre CSA in TA muscle of 3.5 months old male mice. Mean CSA in homozygous mutant (n = 4), heterozygous (n = 4), and controls (n = 3) showed no significant differences ($p > 0.05$ for all comparisons, mean ± SD). Data represents the median (black line) & mean (red dot).

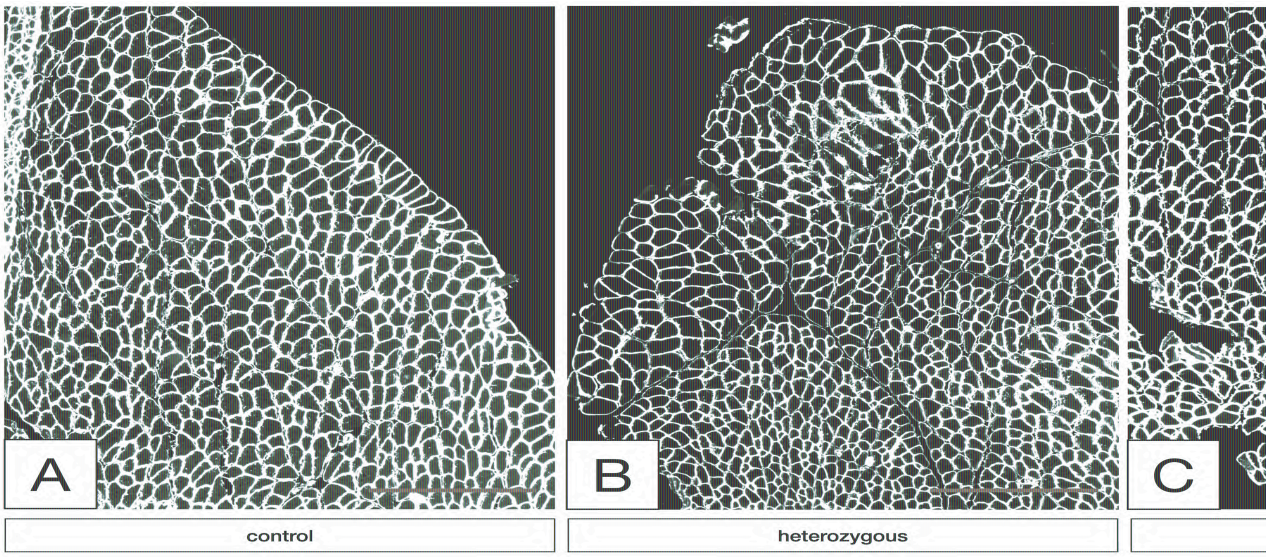

Figure 4.8: Myofibre CSA in TA muscle.

The images display random fields-of-view in TA muscle stained against laminin, which highlights the basal lamina. Concurring with the analysis results control (A), heterozygous (B), and homozygous (C) mice do not show any obvious differences in myofibre CSA. The scale of 500 µm highlighted in red accounts for both images.

In 3.5 months old mice TS muscle myofibre CSA was reduced by 13.6% in homozygous mutants (1.9 ± 1.1 x 10^3 µm^2), and 4.5% increased in heterozygous (2.3 ± 1.2 x 10^3 µm^2), when compared to controls (2.2 ± 1.1 10^3 µm^2). All differences were not statistically significant (p = 0.52, see Figure 4.13).

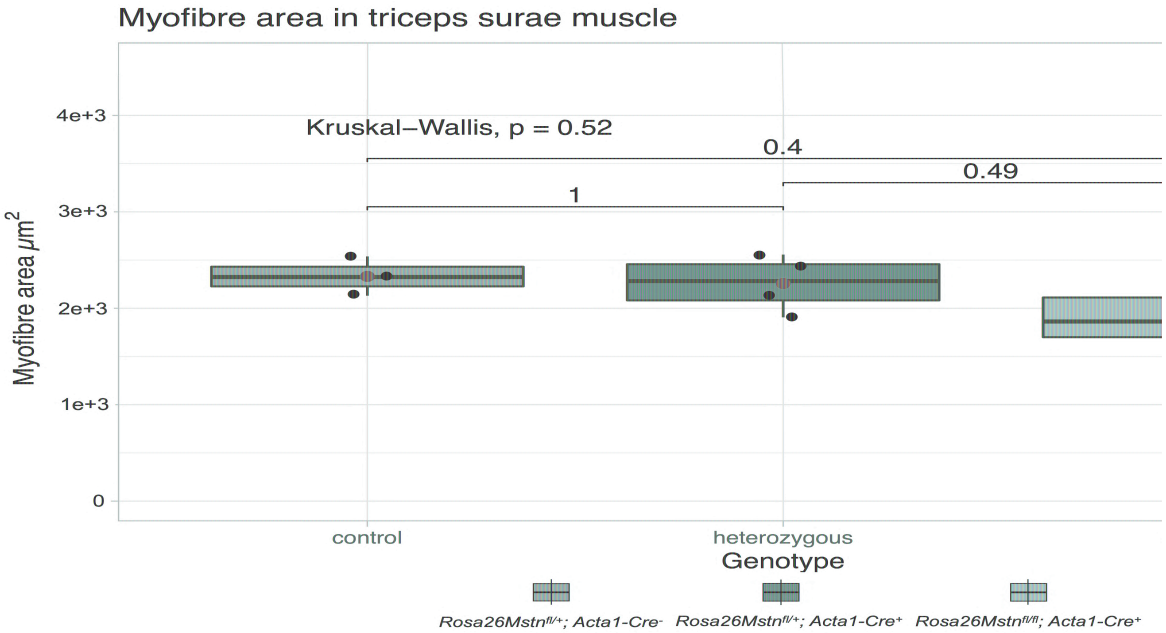

Figure 4.9: Myofibre area (CSA) of TS muscle in male mice.

The figure shows mean myofibre CSA in TS muscle of 3.5 months old male mice. Mean CSA in homozygous mutant (n = 4), heterozygous (n = 4), and controls (n = 3) showed no significant differences (p > 0.05 for all comparisons, mean ± SD). Data represents the median (black line) & mean (red dot).

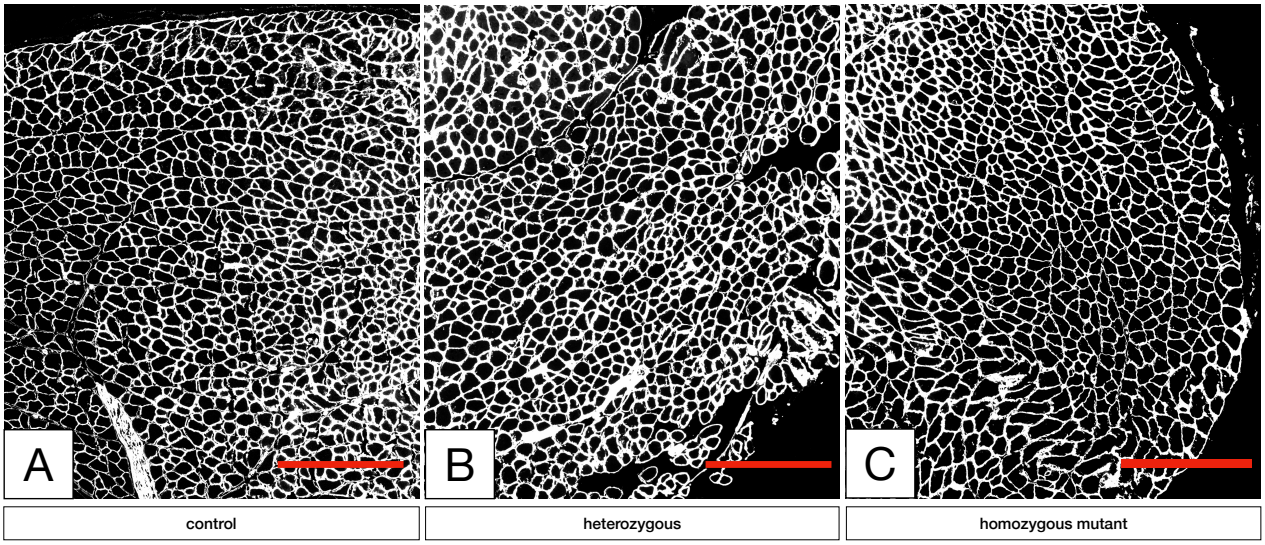

Figure 4.10: Comparison of myofibre CSA in TS muscle.
The images display random fields-of-view in cross sections of TS muscle stained against laminin, which highlights the basal lamina. Control (A), heterozygous (B), and homozygous (C) mice do not show any obvious differences in myofibre CSA. The red scale of 500 µm displayed in C accounts for all images.

4.6. Myofibre type composition in lower limb muscle

To evaluate possible influences of *Mstn* over-expression on myofibre type composition, myofibre number per cross section (slices thickness: 12 µm) was determined in both TA and TS muscle (data not shown). In controls 2.1 ± 0.7 x 10^3 myofibres were counted per cross section, 2.0 ± 0.4 x 10^3 in heterozygous and 1.8 ± 0.8 x 10^3 in homozygous *Mstn* over-expressing mice. In TS muscle controls 3.5 ± 1.8 x 10^3 myofibres were counted per cross section, 3.1 ± 1.3 x 10^3 in heterozygous and 3.6 ± 0.6 x 10^3 in homozygous *Mstn* over-expressing mice ($p > 0.05$ for all comparisons). Analysis of TA muscle myofibre type composition in 3.5 months old mice revealed no significant difference in homozygous mutant and heterozygous, when compared to controls (see Figure 4.11). Expectedly, MYH7-positive fibres (type I) are merely present in TA muscle with 0.7 ± 0.7% in homozygous as well as heterozygous, and 1.1 ± 1.5% in control mice (see Figure 4.11, A). In TA muscle, fibres positive for MYH4 (type IIB) are the most frequently found myofibre type (see Figure 4.11, C) with 48.0 ± 8.5% in homozygous, 48.5 ± 17.3% in heterozygous and 58.2 ± 15.2% in controls. Type IIA (MYH2) myofibres in TA account for 8.1 ± 0.9% in homozygous, 8.7 ± 5.5% in heterozygous and 5.3 ± 3.4% in control mice. Even though this displays a 53%-increase of the proportion of type IIA in homozygous when compared to controls (see Figure 4.11, B), this difference was not significant as well.

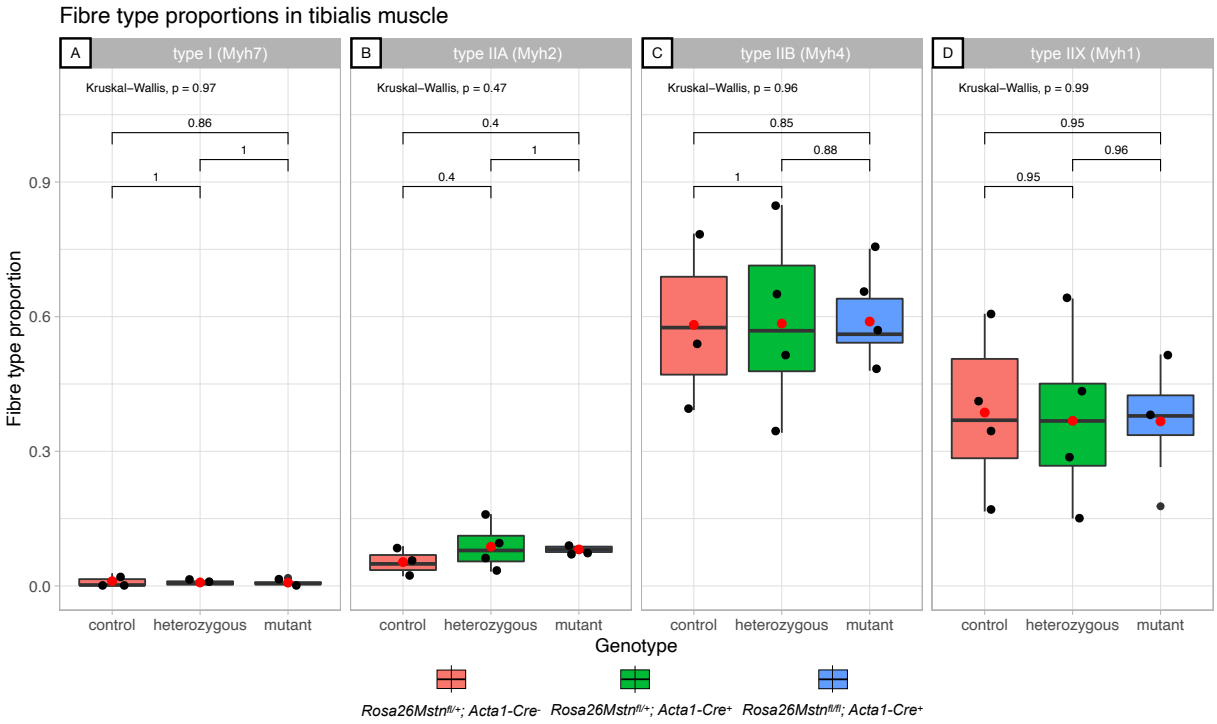

Figure 4.11: Proportion of myofibre types in TA muscle.

The figure shows proportions of each myofibre type found within all myofibres of a TA muscle cross section of 3.5 months old male mice. There was no significant difference, when homozygous mutant (n = 4) and heterozygous (n = 4) were compared to controls (n = 3), $p > 0.05$ for all comparisons. Data represents the median (black line) & mean (red dot).

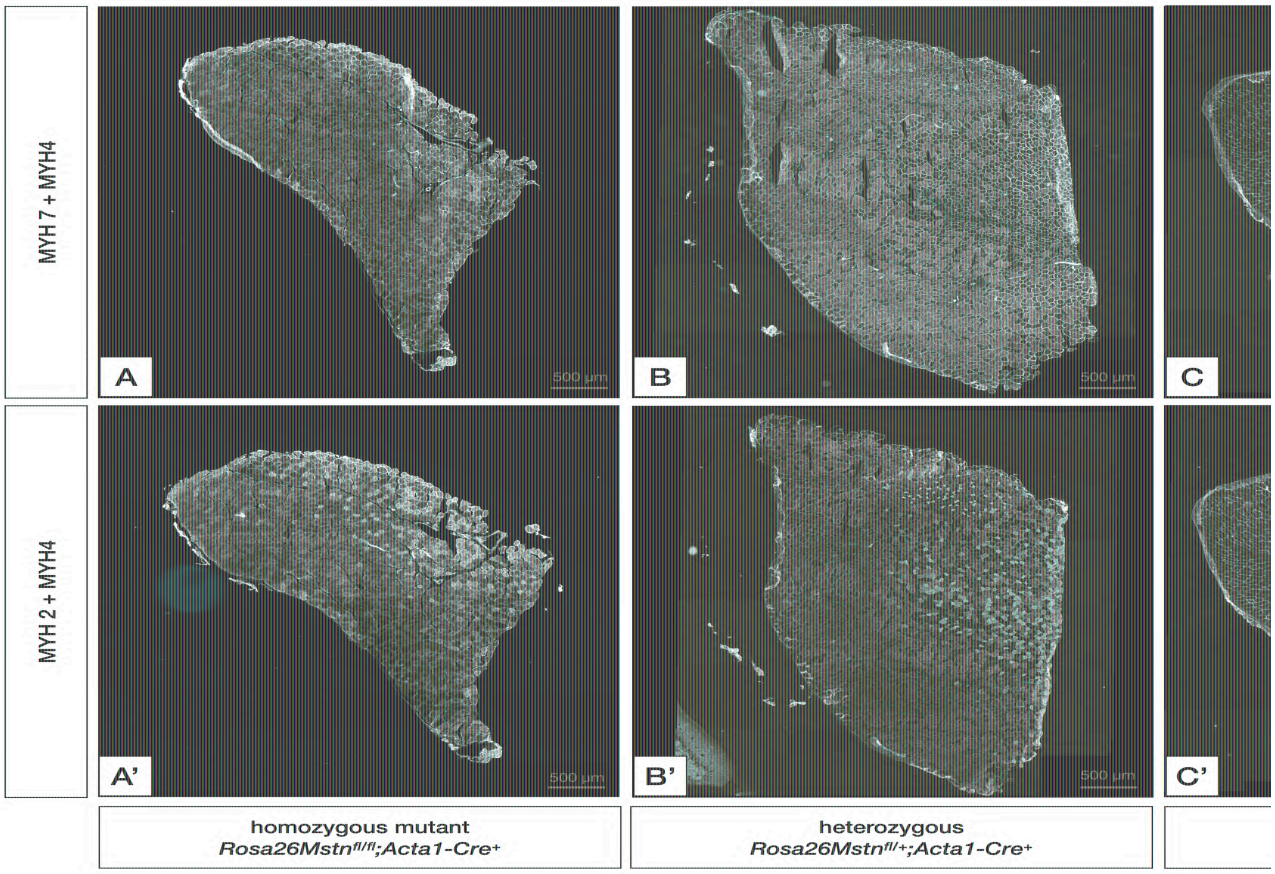

Figure 4.12: Myofibre type composition in TA muscle.
The images show immunohistochemically labeled consecutive cross sections of TA muscle of 3.5 months old male mouse. Only few MYH7-positive myofibres (type I, green) are found in homozygous mutant (A), heterozygous (B) and in controls (C). Higher amounts of myofibres positive for MYH2 (type IIA, green) are visible in all genotypes (A' - C'), without significant differences. MYH4-positive myofibres (type IIB, red), laminin (white), nuclei (blue). Slice thickness: 12 µm.

Analysis of myofibre type proportions in TS muscle revealed no significant difference between the genotypes (see Figure 4.13 and 4.14). MYH7-positive fibres (type I) account for the smallest proportion of myofibres in TS muscle, with 3.1 ± 1.5% in homozygous, 2.6 ± 1.5% in heterozygous, and 5.2 ± 4.6% in control mice (see Figure 4.13, A). The proportion of MYH7-positive fibres is thereby 40% lower in comparison to controls. MYH4-positive (type IIB) fibres make up the largest proportion of myofibres (see Figure 4.13, C) with 54 ± 20% in homozygous, 48 ± 9% in controls and 33 ± 15% in heterozygous. MYH2-positive (type IIA) myofibres in TS account for 14.8 ± 4.3% in homozygous, 15.4 ± 2.2% in heterozygous and 17 ± 3.6% in control mice (see Figure 4.13, B), which is 13% lower in homozygous when compared with controls.
When comparing myofibre type distribution in TS cross sections, a clear pattern within the muscle can be seen, which appears similar across genotypes (see Figure 4.14). Type I fibres are found in the medial and lateral profound muscle compartments. Type IIA myofibres show a similar distribution pattern clustering in the profound muscle compartments (see Figure 4.12 and 4.14). This appears to be similar across genotypes.

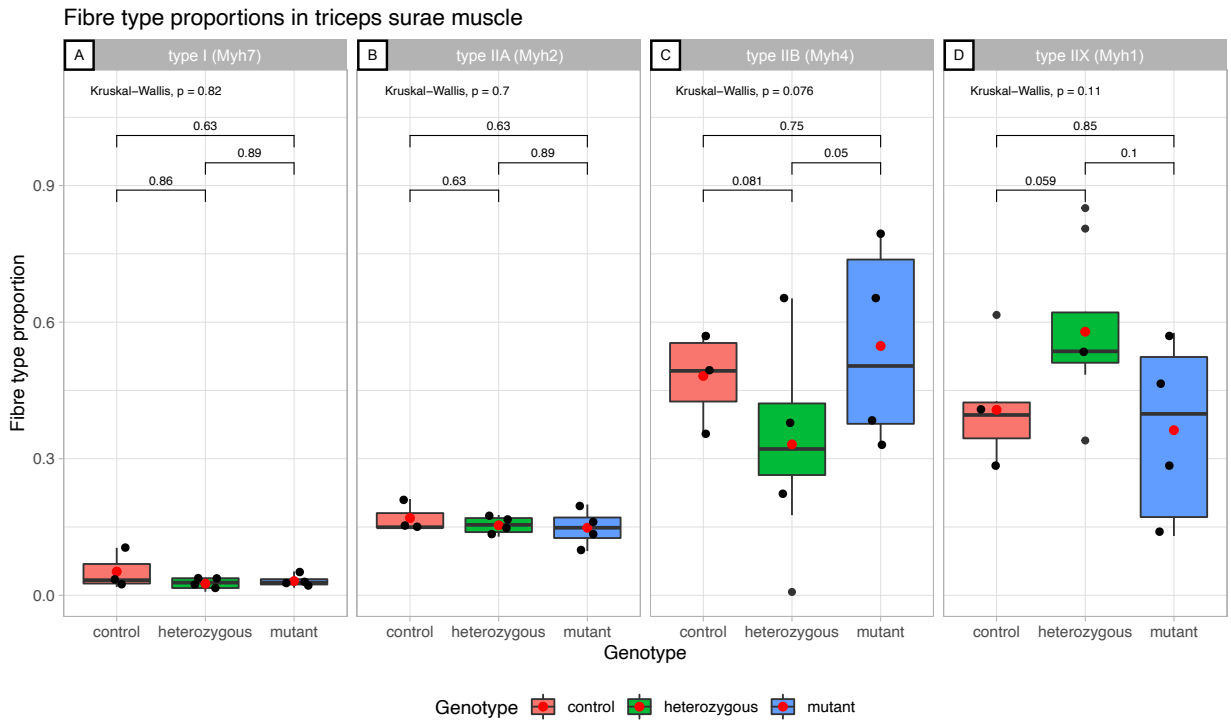

Figure 4.13: Proportion of myofibre types in TS muscle.

The figure shows the proportion of each myofibre type within all detected myofibres in the cross section of TS muscle in 3.5 months old male mice. Analysis revealed no significant difference between homozygous mutant (n = 4), heterozygous (n = 4) and controls (n = 3), $p > 0.05$ for all comparisons. Data represents the median (black line) & mean (red dot).

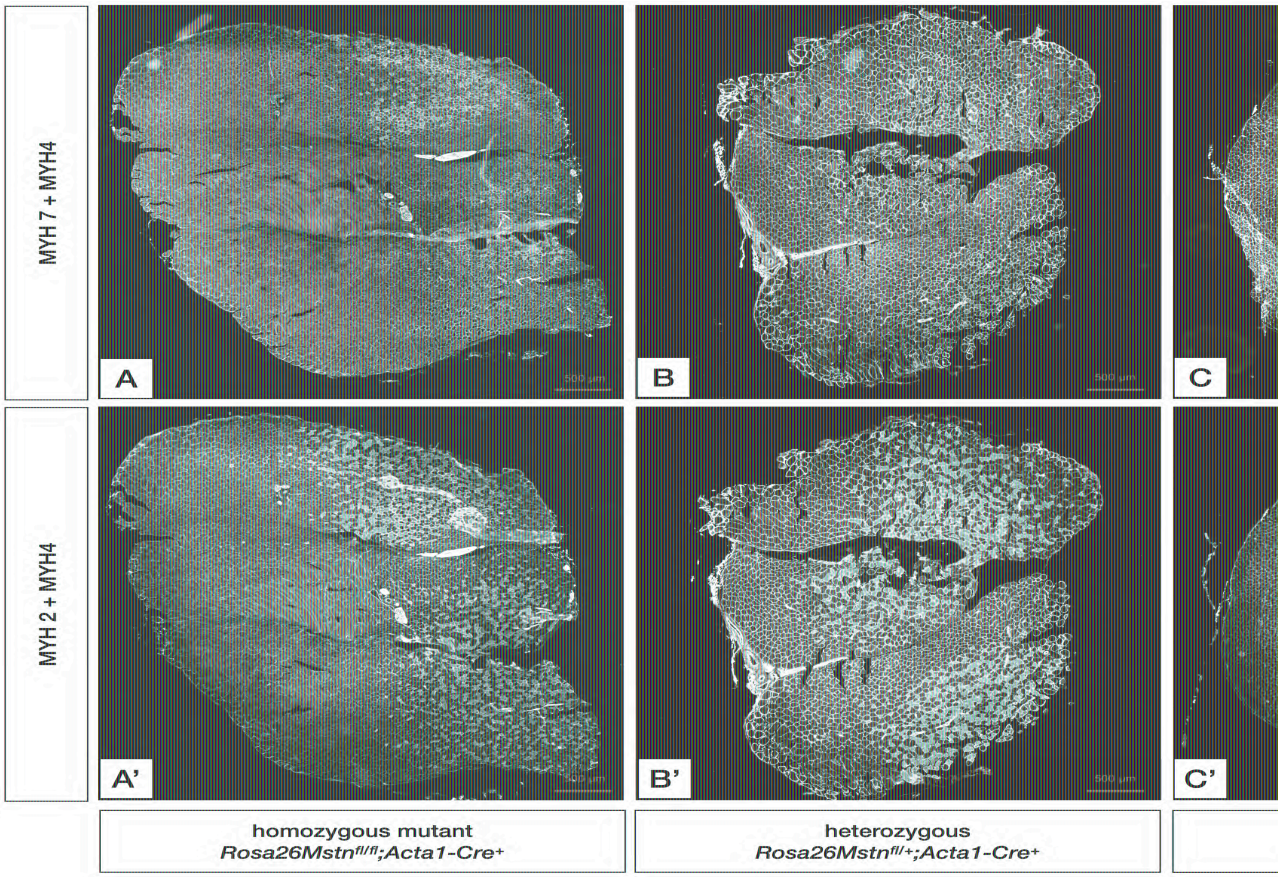

Figure 4.14: Myofibre type composition in TS muscle.

The images show immunohistochemically labeled consecutive cross sections of TS muscle of 3.5 months old male mouse. Similar amounts of MYH7-positive myofibres (type I, green) are found in homozygous mutant (A), heterozygous (B) and in controls (C) within the medial and lateral muscle compartments. Higher amounts of myofibres positive for MYH2 (type IIA, green) are visible in all genotypes (A' - C'), without significant differences. MYH4-positive (type IIB) myofibres (red), laminin (white), nuclei (blue). Slice thickness: 12 µm.

4.7. Skeletal muscle myofibre area by fibre type

The skeletal muscle fibre size was analysed for each fibre type to detect a possible morphological impact by *Mstn* over-expression. Type IIB myofibres display the largest and most frequently found fibre type. In TA muscle these were 6.7% smaller in homozygous mutant (2.5 ± 1.1 x 10^3 µm^2) and 10.3% larger in heterozygous (2.9 ± 1.3 x 10^3 µm^2), when compared to controls (2.7 ± 1.1 x 10^3 µm^2; see Figure 4.15, C). The analysis shows no significant difference between the genotypes for any of the myofibre types (p > 0.5 in all comparisons). Interestingly, myofibre type I were 5.0% larger in homozygous mutant mice when compared to controls (1.3 ± 0.9 x 10^3 µm^2 vs. 1.2 ± 0.8 x 10^3 µm^2), however this difference was not statistically significant (p = 1; Figure 4.15 A). In heterozygous (1.4 ± 1.0 x 10^3 µm^2) type I myofibres were 9.1% larger than in homozygous and even 14.6% larger than in controls, both differences were not significant (p = 0.89 or p = 0.86).

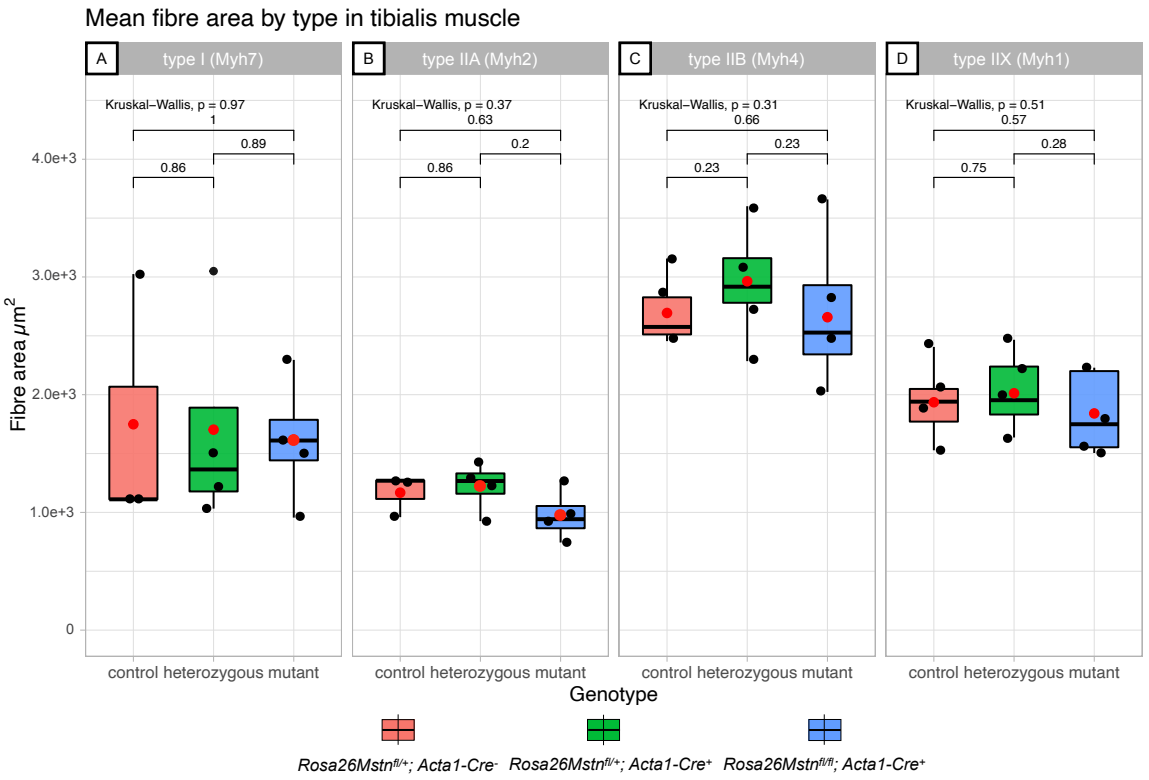

Figure 4.15: Myofibre area by type in TA muscle.
Myofibre area of each fibre type was determined. The analysis showed no significant difference between homozygous mutant (n = 3), heterozygous (n = 4), and controls (n = 3). Data represents the median (black line) & mean (red dot).

In TS muscle type IIB myofibres were 18.8% smaller in homozygous mutant than in controls (2.2 ± 1.1 x 10^3 µm²). In heterozygous type IIB myofibres were 7.3% smaller (2.6 ± 1.2 x 10^3 µm²) than in controls (2.8 ± 1.0 x 10^3 µm²; see Figure 4.16, C). Type I myofibres were 38.2% smaller in homozygous (1.4 ± 0.7 x 10^3 µm²) than in controls (2.2 ± 0.8 x 10^3 µm²), 22.9% smaller in heterozygous (1.7 ± 0.7 x 10^3 µm²) compared to controls (p = 0.11) and 24.8% larger than in homozygous (p = 0.49; see Figure 4.16, A). The analysis showed that none of these differences was of statistical significance for any of the skeletal muscle fibre types (see Figure 4.16, $p > 0.05$ for all comparisons).

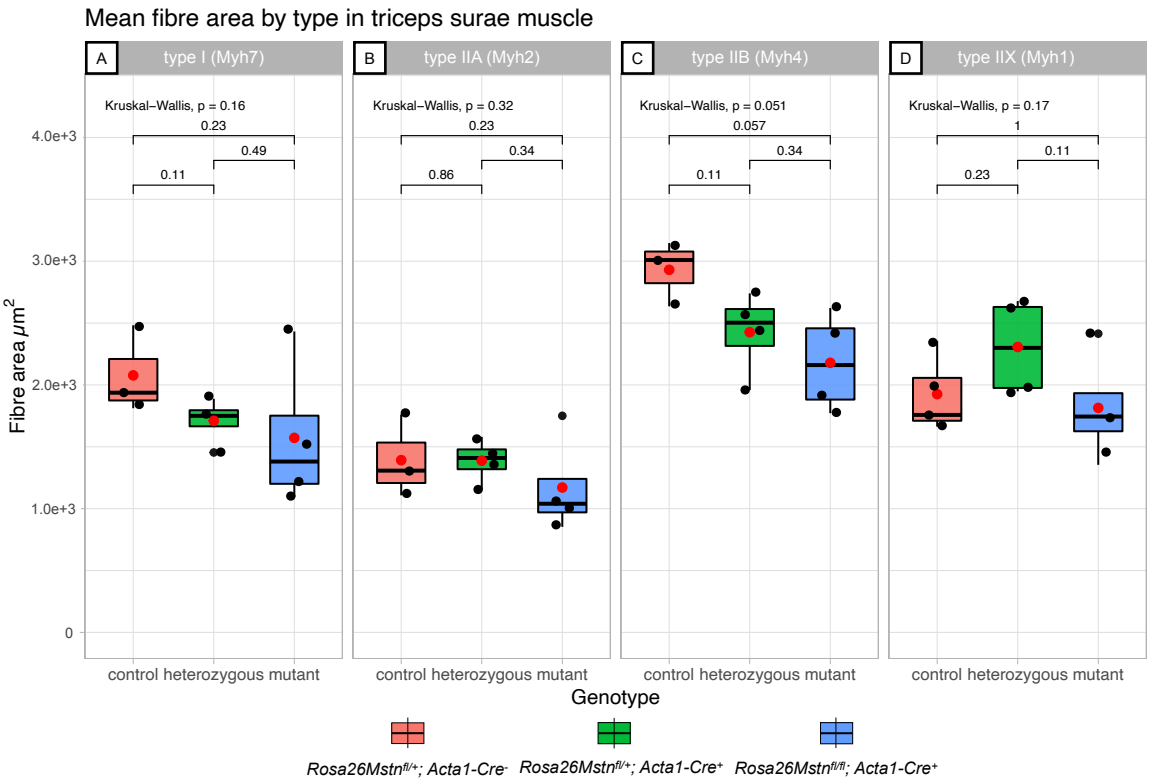

Figure 4.16: Myofibre area by type in TS muscle.

Myofibre area was determined for each myofibre type. No significant differences were found between homozygous mutant (n = 4), heterozygous (n = 4), and controls (n = 3). Graph displays median (black line), data range and mean (red dot).

4.8. Nuclei number per myofibre

Nuclei number was determined using the immunohistochemical staining of lower limb muscle cross sections as described above. In homozygous mutant mice 2.6 ± 0.2 nuclei per myofibre were found, 3.0 ± 0.5 in heterozygous and 2.9 ± 1.0 in controls. Analysis showed no significant differences in mean nuclei count per myofibre in TA muscle (p = 0.41, data not shown). In TS muscle evaluation of mean nuclei number per myofibre showed no significant difference as well (p = 0.11, data not shown).

4.9. Centralised nuclei fraction

Centralised nuclei fraction is defined as the proportion of fibres that show centralised nuclei in relation to all fibres detected in a skeletal muscle cross section. It can be considered as an indicator for muscular tissue damage. The analysis showed no significant impact on centralised nuclei in myostatin over-expressing male mice when compared to controls, both considering TA and TS muscle (see Figure 4.17 + 4.18). Analysing centralised nuclei by skeletal muscle fibre type showed no impact in *Mstn* over-expressing male mice as well (data not shown).

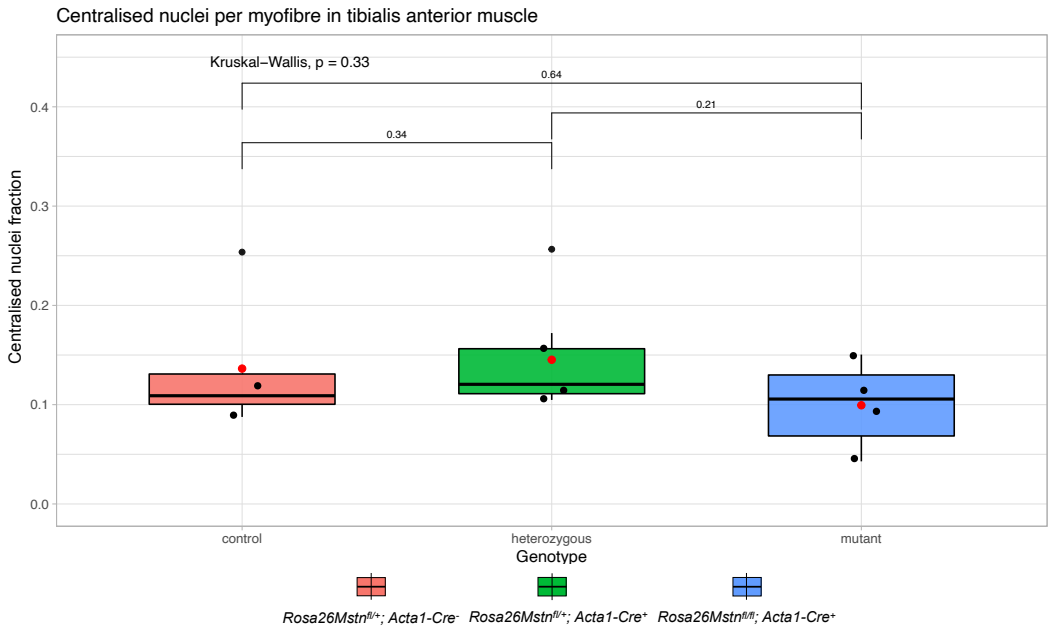

Figure 4.17: Centralised nuclei within skeletal muscle cross sections of TA muscle.

In *Mstn* over-expressing mice there was no significant impact on male mice centralised nuclei fraction. No significant differences in centralised nuclei fraction were found between homozygous mutant (n = 4), heterozygous (n = 4), and controls (n = 3). Significance level $p > 0.05$ for all genotype comparisons. Data represents the median (black line) & mean (red dot).

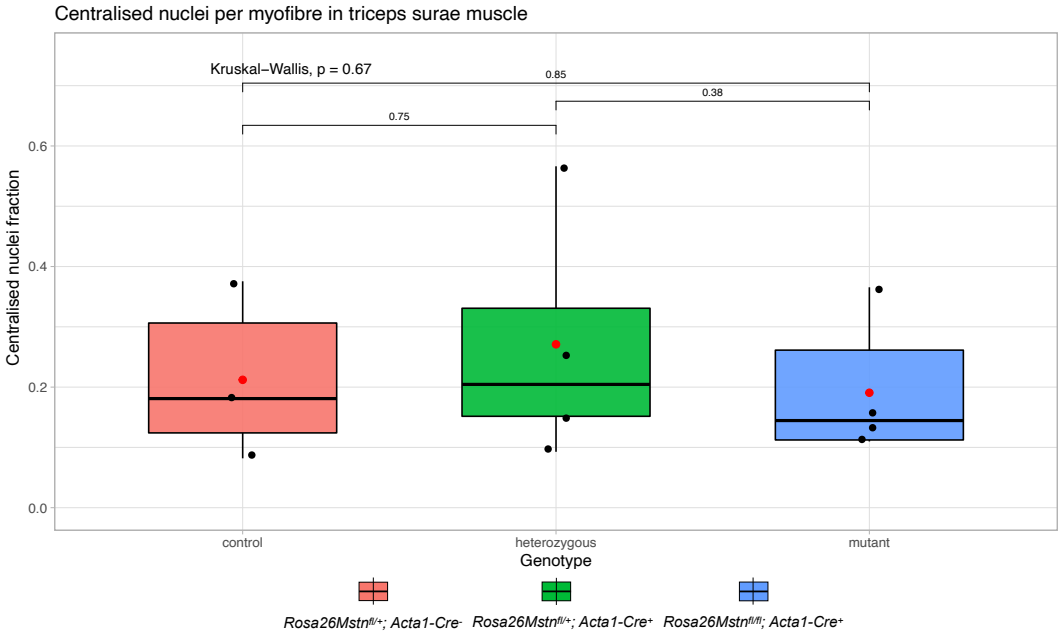

Figure 4.18: Centralised nuclei within skeletal muscle cross sections of TS muscle.

In *Mstn* over-expressing mice there was no significant impact on male mice centralised nuclei fraction. In TS muscle no significant differences in centralised nuclei fraction were found between homozygous mutant (n = 4), heterozygous (n = 4), and controls (n = 3). Significance level $p > 0.05$ for all genotype comparisons. Data represents the median (black line) & mean (red dot).

4.10. *Mstn* over-expression has no significant impact on grip strength

Grip strength measurements were carried out just before euthanisation at 3.5 months as an indicator for possible impairments of muscle function. In female mice mean grip strength was 23% lower in homozygous mutant mice (165.67 ± 13.78 g; n = 3), and 5% lower in heterozygous (226.00 ± 31.46 g; n = 4), when compared to controls (214.36 ± 14.97 g; n = 10). These differences were not significant (p = 0.18, see Figure 4.19).

Mean grip strength in homozygous male mice was 5% lower (223.29 ± 21.01 g; n = 7), and 2% higher in heterozygous (240.50 ± 10.15 g; n = 6), when compared to controls (235.44 ± 15.63 g; n = 9). The differences were not significant as well (Kruskal-Wallis test: p = 0.72).

In both female and male mice *Mstn* over-expression had no significant impact on grip strength. However, grip strength in relation to bodyweight was determined to adjust the measurements to bodyweight differences (data not shown). In female mice mean relative grip strength was 9.43 ± 0.67 g in controls (n = 11), 9.83 ± 1.48 g in heterozygous (n = 4) and 8.05 ± 0.50 g in homozygous mutant mice (n = 3). Thus, relative grip strength was 14.6% lower in female homozygous mutant and 4.2% higher in heterozygous, when compared to controls. In male mice mean relative grip strength was 7.61 ± 0.39 g in controls (n = 9), 7.89 ± 0.33 g in heterozygous (n = 7) and 7.71 ± 0.85 g in homozygous mutant mice (n = 8). This means that relative grip strength was 1.3% higher in male homozygous mutant and 3.7% higher in heterozygous, when compared to controls. However, analyses showed no significant differences across genotypes concerning relative grip strength in both male and female (see Figure 4.19).

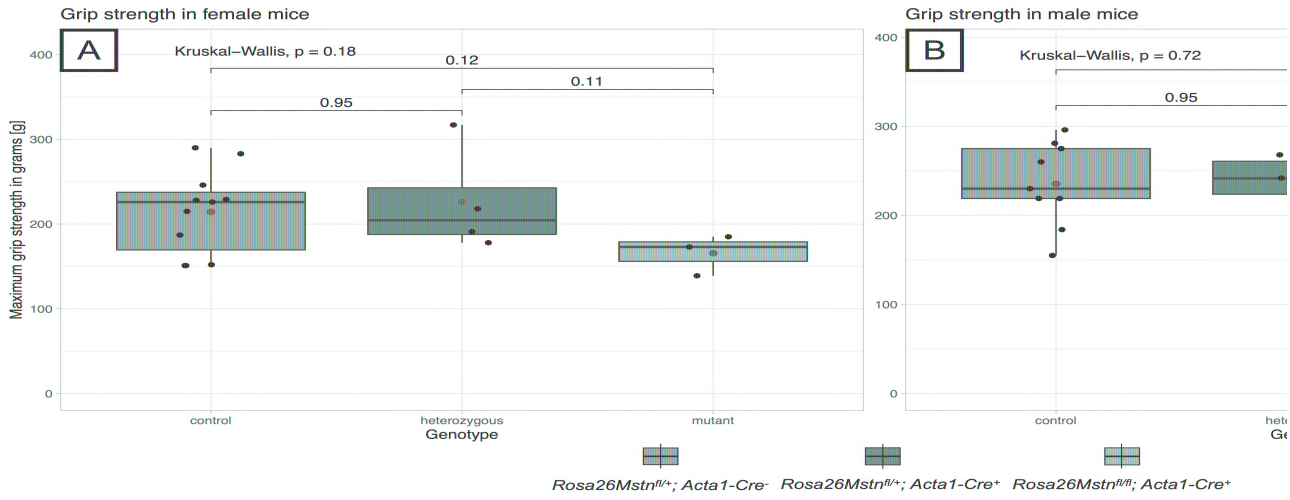

Figure 4.19: Grip strength test.

The figure shows female (A) and male (B) grip strength at 3.5 months of age. In female *Mstn* over-expression had no significant impact (Kruskal-Wallis test resulted in p = 0.18) on grip strength in homozygous mutant mice (n = 3) and heterozygous (n = 4), when compared to controls (n = 10). In male mice, comparison of homozygous mutant mice (n = 7) and heterozygous (n = 6) with controls (n = 9) showed no significant impact on grip strength as well (p = 0.72). The individual values represent the maximum grip strength out of three tries for each mouse. Graph data represents median (black line) & mean (red dot).

4.11. RNA sequencing of murine quadriceps femoris muscle

RNA sequencing was carried out on QF muscles as described above. Here homozygous mutant and control mice were compared to determine possible changes in gene expression. PCA-clustering analysis showed a typical grouping of male and female mice (see Figure 7.4 and 7.5). However, no sufficient grouping of genotypes was found (Figure 4.36). The sample-to-sample distance analysis gives similar results (Figure 4.20).

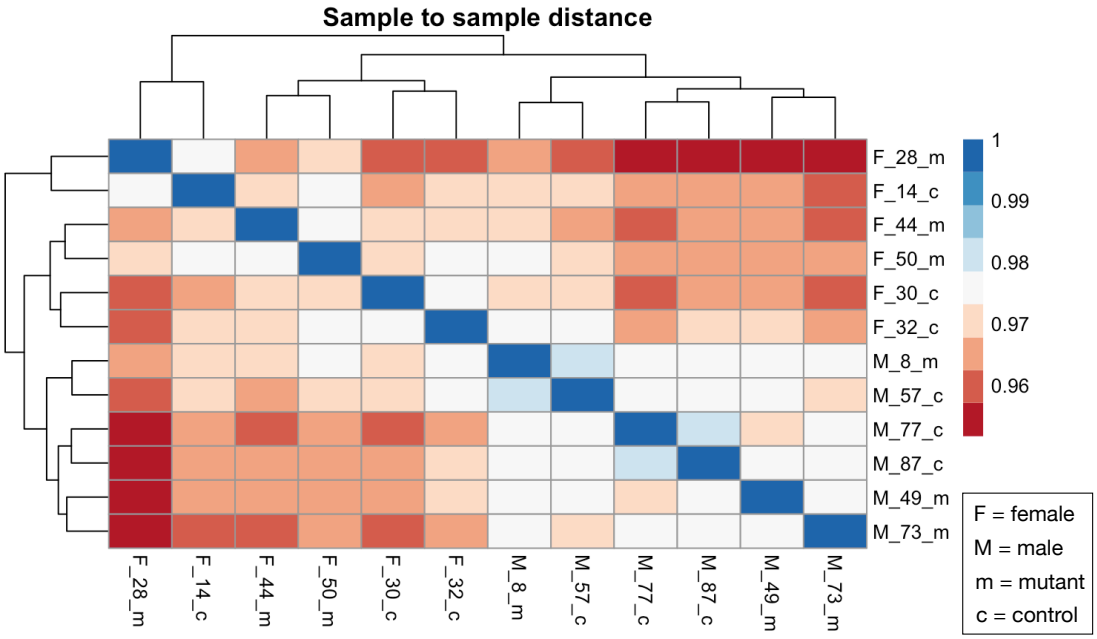

Figure 4.20: Expression pattern on sample-to-sample distance map.
The figure shows the sample-to-sample distance of mutant in comparison to control mice. The visualisation shows that there is a clear clustering of male and female mice. However, there is no clear clustering based on differences between homozygous mutant (n = 3) and controls (n = 3).

Figure 4.21 shows the 10 most up- and down-regulated genes in homozygous mutant mice, when compared to controls. *Cgref1* (Cell Growth Regulator With EF Hand Domain Protein 1) is the most up-regulated gene, whose encoded protein is responsible for calcium-dependent cell-cell adhesion. CGREF1 also inhibits the activation of Activation protein 1 (AP-1), which has transcriptional activity in inflammatory processes and cell proliferation (Madden et al., 1996; Deng et al., 2015). *Nfkbil1* (Nuclear Factor Of Kappa Light Polypeptide Gene Enhancer In B-Cells Inhibitor-Like 1) encodes for a protein involved in negative regulation of immune response (Albertella & Campbell, 1994).
The most down-regulated gene encodes for the Solute Carrier Family 7 Member 3 (SLC7A3), whose function is to mediate uptake of several amino acids (Vékony et al., 2001), which would indicate a catabolic effect by *Mstn* over-expression. Another strongly down-regulated gene is that encoding for Cyclin Dependent Kinase 2 Associated Protein 2 (CDK2AP2), which suppresses cell cycle progression (Liu et al., 2013). LSM domain-containing protein (LSM14) regulates P-body assembly (Yang et al., 2006). These are cytoplasmic storage sites for inactive mRNA, which protect RNA from degradation. Functional clusters of up- or down-regulated genes were analysed

to characterise possible influences of *Mstn* over-expression on cellular and organ processes (see Figure 4.22). *Mstn* over-expression up-regulates expression of genes involved in ion transport and cellular secretion, which might take part in cell communication. However, genes regulating catabolic and mitotic processes are suppressed. In addition, developmental genes in urogenital and kidney development. All in all, this indicates a maintaining regulatory function of MSTN in proliferative and metabolic processes.

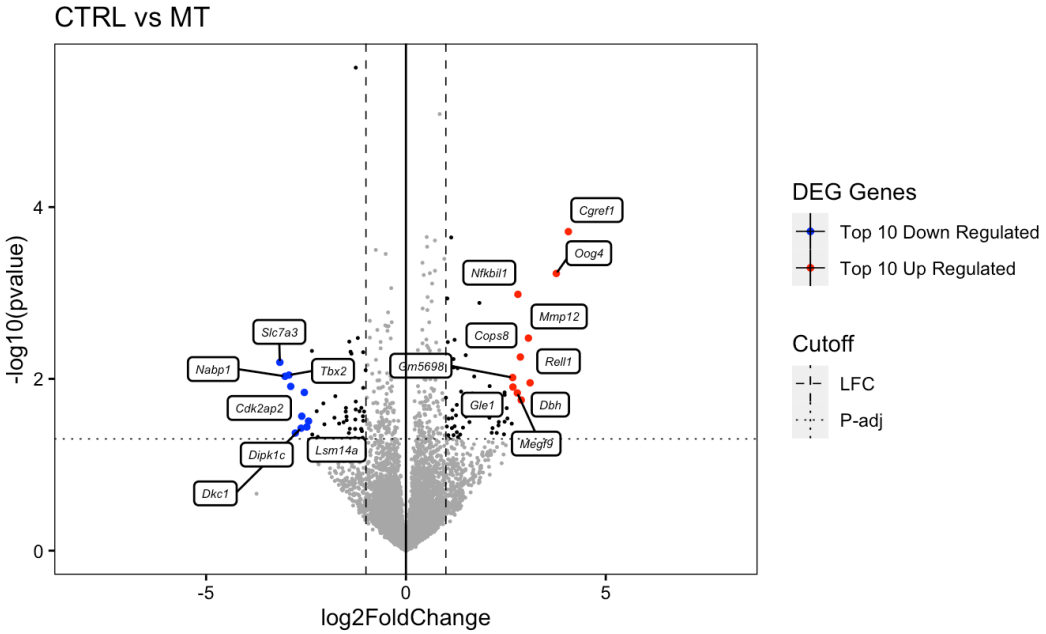

Figure 4.21: Top 10 up- and down-regulated genes.
The figure highlights the 10 most differentially expressed genes of homozygous mutant (n = 3) in comparison to control mice (n = 3), up-regulated genes are highlighted in red, down-regulated genes in blue.

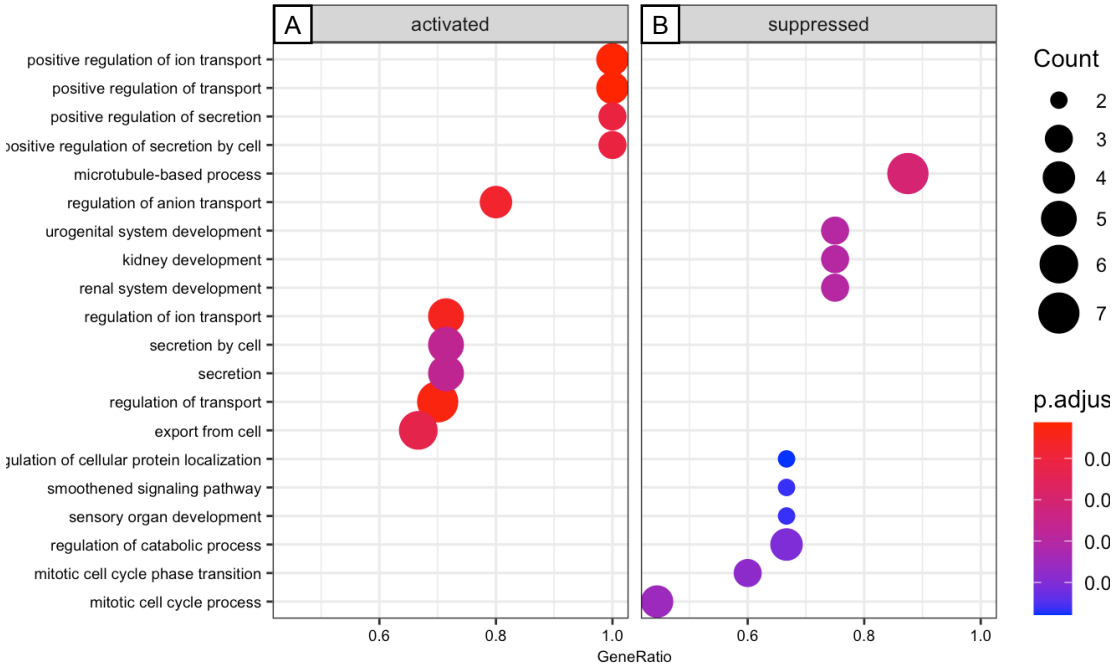

Figure 4.22: Activated and suppressed genes by *Mstn* over-expression over 3.5 months in mice.
The figure shows functional categories of activated and suppressed genes due to *Mstn* over-expression over 3.5 months in mice. *Mstn* over-expression i. a. up-regulates expression of genes involved in immune response, cellular growth (A). Genes involved in regulation of metabolism, mitosis, cell cycle progression, as well as in urogenital and kidney development are down-regulated (B).

5. Discussion

Since MSTN has been identified as a strong inhibitor of muscle growth, the aim of this thesis was to analyse morphological and functional changes in skeletal muscles of *Mstn* over-expressing mice. Therefore, these mice were compared to a heterozygous and a control group. Measurements of body weight, grip strength, weight of lower limb skeletal muscles, MSTN blood level, myofibre size and myofibre type composition were performed, as described above. Moreover, next generation sequencing of skeletal muscle was carried out to determine possible changes in gene expression due to *Mstn* over-expression.

5.1. Previous approaches to genetically modify *Mstn* in animal models

Several animal models have been established to investigate the function of MSTN. A study on mice used promotors of either a WT creatine kinase (MCK), or mutated muscle creatine kinase (MCK-3E), that was placed upstream of the mouse *Mstn* cDNA. These were expressed only in skeletal and cardiac muscles (MCK) or in skeletal muscle alone (MCK-3E)" (Reisz-Porszasz *et al.*, 2003). Hereby, skeletal muscle mass was significantly reduced by 20–22% in 7-weeks old mice. In a model organism for Duchenne muscular dystrophy (mdx mouse line) mutant mice were mated with a mouse line that expresses a transgene coding for an MSTN inhibitor derived from FST (Nakatani *et al.*, 2008). These mice regained muscle mass and strength highlighting the therapeutic potential of MSTN-related pathways (Jin *et al.*, 2019).

Muscle mass hypertrophy could be attained in a similar amount to that of conditional KO-mice by applying a postnatal *Mstn* gene inactivation (Grobet *et al.*, 2003). This finding shows that MSTN not only acts during embryogenesis but also in adolescence.

The aim of the experiments carried out for this thesis was to establish a solid mouse model with decreased skeletal muscle mass. On the basis of that, further genetic modification shall provide the possibility of controlling the onset of this genetic modification to mimic sarcopenia more precisely than by connate gene expression.

5.2. *Mstn* over-expression in mice does not lead to significant changes in overall body weight but reduced skeletal muscle weight

In various species, including cattle, mouse, quail, pigs and humans myostatin deficiency lead to increased muscle mass (Grobet *et al.*, 1997; McPherron *et al.*, 1997; McPherron & Lee, 1997; Lee *et al.*, 2020; Schuelke *et al.*, 2004; Xing *et al.*, 2017). The fact that a single gene had such a profound impact on muscle mass was astonishing and, at the same time, promising to find new ways to fight muscular diseases that go along with a loss of muscle mass and strength, such as sarcopenia. It stands to reason that it did not take long to establish *Mstn* over-expressing animal models to further evaluate its negative role in muscle development and homeostasis. As mentioned before, *Mstn* over-expression using the MCK promoter lead to significant reduction of muscle mass by 20-22%, in TS, QF, and TA muscle (Reisz-Porszasz *et al.*, 2003). Therefore, over-expression of

Mstn (*Rosa26Mstn*$^{fl/fl}$; *Acta1-Cre*$^{+}$) was expected to reduce overall body weight. However, the analysis could not determine a significant effect on body weight in these mice. According to “The Jackson Laboratory” 14 weeks-old male mice weigh 30.8 ± 2.2 g. Mean body weight of all genotypes, that were compared in this thesis, lay within this weight range. As expected, the gene modification (*Rosa26Mstn*$^{fl/fl}$) without expression of the recombinase *Cre* did not have an influence on body weight, either. However, single muscle weight measurements of lower limb muscles showed a significant decrease in homozygous *Mstn* over-expressing male and female mice, compared to heterozygous and controls. Since there was no difference in body weight, the decline in muscle weight should arise from another type of tissue, as discussed below.

Absolute muscle weight was significantly reduced in homozygous male mice. Therefore, further experiments were carried out on male mice, investigating possible morphological effects due to *Mstn* over-expression. Even though, analysis revealed no significant difference on overall bodyweight between genotypes, even small differences in body weight might have an impact on muscle weight. Therefore, absolute and relative muscle weight was examined. Here, male mice showed a significant reduction of lower limb muscle weight in relation to overall bodyweight. At least in terms of body composition this indicates a proper simulation of sarcopenic conditions.

5.3. No significant difference in myofibre size due to *Mstn* over-expression

Skeletal muscles carry out a variety of movements, which require different amounts of force and endurance. These properties strongly depend on the molecular composition of contractile proteins within a myofibre. Especially, MYH isoforms were discovered in the major fibre types. However, there are fluent intermediates, which differ in terms of contraction force, shortening velocity and metabolic characteristics. This explains why muscle performance depends on myofibre type composition. Muscles which are required for stability during standing and gait have a higher proportion of enduring type I myofibres. The reduction of muscle mass by *Mstn* over-expression was demonstrated before (Durieux *et al.*, 2007; Reisz-Porszasz *et al.*, 2003). Consistently, newborn heterozygous *Mstn*$^{+/-}$ pig also show a higher muscle mass (Xing *et al.*, 2017). The results presented in this thesis showed that in TA and TS of male mice muscle *Mstn* over-expression did not lead to a significantly decreased myofibre size. However, a slight tendency towards smaller myofibres in TS muscle was found. This could mean that in 3.5-month-old mice this effect has not reached its full extent or is already lost. Previous research showed that type IIB fibres are most affected by age-related hypotrophy (Lexell, 1995). Across genotypes, IIB myofibres were the largest and most frequently found myofibre type. Interestingly, type I fibres were 5.0% larger in homozygous mutant mice compared to controls and 9.1% larger in heterozygous compared to homozygous and even 14.6% larger than in controls. Even though, both differences were not significant (p = 0.89 and p = 0.86) these results would agree with previous findings that MSTN up-regulates expression of slow MYH isoforms, which appear in type I myofibres (Wang et al., 2012). In TS muscle homozygous mutant mice type IIB myofibres were 18.8% smaller compared to controls. All comparisons did turn out to be statistically insignificant. However, a tendency towards

smaller myofibre size in homozygous *Mstn* over-expressing mice could be detected in all fibre types.

5.4. *Mstn* over-expression does not alter myofibre type composition

MSTN loss-of function mutation leads to significant muscular hypertrophy, which displays an increase in myofibre size (McPherron *et al.*,1997; McPherron & Lee, 1997; Schuelke *et al.*, 2004; Mosher *et al.*, 2007). Accordingly, *Mstn* over-expression was expected to cause opposite morphological changes. These also include an altered myofibre type composition. A differing myofibre distribution pattern could be expected to cause functional differences of the concerning skeletal muscles, due to the differing oxidative capacity, contraction velocity and strength. Previous studies have shown influences of MSTN as well as age-related impact on myofibre composition. Age-related atrophy of skeletal muscles preferentially affects type IIB fibres (Lexell, 1995). Concordantly, $Mstn^{-/-}$ in Belgian Blue cattle and in mice lead to a higher amount of fast IIB fibres (Stavaux *et al.*, 1994; Girgenrath *et al.*, 2005). Heterozygous $MSTN^{+/-}$ pigs showed a significant increase in muscle mass and higher body weight due to fibre hypertrophy. Going along with changes in myofibre type distribution, and alteration of MYH isoforms levels, leading to more fast (type II) glycolytic fibres (Xing *et al.*, 2017). MSTN was proven to up-regulate slow and inhibit fast *Myh* type expression during myogenesis (Wang *et al.*, 2012). Therefore, *Mstn* over-expression could be expected to simulate this pathophysiological aspect of sarcopenia effectively. The results presented here neither show significant difference in overall myofibre number, nor in proportion of fibre types. Type IIB myofibres are most frequently found in all muscles across genotypes. Type I is merely found in TA muscle, consistent with its functional profile presenting a fast contracting and non-persevering muscle. A bigger proportion of intermediate type IIA fibres is found here. However, in TS muscle according to its postural function requiring perseverance a higher amount of type I fibres could be found. But again, *Mstn* over-expression did not influence fibre type proportions in TS.

5.5. Factors of influence for weight difference

It remains unclear which processes cause the weight difference in *Mstn* over-expressing murine lower limb skeletal muscles. It was previously shown that MSTN muscle atrophy leads to decreased expression of structural genes like myosin heavy chain, troponin I and desmin (Durieux *et al.*, 2007). Therefore, a decrease in MYH content and other structural proteins might contribute to the weight reduction. Consistent with that, a study on young men pausing physical exercise for 3 weeks showed the loss of muscle strength was mostly explained by muscle atrophy and a loss of myosin content (Campbell *et al.*, 2013). Besides lowered muscle mass, changes in bone or fat mass have to be considered as well. Bone structure might be impaired in *Mstn*-KO. At least *Mstn*-KO mice show significantly higher trabecular and cortical bone mineral content (Hamrick *et al.*, 2002). An increase in (intramuscular) fat mass replacing healthy muscle tissue might contribute to weight reduction. This was described in *Mstn* over-expressing mice before (Reisz-Porszasz *et al.*,

2003). Water accounts for around two third of body mass. Intravascular fluid accounts for a major proportion of it. Therefore, decreased vascularisation might contribute to weight loss as well. In older man, resistance training increased vascularisation and lead to hypertrophy in type II myofibres (Verdijk *et al.*, 2016).

5.6. Analysis of myofibre structure and indicators for ongoing repair processes

The analysis of nuclei number and centralised nuclei in myofibres intended to show possible damages or ongoing regeneration in myofibres, as the nuclei leave the subsarcolemmal position during these processes (Dumont *et al.*, 2015). However, no significant difference between the genotypes could be detected in nuclei number as well as centralised nuclei fraction. Therefore, it was not possible to conclude any structural impairments by the over-expression of *Mstn* in homozygous or heterozygous mutant mice. Also, it was of interest if a certain myofibre type showed higher signs of damage or repair. But again, analysis revealed no significant difference between the fibre types. In conclusion, these results do not indicate any significant impairment of muscle structure or increased repair processes due to *Mstn* over-expression.

5.7. Grip strength was not affected by the morphological changes due to *Mstn* over-expression

Low grip strength displays a strong indicator for unfavourable outcomes such as prolonged hospitalisation, impaired quality of life and death (Leong *et al.*, 2015). In humans, a lowered hand grip strength correlates with a decrease in global muscle strength (Rantanen *et al.*, 1994). Therefore, *Mstn* over-expression was predicted to have a negative effect on overall strength, which was determined based on grip strength measurements. The analysis showed no significant difference between the different genotypes in male as well as female mice. During the measurement procedure the mice showed strong differences in behaviour, which appeared to have a major impact on the measured values. Even though, different techniques were tested to perform the grip strength test, to ensure valid and reproducible measurements, the variation in behaviour could not be eradicated. Therefore, the informative value of these results remains questionable. However, *Mstn*-KO in mice showed no increase in specific force (sF_0), which is maximum isometric force F_0 divided by CSA, compared with WT (Mendiaz *et al.*, 2011). So, *Mstn* over-expression is not necessarily expected to result in a significant reduction of grip strength. Detailed electrophysiological analysis of mutant mices' skeletal muscle could reveal possible altered ability of force generation and avoid the behaviour-related measurement difficulties.

5.8. RNA sequencing of murine quadriceps femoris muscle reveals no significant changes in transcriptome by *Mstn* over-expression

To obtain insights into possible transcriptional changes of skeletal muscle that might be caused by *Mstn* over-expression, RNA sequencing was performed using QF muscle tissue of homozygous

mutant and controls. Gene expression analyses included evaluation of functional clusters of up- or down-regulated genes, to further characterise possible influences of *Mstn* over-expression on cellular and organ processes. Up-regulated genes, such as *Cgref1* and *Nfkbil1* are involved in immune modulatory processes and inhibit cell proliferation (Madden et al., 1996; Deng et al., 2015; Albertella & Campbell, 1994). Genes like *Slc7a3, Cdk2ap2* and *LSM14* are suppressed, down-regulating protein uptake, cell cycle progression and RNA degradation. This pattern shows that *Mstn* over-expression can cause inhibition of catabolic processes but also suppress proliferation, indicating a homeostatic regulatory function.

A study on gene expression in mice after postnatal *Mstn*-KO showed that post developmental MSTN deficiency did not influence expression levels of genes encoding slow MYH isoforms or metabolic proteins (Welle *et al.*, 2009). This contradicts other findings in *Mstn* deficient myoblasts (Wang *et al.*, 2012). Instead, *Mstn*-KO lead to significantly reduced gene expression of collagens. Ageing, the major factor influencing sarcopenia, was found to be associated with increased levels of inflammatory cytokines, which suggests a partial involvement of a chronic inflammation in the loss of muscle mass and strength (Krabbe *et al.*, 2004). Some important inflammatory cytokines (CRP, IL-6 and TNF-α) were investigated towards their impact on sarcopenia in a study on 120 older men and women (mean age: 66.7 ± 7.7 years) of which 40 met the criteria for sarcopenia of the EWGSOP1 (Asoudeh *et al.*, 2022). However, no significant association of inflammatory cytokine levels and the presence of sarcopenia was observed.

6. Conclusions and outlook

High focus has been given to analyse the impact of MSTN on skeletal muscle using knockout models. These revealed significant morphological changes by the loss of myostatin's function. Over-expression of *Mstn* was hypothesised to lead to opposite effects. The results of this thesis show that skeletal muscle-specific over-expression of *Mstn* leads to a decrease in skeletal muscle weight in homozygous mutant mice. However, no significant morphological changes could be detected in lower limb muscles. No functional impairment in terms of grip strength could be found. Analyses of gene expression due to *Mstn* over-expression revealed a pattern of up- and down-regulated gene that indicates a maintaining regulatory function of MSTN.

All in all, these results show that conditional *Mstn* over-expression has no fatal effect on mice, but a distinct, yet limited impact on skeletal muscle. However, the validity of these results has some limitations. Only a specific point in time was observed, which means that later and possibly more pronounced effects would not yet be apparent at that time, or that they might already lost. A tendency towards smaller myofibre CSA in TS muscle in mutant mice could be an indicator for that. Additionally, the focus of these experiments lay on skeletal muscle alone, but other adjacent tissues could be of interest to unravel processes in sarcopenia e. g. neuronal interaction with muscle cells in subsequent studies (Marš et al., 2020).

Future experiments should examine possible effects on skeletal muscle i. a. in later adolescence. Another research subject could be the onset and/or duration of *Mstn* over-expression. An inducible genetic modification could allow investigation to this matter.

Since, overall body weight is not affected by *Mstn* over-expression, further investigation could also try to explain how the decline in muscle weight is compensated. High-resolution CT/MRI scans of the entire body could reveal compositional differences.

So far, therapeutic approaches for sarcopenic conditions like targeted therapy via antibody inactivation of MSTN have not been able to provide a breakthrough that would restore strength and performance. Despite the impressive phenotype caused by dysfunctional MSTN the pathomechanisms involved in sarcopenic conditions are most likely more complex. Thus, investigating signalling pathway interactions e. g. with GDF11, which has partly overlapping functions with MSTN, might be of interest (Lee *et al.*, 2005).

Possible future projects could investigate whether the regenerative capacity in the skeletal muscle of *Mstn* over-expressing mice is compromised, when compared to the control group. Moreover, detailed electrophysiological analyses of mutant mice's skeletal muscle might reveal a possible altered ability of force generation. Such measurements could avoid the behaviour-related measurement difficulties when performing the grip strength test.

7. Supplementary data

Table 7.1 Descriptive statistics of male mice bodyweight and grip strength

	n	mean	sd	median	trimmed	mad	min	max	range	skew	kurtosis	se
Body weight in [g]	23	30.26	3.26	29.94	30.18	3.23	23.53	36.98	13.45	0.16	-0.47	0.68
Maximum grip strength	22	232.95	43.79	230.50	232.67	40.77	155.00	323.00	168.00	-0.01	-0.73	9.34

Table 7.2 Single skeletal muscle weight of female mice in [g] mean ± SD

	mutant	heterozygous	control
tibialis anterior muscle	0.037 ± 0.004	0.046 ± 0.001	0.047 ± 0.006
triceps surae muscle	0.098 ± 0.004	0.121 ± 0.018	0.123 ± 0.016
quadriceps muscle	0.122 ± 0.005	0.161 ± 0.025	0.151 ± 0.022

Table 7.3 Single skeletal muscle weight of male mice in [g] mean ± SD

	mutant	heterozygous	control
tibialis anterior muscle	0.038 ± 0.009	0.057 ± 0.004	0.061 ± 0.007
triceps surae muscle	0.128 ± 0.028	0.172 ± 0.015	0.175 ± 0.014
quadriceps muscle	0.149 ± 0.032	0.223 ± 0.021	0.226 ± 0.031

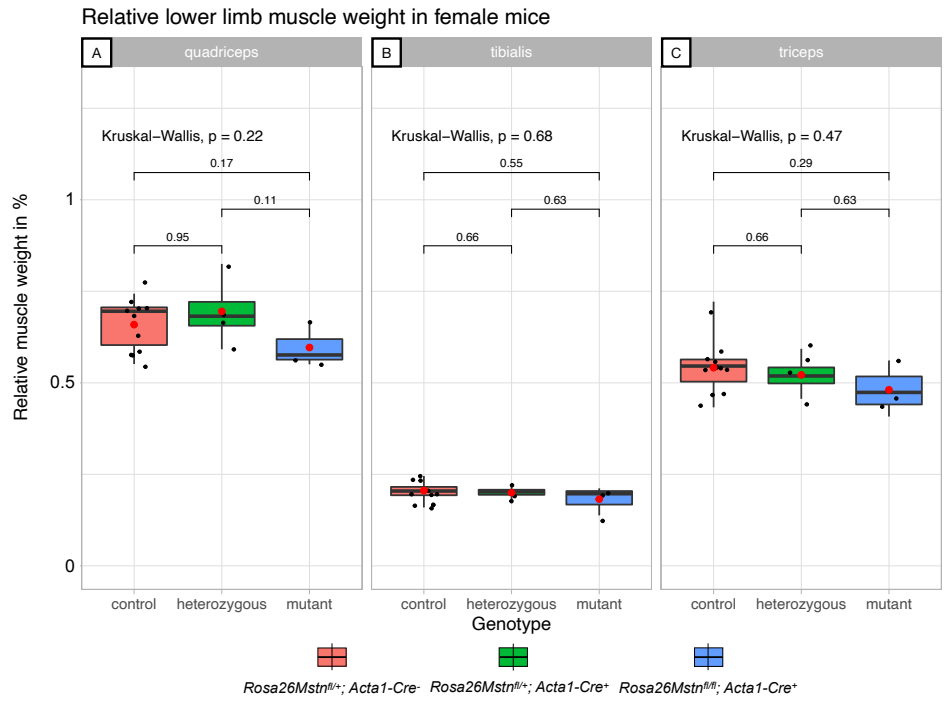

Figure 7.1: Relative skeletal muscle weight of female mice's lower limb muscles

Analysis of skeletal muscle weight of 3.5 months old mice showed no significant difference of relative muscle weight in QF, TA or TS muscles in homozygous mutant mice (n = 4), compared to heterozygous (n = 4) and controls (n = 4). Data represents the median (black line) & mean (red dot).

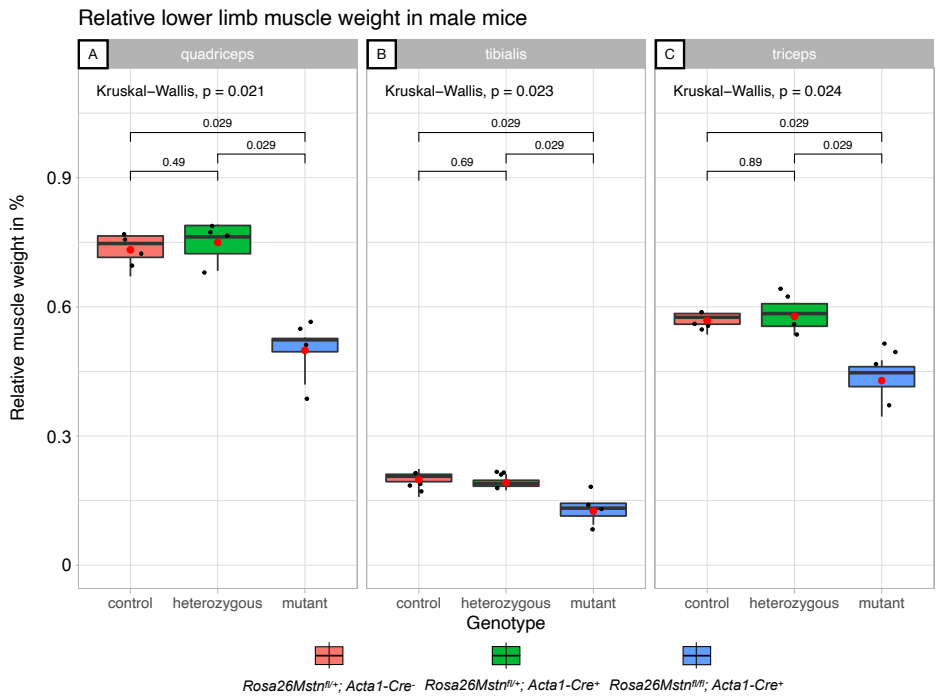

Figure 7.2: Relative skeletal muscle weight of male mice's lower limb muscles

Analysis of skeletal muscle weight of 3.5 months old mice showed a significant reduction of relative muscle weight in all lower limb muscles in homozygous mutant mice (n = 4), compared to heterozygous (n = 4) and controls (n = 4). Data represents the median (black line) & mean (red dot).

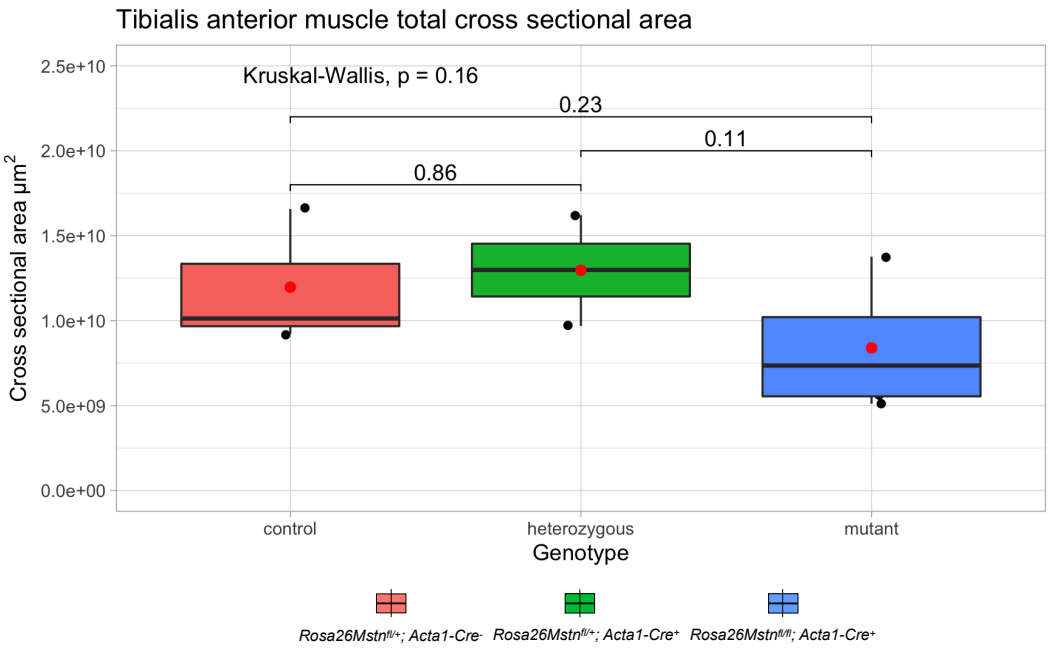

Figure 7.3: Total cross sectional area of TA muscle in male mice.

Total myofibre CSA of TA muscle in 3.5 months old male mice. In homozygous mutant CSA was 12.5% lower (2.1 ± 1.1 x 10^3 µm^2), in comparison to controls (2.4 ± 1.2 x 10^3 µm^2), and 16% lower than in heterozygous mice (2.5 ± 1.3 x 10^3 µm^2). $p > 0.05$ for all comparisons, mean ± SD). control n = 3; heterozygous n = 4; homozygous mutant n = 4. Data represents the median (black line) & mean (red dot).

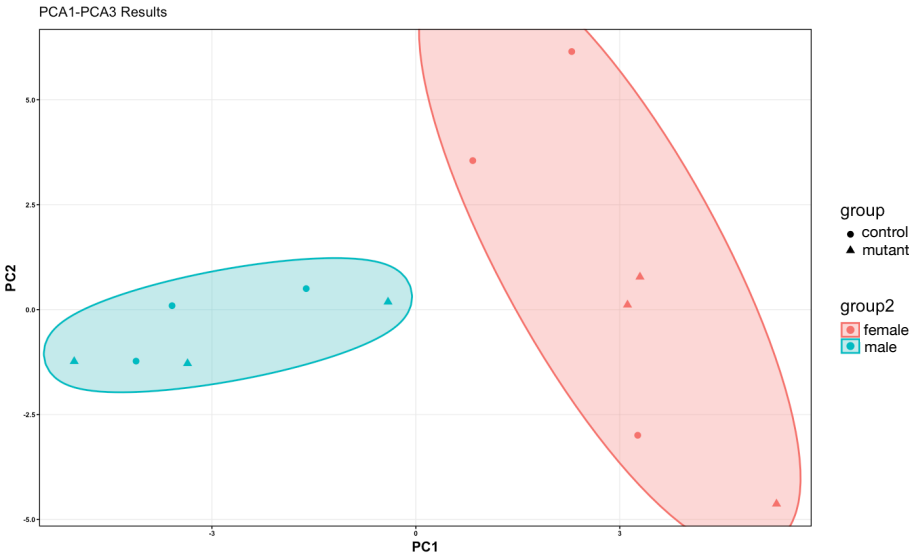

Figure 7.4: PCA clustering.

The figure shows PCA clustering of mutant and control mice. The visualisation shows that there is a clear separation of male and female mice by PCA. However, the genotypes do not cluster properly (m=mutant/ homozygous, n =3; c= control, n=3; F =female, M = male).

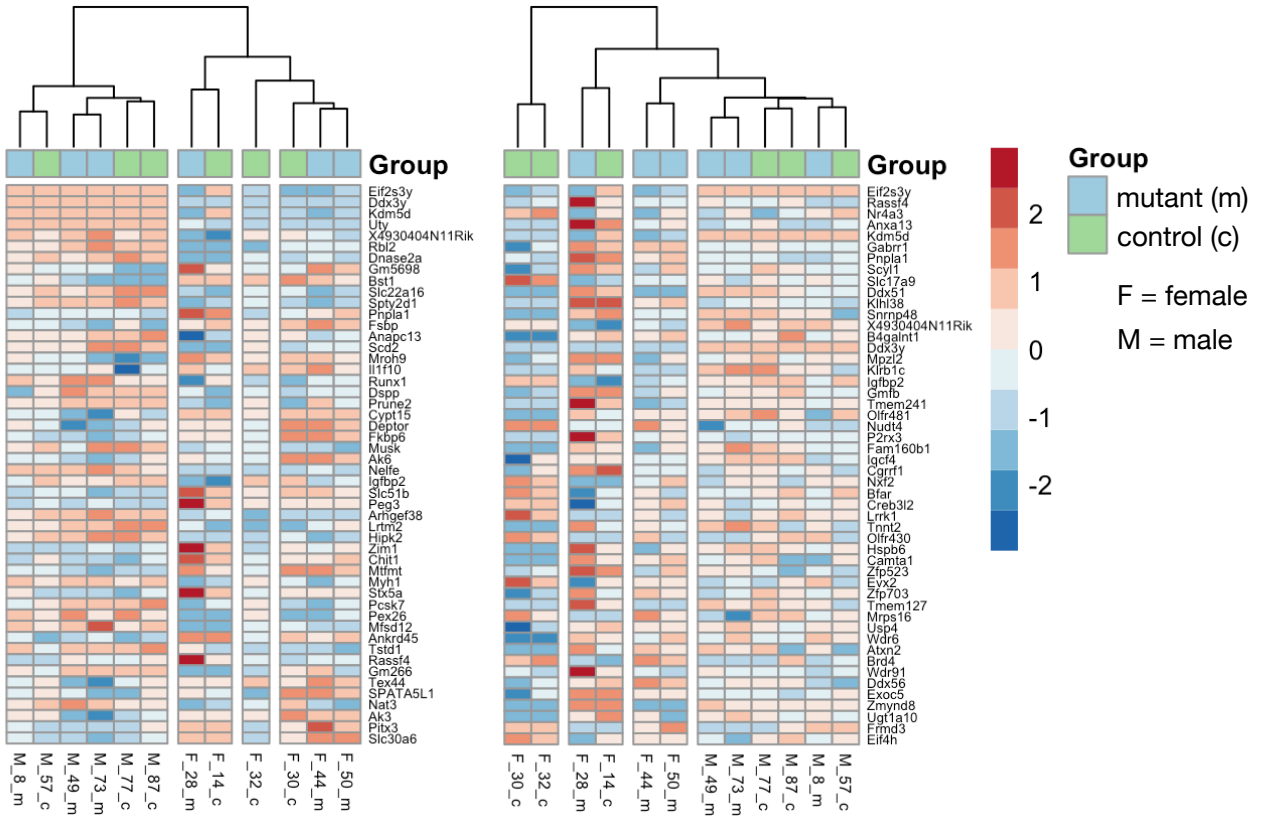

Figure 7.5: Top 50 differentially expressed genes for PC1 and PC2.

The figure shows the 50 most differentially expressed genes of homozygous mutant in comparison to control mice for PC1 (left) and PC2 (right). The visualisation shows that there is no radical impact of *Mstn* over-expression on gene expression patterns (homozygous mutant, n = 3; control, n = 3; female, male).

8. Bibliography

1 **Abellan van Kan, G., Rolland, Y., Andrieu, S., Bauer, J., Beauchet, O., Bonnefoy, M., Cesari, M., Donini, L. M., Gillette Guyonnet, S., Inzitari, M., Nourhashemi, F., Onder, G., Ritz, P., Salva, A., Visser, M., & Vellas, B.** (2009). Gait speed at usual pace as a predictor of adverse outcomes in community-dwelling older people an International Academy on Nutrition and Aging (IANA) Task Force. The journal of nutrition, health & aging, 13(10), 881–889. https://doi.org/10.1007/s12603-009-0246-z

Albertella, M. R., & Campbell, R. D. (1994). Characterization of a novel gene in the human major histocompatibility complex that encodes a potential new member of the I kappa B family of proteins. Human molecular genetics, 3(5), 793–799. https://doi.org/10.1093/hmg/3.5.793

3 **Arentson-Lantz, E. J., English, K. L., Paddon-Jones, D., & Fry, C. S.** (2016). Fourteen days of bed rest induces a decline in satellite cell content and robust atrophy of skeletal muscle fibers in middle-aged adults. Journal of applied physiology (Bethesda, Md. : 1985), 120(8), 965–975. https://doi.org/10.1152/japplphysiol.00799.2015

4 **Asoudeh, F., Dashti, F., Raeesi, S., Heshmat, R., Bidkhori, M., Jalilian, Z., & Hashemi, R.** (2022). Inflammatory cytokines and sarcopenia in Iranian adults-results from SARIR study. Scientific reports, 12(1), 5471. https://doi.org/10.1038/s41598-022-09139-3

5 **Babcock, L. W., Knoblauch, M., & Clarke, M. S.** (2015). The role of myostatin and activin receptor IIB in the regulation of unloading-induced myofiber type-specific skeletal muscle atrophy. Journal of applied physiology (Bethesda, Md. : 1985), 119(6), 633–642. https://doi.org/10.1152/japplphysiol.00762.2014

6 **Bagheri, R., Rashidlamir, A., Motevalli, M. S., Elliott, B. T., Mehrabani, J., & Wong, A.** (2019). Effects of upper-body, lower-body, or combined resistance training on the ratio of follistatin and myostatin in middle-aged men. European journal of applied physiology, 119(9), 1921–1931. https://doi.org/10.1007/s00421-019-04180-z

7 **Baig, M. H., Ahmad, K., Moon, J. S., Park, S. Y., Ho Lim, J., Chun, H. J., Qadri, A. F., Hwang, Y. C., Jan, A. T., Ahmad, S. S., Ali, S., Shaikh, S., Lee, E. J., & Choi, I.** (2022). Myostatin and its Regulation: A Comprehensive Review of Myostatin Inhibiting Strategies. Frontiers in physiology, 13, 876078. https://doi.org/10.3389/fphys.2022.876078

8 **Baker, R. E., Schnell, S., & Maini, P. K.** (2006). A clock and wavefront mechanism for somite formation. Developmental biology, 293(1), 116–126. https://doi.org/10.1016/j.ydbio.2006.01.018

9 **Baracos, V., Rodemann, H. P., Dinarello, C. A., & Goldberg, A. L.** (1983). Stimulation of muscle protein degradation and prostaglandin E2 release by leukocytic pyrogen (interleukin-1). A mechanism for the increased degradation of muscle proteins during fever. The New England journal of medicine, 308(10), 553–558. https://doi.org/10.1056/NEJM198303103081002

10 **Beaudart, C., Biver, E., Bruyère, O., Cooper, C., Al-Daghri, N., Reginster, J. Y., & Rizzoli, R.** (2018). Quality of life assessment in musculo-skeletal health. Aging clinical and experimental research, 30(5), 413–418. https://doi.org/10.1007/s40520-017-0794-8

11 **Bell, K. E., von Allmen, M. T., Devries, M. C., & Phillips, S. M.** (2016). Muscle Disuse as a Pivotal Problem in Sarcopenia-related Muscle Loss and Dysfunction. The Journal of frailty & aging, 5(1), 33–41. https://doi.org/10.14283/jfa.2016.78

12 **Benny Klimek, M. E., Aydogdu, T., Link, M. J., Pons, M., Koniaris, L. G., & Zimmers, T. A.** (2010). Acute inhibition of myostatin-family proteins preserves skeletal muscle in mouse models of cancer cachexia. Biochemical and biophysical research communications, 391(3), 1548–1554. https://doi.org/10.1016/j.bbrc.2009.12.123

13 **Bischoff-Ferrari, H. A., Orav, J. E., Kanis, J. A., Rizzoli, R., Schlögl, M., Staehelin, H. B., Willett, W. C., & Dawson-Hughes, B.** (2015). Comparative performance of current definitions of sarcopenia against the prospective incidence of falls among community-dwelling seniors age 65 and older. Osteoporosis international : a journal established as result of cooperation between the European Foundation for Osteoporosis and the National Osteoporosis Foundation of the USA, 26(12), 2793–2802. https://doi.org/10.1007/s00198-015-3194-y

14 **Blanco-Reina, E., Ocaña-Riola, R., Ariza-Zafra, G., García-Merino, M. R., Aguilar-Cano, L., Valdellós, J., Torres-Blanco, C., & Bellido-Estévez, I.** (2022). Prevalence and Clinical Conditions Related to Sarcopaenia among Older Persons Living in the Community. Journal of clinical medicine, 11(13), 3814. https://doi.org/10.3390/jcm11133814

15 **Bodine, S. C., Stitt, T. N., Gonzalez, M., Kline, W. O., Stover, G. L., Bauerlein, R., Zlotchenko, E., Scrimgeour, A., Lawrence, J. C., Glass, D. J., & Yancopoulos, G. D.** (2001). Akt/mTOR pathway is a crucial regulator of skeletal muscle hypertrophy and can prevent muscle atrophy in vivo. Nature cell biology, 3(11), 1014–1019. https://doi.org/10.1038/ncb1101-1014

16 **Bogdanovich, S., Perkins, K. J., Krag, T. O., Whittemore, L. A., & Khurana, T. S.** (2005). Myostatin propeptide-mediated amelioration of dystrophic pathophysiology. FASEB journal : official publication of the Federation of American Societies for Experimental Biology, 19(6), 543–549. https://doi.org/10.1096/fj.04-2796com

17 **Bouabe, H., Fässler, R., & Heesemann, J.** (2008). Improvement of reporter activity by IRES-mediated polycistronic reporter system. Nucleic acids research, 36(5), e28. https://doi.org/10.1093/nar/gkm1119

18 **Brack, A. S., Bildsoe, H., & Hughes, S. M.** (2005). Evidence that satellite cell decrement contributes to preferential decline in nuclear number from large fibres during murine age-related muscle atrophy. Journal of cell science, 118(Pt 20), 4813–4821. https://doi.org/10.1242/jcs.02602

19 **Burke, D. G., Candow, D. G., Chilibeck, P. D., MacNeil, L. G., Roy, B. D., Tarnopolsky, M. A., & Ziegenfuss, T.** (2008). Effect of creatine supplementation and resistance-exercise training on muscle insulin-like growth factor in young adults. International journal of sport nutrition and exercise metabolism, 18(4), 389–398. https://doi.org/10.1123/ijsnem.18.4.389

20 **Campbell, E. L., Seynnes, O. R., Bottinelli, R., McPhee, J. S., Atherton, P. J., Jones, D. A., Butler-Browne, G., & Narici, M. V.** (2013). Skeletal muscle adaptations to physical inactivity and subsequent retraining in young men. Biogerontology, 14(3), 247–259. https://doi.org/10.1007/s10522-013-9427-6

21 **Camporez, J. P., Petersen, M. C., Abudukadier, A., Moreira, G. V., Jurczak, M. J., Friedman, G., Haqq, C. M., Petersen, K. F., & Shulman, G. I.** (2016). Anti-myostatin antibody increases muscle mass and strength and improves insulin sensitivity in old mice. Proceedings of the National Academy of Sciences of the United States of America, 113(8), 2212–2217. https://doi.org/10.1073/pnas.1525795113

22 **Carbone, J. W., McClung, J. P., & Pasiakos, S. M.** (2012). Skeletal muscle responses to negative energy balance: effects of dietary protein. Advances in nutrition (Bethesda, Md.), 3(2), 119–126. https://doi.org/10.3945/an.111.001792

23 **Carraro, U., Kern, H., Gava, P., Hofer, C., Loefler, S., Gargiulo, P., Mosole, S., Zampieri, S., Gobbo, V., Ravara, B., Piccione, F., Marcante, A., Baba, A., Schils, S., Pond, A., & Gava, F.** (2015). Biology of Muscle Atrophy and of its Recovery by FES in Aging and Mobility Impairments: Roots and By-Products. European journal of translational myology, 25(4), 221–230. https://doi.org/10.4081/ejtm.2015.5272

24 **Cawthon P. M.** (2015). Assessment of Lean Mass and Physical Performance in Sarcopenia. Journal of clinical densitometry : the official journal of the International Society for Clinical Densitometry, 18(4), 467–471. https://doi.org/10.1016/j.jocd.2015.05.063

25 **Christ, B., & Ordahl, C. P.** (1995). Early stages of chick somite development. Anatomy and embryology, 191(5), 381–396. https://doi.org/10.1007/BF00304424

Cisterna, B., Giagnacovo, M., Costanzo, M., Fattoretti, P., Zancanaro, C., Pellicciari, C., & Malatesta, M. (2016). Adapted physical exercise enhances activation and differentiation potential of satellite cells in the skeletal muscle of old mice. Journal of anatomy, 228(5), 771–783. https://doi.org/10.1111/joa.12429

Coker, R. H., Hays, N. P., Williams, R. H., Wolfe, R. R., & Evans, W. J. (2015). Bed rest promotes reductions in walking speed, functional parameters, and aerobic fitness in older, healthy adults. The journals of gerontology. Series A, Biological sciences and medical sciences, 70(1), 91–96. https://doi.org/10.1093/gerona/glu123

Cornelison, D. D., Wilcox-Adelman, S. A., Goetinck, P. F., Rauvala, H., Rapraeger, A. C., & Olwin, B. B. (2004). Essential and separable roles for Syndecan-3 and Syndecan-4 in skeletal muscle development and regeneration. Genes & development, 18(18), 2231–2236. https://doi.org/10.1101/gad.1214204

Costantin L. L. (1975). Contractile activation in skeletal muscle. Progress in biophysics and molecular biology, 29(2), 197–224. https://doi.org/10.1016/0079-6107(76)90023-7

Cruz-Jentoft, A. J., Bahat, G., Bauer, J., Boirie, Y., Bruyère, O., Cederholm, T., Cooper, C., Landi, F., Rolland, Y., Sayer, A. A., Schneider, S. M., Sieber, C. C., Topinkova, E., Vandewoude, M., Visser, M., Zamboni, M., & Writing Group for the European Working Group on Sarcopenia in Older People 2 (EWGSOP2), and the Extended Group for EWGSOP2 (2019). Sarcopenia: revised European consensus on definition and diagnosis. *Age and ageing*, *48*(1), 16–31. https://doi.org/10.1093/ageing/afy169

DeFronzo, R. A., Jacot, E., Jequier, E., Maeder, E., Wahren, J., & Felber, J. P. (1981). The effect of insulin on the disposal of intravenous glucose. Results from indirect calorimetry and hepatic and femoral venous catheterization. Diabetes, 30(12), 1000–1007. https://doi.org/10.2337/diab.30.12.1000

Deng, W., Wang, L., Xiong, Y., Li, J., Wang, Y., Shi, T., & Ma, D. (2015). The novel secretory protein CGREF1 inhibits the activation of AP-1 transcriptional activity and cell proliferation. The international journal of biochemistry & cell biology, 65, 32–39. https://doi.org/10.1016/j.biocel.2015.05.019

Dobin, A., Davis, C. A., Schlesinger, F., Drenkow, J., Zaleski, C., Jha, S., Batut, P., Chaisson, M., & Gingeras, T. R. (2013). STAR: ultrafast universal RNA-seq aligner. Bioinformatics (Oxford, England), 29(1), 15–21. https://doi.org/10.1093/bioinformatics/bts635

Druet, T., Ahariz, N., Cambisano, N., Tamma, N., Michaux, C., Coppieters, W., Charlier, C., & Georges, M. (2014). Selection in action: dissecting the molecular underpinnings of the increasing muscle mass of Belgian Blue Cattle. BMC genomics, 15(1), 796. https://doi.org/10.1186/1471-2164-15-796

Dumont, N. A., Bentzinger, C. F., Sincennes, M. C., & Rudnicki, M. A. (2015). Satellite Cells and Skeletal Muscle Regeneration. Comprehensive Physiology, 5(3), 1027–1059. https://doi.org/10.1002/cphy.c140068

Durieux, A. C., Amirouche, A., Banzet, S., Koulmann, N., Bonnefoy, R., Pasdeloup, M., Mouret, C., Bigard, X., Peinnequin, A., & Freyssenet, D. (2007). Ectopic expression of myostatin induces atrophy of adult skeletal muscle by decreasing muscle gene expression. Endocrinology, 148(7), 3140–3147. https://doi.org/10.1210/en.2006-1500

Egerman, M. A., Cadena, S. M., Gilbert, J. A., Meyer, A., Nelson, H. N., Swalley, S. E., Mallozzi, C., Jacobi, C., Jennings, L. L., Clay, I., Laurent, G., Ma, S., Brachat, S., Lach-Trifilieff, E., Shavlakadze, T., Trendelenburg, A. U., Brack, A. S., & Glass, D. J. (2015). GDF11 Increases with Age and Inhibits Skeletal Muscle Regeneration. Cell metabolism, 22(1), 164–174. https://doi.org/10.1016/j.cmet.2015.05.010

Esquela, A. F., & Lee, S. J. (2003). Regulation of metanephric kidney development by growth/differentiation factor 11. Developmental biology, 257(2), 356–370. https://doi.org/10.1016/s0012-1606(03)00100-3

Fan, C. M., & Tessier-Lavigne, M. (1994). Patterning of mammalian somites by surface ectoderm and notochord: evidence for sclerotome induction by a hedgehog homolog. Cell, 79(7), 1175–1186. https://doi.org/10.1016/0092-8674(94)90009-4

Flores-Opazo, M., McGee, S. L., & Hargreaves, M. (2020). Exercise and GLUT4. Exercise and sport sciences reviews, 48(3), 110–118. https://doi.org/10.1249/JES.0000000000000224

Fortier, M., Comunale, F., Kucharczak, J., Blangy, A., Charrasse, S., & Gauthier-Rouvière, C. (2008). RhoE controls myoblast alignment prior fusion through RhoA and ROCK. *Cell death and differentiation*, *15*(8), 1221–1231. https://doi.org/10.1038/cdd.2008.34

Friedrich, G., & Soriano, P. (1991). Promoter traps in embryonic stem cells: a genetic screen to identify and mutate developmental genes in mice. Genes & development, 5(9), 1513–1523. https://doi.org/10.1101/gad.5.9.1513

Frontera, W. R., & Ochala, J. (2015). Skeletal muscle: a brief review of structure and function. Calcified tissue international, 96(3), 183–195. https://doi.org/10.1007/s00223-014-9915-y

Giallauria, F., Cittadini, A., Smart, N. A., & Vigorito, C. (2016). Resistance training and sarcopenia. *Monaldi archives for chest disease = Archivio Monaldi per le malattie del torace*, *84*(1-2), 738. https://doi.org/10.4081/monaldi.2015.738

Girgenrath, S., Song, K., & Whittemore, L. A. (2005). Loss of myostatin expression alters fiber-type distribution and expression of myosin heavy chain isoforms in slow- and fast-type skeletal muscle. Muscle & nerve, 31(1), 34–40. https://doi.org/10.1002/mus.20175

González-Alonso J. (2012). Human thermoregulation and the cardiovascular system. Experimental physiology, 97(3), 340–346. https://doi.org/10.1113/expphysiol.2011.058701

Gonzalez-Cadavid, N. F., Taylor, W. E., Yarasheski, K., Sinha-Hikim, I., Ma, K., Ezzat, S., Shen, R., Lalani, R., Asa, S., Mamita, M., Nair, G., Arver, S., & Bhasin, S. (1998). Organization of the human myostatin gene and expression in healthy men and HIV-infected men with muscle wasting. Proceedings of the National Academy of Sciences of the United States of America, 95(25), 14938–14943. https://doi.org/10.1073/pnas.95.25.14938

Goodpaster, B. H., Park, S. W., Harris, T. B., Kritchevsky, S. B., Nevitt, M., Schwartz, A. V., Simonsick, E. M., Tylavsky, F. A., Visser, M., & Newman, A. B. (2006). The loss of skeletal muscle strength, mass, and quality in older adults: the health, aging and body composition study. The journals of gerontology. Series A, Biological sciences and medical sciences, 61(10), 1059–1064. https://doi.org/10.1093/gerona/61.10.1059

Grobet, L., Martin, L. J., Poncelet, D., Pirottin, D., Brouwers, B., Riquet, J., Schoeberlein, A., Dunner, S., Ménissier, F., Massabanda, J., Fries, R., Hanset, R., & Georges, M. (1997). A deletion in the bovine myostatin gene causes the double-muscled phenotype in cattle. Nature genetics, 17(1), 71–74. https://doi.org/10.1038/ng0997-71

Grobet, L., Pirottin, D., Farnir, F., Poncelet, D., Royo, L. J., Brouwers, B., Christians, E., Desmecht, D., Coignoul, F., Kahn, R., & Georges, M. (2003). Modulating skeletal muscle mass by postnatal, muscle-specific inactivation of the myostatin gene. Genesis (New York, N.Y. : 2000), 35(4), 227–238. https://doi.org/10.1002/gene.10188

Grounds M. D. (2014). Therapies for sarcopenia and regeneration of old skeletal muscles: more a case of old tissue architecture than old stem cells. Bioarchitecture, 4(3), 81–87. https://doi.org/10.4161/bioa.29668

Gustafsson, M. K., Pan, H., Pinney, D. F., Liu, Y., Lewandowski, A., Epstein, D. J., & Emerson, C. P., Jr (2002). Myf5 is a direct target of long-range Shh signaling and Gli regulation for muscle specification. Genes & development, 16(1), 114–126. https://doi.org/10.1101/gad.940702

Hamilton, D. L., & Abremski, K. (1984). Site-specific recombination by the bacteriophage P1 lox-Cre system. Cre-mediated synapsis of two lox sites. Journal of molecular biology, 178(2), 481–486. https://doi.org/10.1016/0022-2836(84)90154-2

Hamrick, M. W., McPherron, A. C., & Lovejoy, C. O. (2002). Bone mineral content and density in the humerus of adult myostatin-deficient mice. Calcified tissue international, 71(1), 63–68. https://doi.org/10.1007/s00223-001-1109-8

Heymsfield, S. B., Gallagher, D., Kotler, D. P., Wang, Z., Allison, D. B., & Heshka, S. (2002). Body-size dependence of resting energy expenditure can be attributed to nonenergetic homogeneity of fat-free mass. American journal of physiology. Endocrinology and metabolism, 282(1), E132–E138. https://doi.org/10.1152/ajpendo.2002.282.1.E132

Heymsfield, S. B., Gonzalez, M. C., Lu, J., Jia, G., & Zheng, J. (2015). Skeletal muscle mass and quality: evolution of modern measurement concepts in the context of sarcopenia. The Proceedings of the Nutrition Society, 74(4), 355–366. https://doi.org/10.1017/S0029665115000129

Hirsinger, E., Jouve, C., Dubrulle, J., & Pourquié, O. (2000). Somite formation and patterning. International review of cytology, 198, 1–65. https://doi.org/10.1016/s0074-7696(00)98002-1

Hoess, R., Abremski, K., & Sternberg, N. (1984). The nature of the interaction of the P1 recombinase Cre with the recombining site loxP. Cold Spring Harbor symposia on quantitative biology, 49, 761–768. https://doi.org/10.1101/sqb.1984.049.01.086

Hsu, K. J., Liao, C. D., Tsai, M. W., & Chen, C. N. (2019). Effects of Exercise and Nutritional Intervention on Body Composition, Metabolic Health, and Physical Performance in Adults with Sarcopenic Obesity: A Meta-Analysis. Nutrients, 11(9), 2163. https://doi.org/10.3390/nu11092163

Janssen, I., Heymsfield, S. B., Wang, Z. M., & Ross, R. (2000). Skeletal muscle mass and distribution in 468 men and women aged 18-88 yr. Journal of applied physiology (Bethesda, Md. : 1985), 89(1), 81–88. https://doi.org/10.1152/jappl.2000.89.1.81

Jin, Q., Qiao, C., Li, J., Xiao, B., Li, J., & Xiao, X. (2019). A GDF11/myostatin inhibitor, GDF11 propeptide-Fc, increases skeletal muscle mass and improves muscle strength in dystrophic mdx mice. Skeletal muscle, 9(1), 16. https://doi.org/10.1186/s13395-019-0197-y

Kassar-Duchossoy, L., Giacone, E., Gayraud-Morel, B., Jory, A., Gomès, D., & Tajbakhsh, S. (2005). Pax3/Pax7 mark a novel population of primitive myogenic cells during development. Genes & development, 19(12), 1426–1431. https://doi.org/10.1101/gad.345505

Kim, H., Hirano, H., Edahiro, A., Ohara, Y., Watanabe, Y., Kojima, N., Kim, M., Hosoi, E., Yoshida, Y., Yoshida, H., & Shinkai, S. (2016). Sarcopenia: Prevalence and associated factors based on different suggested definitions in community-dwelling older adults. Geriatrics & gerontology international, 16 Suppl 1, 110–122. https://doi.org/10.1111/ggi.12723

Kim, H., Kim, M., Kojima, N., Fujino, K., Hosoi, E., Kobayashi, H., Somekawa, S., Niki, Y., Yamashiro, Y., & Yoshida, H. (2016). Exercise and Nutritional Supplementation on Community-Dwelling Elderly Japanese Women With Sarcopenic Obesity: A Randomized Controlled Trial. Journal of the American Medical Directors Association, 17(11), 1011–1019. https://doi.org/10.1016/j.jamda.2016.06.016

Kim, M., & Won, C. W. (2020). Sarcopenia in Korean Community-Dwelling Adults Aged 70 Years and Older: Application of Screening and Diagnostic Tools From the Asian Working Group for Sarcopenia 2019 Update. Journal of the American Medical Directors Association, 21(6), 752–758. https://doi.org/10.1016/j.jamda.2020.03.018

Kim, S., Jung, P. Y., Lee, J. S., Hwang, S., Sohn, J. H., Yoon, Y., Bae, K. S., & Eom, Y. W. (2021). Cultured human skeletal muscle satellite cells exhibit characteristics of mesenchymal stem cells and play anti-inflammatory roles through prostaglandin E2 and hepatocyte growth factors. Cell biology international, 45(12), 2443–2451. https://doi.org/10.1002/cbin.11688

Kondás, K., Szláma, G., Trexler, M., & Patthy, L. (2008). Both WFIKKN1 and WFIKKN2 have high affinity for growth and differentiation factors 8 and 11. The Journal of biological chemistry, 283(35), 23677–23684. https://doi.org/10.1074/jbc.M803025200

Kos C. H. (2004). Cre/loxP system for generating tissue-specific knockout mouse models. Nutrition reviews, 62(6 Pt 1), 243–246. https://doi.org/10.1301/nr2004.jun243-246

Krabbe, K. S., Pedersen, M., & Bruunsgaard, H. (2004). Inflammatory mediators in the elderly. Experimental gerontology, 39(5), 687–699. https://doi.org/10.1016/j.exger.2004.01.009

Latres, E., Pangilinan, J., Miloscio, L., Bauerlein, R., Na, E., Potocky, T. B., Huang, Y., Eckersdorff, M., Rafique, A., Mastaitis, J., Lin, C., Murphy, A. J., Yancopoulos, G. D., Gromada, J., & Stitt, T. (2015). Myostatin blockade with a fully human monoclonal antibody induces muscle hypertrophy and reverses muscle atrophy in young and aged mice. Skeletal muscle, 5, 34. https://doi.org/10.1186/s13395-015-0060-8

LeBrasseur, N. K., Schelhorn, T. M., Bernardo, B. L., Cosgrove, P. G., Loria, P. M., & Brown, T. A. (2009). Myostatin inhibition enhances the effects of exercise on performance and metabolic outcomes in aged mice. The journals of gerontology. Series A, Biological sciences and medical sciences, 64(9), 940–948. https://doi.org/10.1093/gerona/glp068

Lee S. J. (2004). Regulation of muscle mass by myostatin. Annual review of cell and developmental biology, 20, 61–86. https://doi.org/10.1146/annurev.cellbio.20.012103.135836

Lee, J., Kim, D. H., & Lee, K. (2020). Muscle Hyperplasia in Japanese Quail by Single Amino Acid Deletion in MSTN Propeptide. International journal of molecular sciences, 21(4), 1504. https://doi.org/10.3390/ijms21041504

Lee, M., Oikawa, S., Ushida, T., Suzuki, K., & Akimoto, T. (2019). Effects of Exercise Training on Growth and Differentiation Factor 11 Expression in Aged Mice. Frontiers in physiology, 10, 970. https://doi.org/10.3389/fphys.2019.00970

Lee, S. J., Huynh, T. V., Lee, Y. S., Sebald, S. M., Wilcox-Adelman, S. A., Iwamori, N., Lepper, C., Matzuk, M. M., & Fan, C. M. (2012). Role of satellite cells versus myofibers in muscle hypertrophy induced by inhibition of the myostatin/activin signaling pathway. Proceedings of the National Academy of Sciences of the United States of America, 109(35), E2353–E2360. https://doi.org/10.1073/pnas.1206410109

Lee, S. J., Reed, L. A., Davies, M. V., Girgenrath, S., Goad, M. E., Tomkinson, K. N., Wright, J. F., Barker, C., Ehrmantraut, G., Holmstrom, J., Trowell, B., Gertz, B., Jiang, M. S., Sebald, S. M., Matzuk, M., Li, E., Liang, L. F., Quattlebaum, E., Stotish, R. L., & Wolfman, N. M. (2005). Regulation of muscle growth by multiple ligands signaling through activin type II receptors. Proceedings of the National Academy of Sciences of the United States of America, 102(50), 18117–18122. https://doi.org/10.1073/pnas.0505996102

Leong, D. P., Teo, K. K., Rangarajan, S., Lopez-Jaramillo, P., Avezum, A., Jr, Orlandini, A., Seron, P., Ahmed, S. H., Rosengren, A., Kelishadi, R., Rahman, O., Swaminathan, S., Iqbal, R., Gupta, R., Lear, S. A., Oguz, A., Yusoff, K., Zatonska, K., Chifamba, J., Igumbor, E., … Prospective Urban Rural Epidemiology (PURE) Study investigators (2015). Prognostic value of grip strength: findings from the Prospective Urban Rural Epidemiology (PURE) study. Lancet (London, England), 386(9990), 266–273. https://doi.org/10.1016/S0140-6736(14)62000-6

Lexell, J., Taylor, C. C., & Sjöström, M. (1988). What is the cause of the ageing atrophy? Total number, size and proportion of different fiber types studied in whole vastus lateralis muscle from 15- to 83-year-old men. Journal of the neurological sciences, 84(2-3), 275–294. https://doi.org/10.1016/0022-510x(88)90132-3

Linke W. A. (2018). Titin Gene and Protein Functions in Passive and Active Muscle. Annual review of physiology, 80, 389–411. https://doi.org/10.1146/annurev-physiol-021317-121234

Liu, Q., Liu, X., Gao, J., Shi, X., Hu, X., Wang, S., & Luo, Y. (2013). Overexpression of DOC-1R inhibits cell cycle G1/S transition by repressing CDK2 expression and activation. International journal of biological sciences, 9(6), 541–549. https://doi.org/10.7150/ijbs.5763

Loffredo, F. S., Steinhauser, M. L., Jay, S. M., Gannon, J., Pancoast, J. R., Yalamanchi, P., Sinha, M., Dall'Osso, C., Khong, D., Shadrach, J. L., Miller, C. M., Singer, B. S., Stewart, A., Psychogios, N., Gerszten, R. E., Hartigan, A. J., Kim, M. J., Serwold, T., Wagers, A. J., & Lee, R. T. (2013). Growth differentiation factor 11 is a circulating factor that reverses age-related cardiac hypertrophy. Cell, 153(4), 828–839. https://doi.org/10.1016/j.cell.2013.04.015

Louis, M., Van Beneden, R., Dehoux, M., Thissen, J. P., & Francaux, M. (2004). Creatine increases IGF-I and myogenic regulatory factor mRNA in C(2)C(12) cells. FEBS letters, 557(1-3), 243–247. https://doi.org/10.1016/s0014-5793(03)01504-7

Love, M. I., Huber, W., & Anders, S. (2014). Moderated estimation of fold change and dispersion for RNA-seq data with DESeq2. Genome biology, 15(12), 550. https://doi.org/10.1186/s13059-014-0550-8

Madden, S. L., Galella, E. A., Riley, D., Bertelsen, A. H., & Beaudry, G. A. (1996). Induction of cell growth regulatory genes by p53. *Cancer research*, *56*(23), 5384–5390.

Maggio, M., Ceda, G. P., Ticinesi, A., De Vita, F., Gelmini, G., Costantino, C., Meschi, T., Kressig, R. W., Cesari, M., Fabi, M., & Lauretani, F. (2016). Instrumental and Non-Instrumental Evaluation of 4-Meter Walking Speed in Older Individuals. PloS one, 11(4), e0153583. https://doi.org/10.1371/journal.pone.0153583

Marš, T., Miš, K., Meznarič, M., Prpar Mihevc, S., Jan, V., Haugen, F., Rogelj, B., Rustan, A. C., Thoresen, G. H., Pirkmajer, S., & Nikolić, N. (2021). Innervation and electrical pulse stimulation - in vitro effects on human skeletal muscle cells. Applied physiology, nutrition, and metabolism = Physiologie appliquee, nutrition et metabolisme, 46(4), 299–308. https://doi.org/10.1139/apnm-2019-0575

Massagué, J., & Gomis, R. R. (2006). The logic of TGFbeta signaling. FEBS letters, 580(12), 2811–2820. https://doi.org/10.1016/j.febslet.2006.04.033

Mayeuf-Louchart, A., Hardy, D., Thorel, Q., Roux, P., Gueniot, L., Briand, D., Mazeraud, A., Bouglé, A., Shorte, S. L., Staels, B., Chrétien, F., Duez, H., & Danckaert, A. (2018). MuscleJ: a high-content analysis method to study skeletal muscle with a new Fiji tool. Skeletal muscle, 8(1), 25. https://doi.org/10.1186/s13395-018-0171-0

McPherron, A. C., & Lee, S. J. (1997). Double muscling in cattle due to mutations in the myostatin gene. Proceedings of the National Academy of Sciences of the United States of America, 94(23), 12457–12461. https://doi.org/10.1073/pnas.94.23.12457

McPherron, A. C., Huynh, T. V., & Lee, S. J. (2009). Redundancy of myostatin and growth/differentiation factor 11 function. BMC developmental biology, 9, 24. https://doi.org/10.1186/1471-213X-9-24

McPherron, A. C., Lawler, A. M., & Lee, S. J. (1997). Regulation of skeletal muscle mass in mice by a new TGF-beta superfamily member. Nature, 387(6628), 83–90. https://doi.org/10.1038/387083a0

McPherron, A. C., Lawler, A. M., & Lee, S. J. (1999). Regulation of anterior/posterior patterning of the axial skeleton by growth/differentiation factor 11. Nature genetics, 22(3), 260–264. https://doi.org/10.1038/10320

Mendias, C. L., Kayupov, E., Bradley, J. R., Brooks, S. V., & Claflin, D. R. (2011). Decreased specific force and power production of muscle fibers from myostatin-deficient mice are associated with a suppression of protein degradation. Journal of applied physiology (Bethesda, Md. : 1985), 111(1), 185–191. https://doi.org/10.1152/japplphysiol.00126.2011

Mendias, C. L., Marcin, J. E., Calerdon, D. R., & Faulkner, J. A. (2006). Contractile properties of EDL and soleus muscles of myostatin-deficient mice. Journal of applied physiology (Bethesda, Md. : 1985), 101(3), 898–905. https://doi.org/10.1152/japplphysiol.00126.2006

Metzger, D., & Chambon, P. (2001). Site- and time-specific gene targeting in the mouse. Methods (San Diego, Calif.), 24(1), 71–80. https://doi.org/10.1006/meth.2001.1159

Mijnarends, D. M., Luiking, Y. C., Halfens, R., Evers, S., Lenaerts, E., Verlaan, S., Wallace, M., Schols, J., & Meijers, J. (2018). Muscle, Health and Costs: A Glance at their Relationship. The journal of nutrition, health & aging, 22(7), 766–773. https://doi.org/10.1007/s12603-018-1058-9

Miniou, P., Tiziano, D., Frugier, T., Roblot, N., Le Meur, M., & Melki, J. (1999). Gene targeting restricted to mouse striated muscle lineage. Nucleic acids research, 27(19), e27. https://doi.org/10.1093/nar/27.19.e27

Mirzoev T. M. (2020). Skeletal Muscle Recovery from Disuse Atrophy: Protein Turnover Signaling and Strategies for Accelerating Muscle Regrowth. International journal of molecular sciences, 21(21), 7940. https://doi.org/10.3390/ijms21217940

Miyazaki, J., Takaki, S., Araki, K., Tashiro, F., Tominaga, A., Takatsu, K., & Yamamura, K. (1989). Expression vector system based on the chicken beta-actin promoter directs efficient production of interleukin-5. Gene, 79(2), 269–277. https://doi.org/10.1016/0378-1119(89)90209-6

Mosher, D. S., Quignon, P., Bustamante, C. D., Sutter, N. B., Mellersh, C. S., Parker, H. G., & Ostrander, E. A. (2007). A mutation in the myostatin gene increases muscle mass and enhances racing performance in heterozygote dogs. PLoS genetics, 3(5), e79. https://doi.org/10.1371/journal.pgen.0030079

Nakanishi, R., Hirayama, Y., Tanaka, M., Maeshige, N., Kondo, H., Ishihara, A., Roy, R. R., & Fujino, H. (2016). Nucleoprotein supplementation enhances the recovery of rat soleus mass with reloading after hindlimb unloading-induced atrophy via myonuclei accretion and increased protein synthesis. Nutrition research (New York, N.Y.), 36(12), 1335–1344. https://doi.org/10.1016/j.nutres.2016.10.007

Nakatani, M., Takehara, Y., Sugino, H., Matsumoto, M., Hashimoto, O., Hasegawa, Y., Murakami, T., Uezumi, A., Takeda, S., Noji, S., Sunada, Y., & Tsuchida, K. (2008). Transgenic expression of a myostatin inhibitor derived from follistatin increases skeletal muscle mass and ameliorates dystrophic pathology in mdx mice. FASEB journal : official publication of the Federation of American Societies for Experimental Biology, 22(2), 477–487. https://doi.org/10.1096/fj.07-8673com

Newman, A. B., Kupelian, V., Visser, M., Simonsick, E. M., Goodpaster, B. H., Kritchevsky, S. B., Tylavsky, F. A., Rubin, S. M., & Harris, T. B. (2006). Strength, but not muscle mass, is associated with mortality in the health, aging and body composition study cohort. The journals of gerontology. Series A, Biological sciences and medical sciences, 61(1), 72–77. https://doi.org/10.1093/gerona/61.1.72

Olson, K. A., Beatty, A. L., Heidecker, B., Regan, M. C., Brody, E. N., Foreman, T., Kato, S., Mehler, R. E., Singer, B. S., Hveem, K., Dalen, H., Sterling, D. G., Lawn, R. M., Schiller, N. B., Williams, S. A., Whooley, M. A., & Ganz, P. (2015). Association of growth differentiation factor 11/8, putative anti-ageing factor, with cardiovascular outcomes and overall mortality in humans: analysis of the Heart and Soul and HUNT3 cohorts. European heart journal, 36(48), 3426–3434. https://doi.org/10.1093/eurheartj/ehv385

Oustanina, S., Hause, G., & Braun, T. (2004). Pax7 directs postnatal renewal and propagation of myogenic satellite cells but not their specification. The EMBO journal, 23(16), 3430–3439. https://doi.org/10.1038/sj.emboj.7600346

Patel, H. P., Syddall, H. E., Jameson, K., Robinson, S., Denison, H., Roberts, H. C., Edwards, M., Dennison, E., Cooper, C., & Aihie Sayer, A. (2013). Prevalence of sarcopenia in community-dwelling older people in the UK using the European Working Group on Sarcopenia in Older People (EWGSOP) definition: findings from the Hertfordshire Cohort Study (HCS). Age and ageing, 42(3), 378–384. https://doi.org/10.1093/ageing/afs197

Personius, K. E., Jayaram, A., Krull, D., Brown, R., Xu, T., Han, B., Burgess, K., Storey, C., Shah, B., Tawil, R., & Welle, S. (2010). Grip force, EDL contractile properties, and voluntary wheel running after postdevelopmental myostatin depletion in mice. Journal of applied physiology (Bethesda, Md. : 1985), 109(3), 886–894. https://doi.org/10.1152/japplphysiol.00300.2010

Peters, T. M., & Brazeau, A. S. (2019). Exercise in Pregnant Women with Diabetes. Current diabetes reports, 19(9), 80. https://doi.org/10.1007/s11892-019-1204-8

Piatkevich, K. D., & Verkhusha, V. V. (2011). Guide to red fluorescent proteins and biosensors for flow cytometry. Methods in cell biology, 102, 431–461. https://doi.org/10.1016/B978-0-12-374912-3.00017-1

Pierik, V. D., Meskers, C., Van Ancum, J. M., Numans, S. T., Verlaan, S., Scheerman, K., Kruizinga, R. C., & Maier, A. B. (2017). High risk of malnutrition is associated with low muscle mass in older hospitalized patients - a prospective cohort study. BMC geriatrics, 17(1), 118. https://doi.org/10.1186/s12877-017-0505-5

Podsiadlo, D., & Richardson, S. (1991). The timed "Up & Go": a test of basic functional mobility for frail elderly persons. Journal of the American Geriatrics Society, 39(2), 142–148. https://doi.org/10.1111/j.1532-5415.1991.tb01616.x

Popov D. V. (2018). Adaptation of Skeletal Muscles to Contractile Activity of Varying Duration and Intensity: The Role of PGC-1α. Biochemistry. Biokhimiia, 83(6), 613–628. https://doi.org/10.1134/S0006297918060019

Proctor, D. N., Sinning, W. E., Walro, J. M., Sieck, G. C., & Lemon, P. W. (1995). Oxidative capacity of human muscle fiber types: effects of age and training status. Journal of applied physiology (Bethesda, Md. : 1985), 78(6), 2033–2038. https://doi.org/10.1152/jappl.1995.78.6.2033

Quiroz-Rothe, E., & Rivero, J. L. (2004). Coordinated expression of myosin heavy chains, metabolic enzymes, and morphological features of porcine skeletal muscle fiber types. Microscopy research and technique, 65(1-2), 43–61. https://doi.org/10.1002/jemt.20090

Rantanen, T., Era, P., & Heikkinen, E. (1994). Maximal isometric strength and mobility among 75-year-old men and women. Age and ageing, 23(2), 132–137. https://doi.org/10.1093/ageing/23.2.132

Rebbapragada, A., Benchabane, H., Wrana, J. L., Celeste, A. J., & Attisano, L. (2003). Myostatin signals through a transforming growth factor beta-like signaling pathway to block adipogenesis. Molecular and cellular biology, 23(20), 7230–7242. https://doi.org/10.1128/MCB.23.20.7230-7242.2003

Reisz-Porszasz, S., Bhasin, S., Artaza, J. N., Shen, R., Sinha-Hikim, I., Hogue, A., Fielder, T. J., & Gonzalez-Cadavid, N. F. (2003). Lower skeletal muscle mass in male transgenic mice with muscle-specific overexpression of myostatin. American journal of physiology. Endocrinology and metabolism, 285(4), E876–E888. https://doi.org/10.1152/ajpendo.00107.2003

Sampath Kumar, A., Maiya, A. G., Shastry, B. A., Vaishali, K., Ravishankar, N., Hazari, A., Gundmi, S., & Jadhav, R. (2019). Exercise and insulin resistance in type 2 diabetes mellitus: A systematic review and meta-analysis. Annals of physical and rehabilitation medicine, 62(2), 98–103. https://doi.org/10.1016/j.rehab.2018.11.001

Sartori, R., Milan, G., Patron, M., Mammucari, C., Blaauw, B., Abraham, R., & Sandri, M. (2009). Smad2 and 3 transcription factors control muscle mass in adulthood. American journal of physiology. Cell physiology, 296(6), C1248–C1257. https://doi.org/10.1152/ajpcell.00104.2009

Saunders, M. A., Good, J. M., Lawrence, E. C., Ferrell, R. E., Li, W. H., & Nachman, M. W. (2006). Human adaptive evolution at Myostatin (GDF8), a regulator of muscle growth. *American journal of human genetics*, *79*(6), 1089–1097.

Schiaffino, S., & Reggiani, C. (2011). Fiber types in mammalian skeletal muscles. Physiological reviews, 91(4), 1447–1531. https://doi.org/10.1152/physrev.00031.2010

Schindelin, J., Arganda-Carreras, I., Frise, E., Kaynig, V., Longair, M., Pietzsch, T., Preibisch, S., Rueden, C., Saalfeld, S., Schmid, B., Tinevez, J. Y., White, D. J., Hartenstein, V., Eliceiri, K., Tomancak, P., & Cardona, A. (2012). Fiji: an open-source platform for biological-image analysis. Nature methods, 9(7), 676–682. https://doi.org/10.1038/nmeth.2019

Schuelke, M., Wagner, K. R., Stolz, L. E., Hübner, C., Riebel, T., Kömen, W., Braun, T., Tobin, J. F., & Lee, S. J. (2004). Myostatin mutation associated with gross muscle hypertrophy in a child. The New England journal of medicine, 350(26), 2682–2688. https://doi.org/10.1056/NEJMoa040933

Schwander, M., Leu, M., Stumm, M., Dorchies, O. M., Ruegg, U. T., Schittny, J., & Müller, U. (2003). Beta1 integrins regulate myoblast fusion and sarcomere assembly. *Developmental cell*, *4*(5), 673–685. https://doi.org/10.1016/s1534-5807(03)00118-7

Seale, P., Sabourin, L. A., Girgis-Gabardo, A., Mansouri, A., Gruss, P., & Rudnicki, M. A. (2000). Pax7 is required for the specification of myogenic satellite cells. Cell, 102(6), 777–786. https://doi.org/10.1016/s0092-8674(00)00066-0

Seiliez, I., Sabin, N., & Gabillard, J. C. (2012). Myostatin inhibits proliferation but not differentiation of trout myoblasts. Molecular and cellular endocrinology, 351(2), 220–226. https://doi.org/10.1016/j.mce.2011.12.011

Shi, X., & Garry, D. J. (2006). Muscle stem cells in development, regeneration, and disease. *Genes & development*, *20*(13), 1692–1708. https://doi.org/10.1101/gad.1419406

Sica, R. E., & McComas, A. J. (1971). Fast and slow twitch units in a human muscle. Journal of neurology, neurosurgery, and psychiatry, 34(2), 113–120. https://doi.org/10.1136/jnnp.34.2.113

Sinha, M., Jang, Y. C., Oh, J., Khong, D., Wu, E. Y., Manohar, R., Miller, C., Regalado, S. G., Loffredo, F. S., Pancoast, J. R., Hirshman, M. F., Lebowitz, J., Shadrach, J. L., Cerletti, M., Kim, M. J., Serwold, T., Goodyear, L. J., Rosner, B., Lee, R. T., & Wagers, A. J. (2014). Restoring systemic GDF11 levels reverses age-related dysfunction in mouse skeletal muscle. Science (New York, N.Y.), 344(6184), 649–652. https://doi.org/10.1126/science.1251152

Snijders, T., Wall, B. T., Dirks, M. L., Senden, J. M., Hartgens, F., Dolmans, J., Losen, M., Verdijk, L. B., & van Loon, L. J. (2014). Muscle disuse atrophy is not accompanied by changes in skeletal muscle satellite cell content. Clinical science (London, England : 1979), 126(8), 557–566. https://doi.org/10.1042/CS20130295

Sousa-Victor, P., & Muñoz-Cánoves, P. (2016). Regenerative decline of stem cells in sarcopenia. Molecular aspects of medicine, 50, 109–117. https://doi.org/10.1016/j.mam.2016.02.002

Souza, T. A., Chen, X., Guo, Y., Sava, P., Zhang, J., Hill, J. J., Yaworsky, P. J., & Qiu, Y. (2008). Proteomic identification and functional validation of activins and bone morphogenetic protein 11 as candidate novel muscle mass regulators. Molecular endocrinology (Baltimore, Md.), 22(12), 2689–2702. https://doi.org/10.1210/me.2008-0290

St Andre, M., Johnson, M., Bansal, P. N., Wellen, J., Robertson, A., Opsahl, A., Burch, P. M., Bialek, P., Morris, C., & Owens, J. (2017). A mouse anti-myostatin antibody increases muscle mass and improves muscle strength and contractility in the mdx mouse model of Duchenne muscular dystrophy and its humanized equivalent, domagrozumab (PF-06252616), increases muscle volume in cynomolgus monkeys. Skeletal muscle, 7(1), 25. https://doi.org/10.1186/s13395-017-0141-y

Stavaux, D., Art, T., McEntee, K., Reznick, M., & Lekeux, P. (1994). Muscle fibre type and size, and muscle capillary density in young double-muscled blue Belgian cattle. Zentralblatt fur Veterinarmedizin. Reihe A, 41(3), 229–236. https://doi.org/10.1111/j.1439-0442.1994.tb00089.x

Suh, J., & Lee, Y. S. (2020). Similar sequences but dissimilar biological functions of GDF11 and myostatin. Experimental & molecular medicine, 52(10), 1673–1693. https://doi.org/10.1038/s12276-020-00516-4

Suh, J., Kim, N. K., Lee, S. H., Eom, J. H., Lee, Y., Park, J. C., Woo, K. M., Baek, J. H., Kim, J. E., Ryoo, H. M., Lee, S. J., & Lee, Y. S. (2020). GDF11 promotes osteogenesis as opposed to MSTN, and follistatin, a MSTN/GDF11 inhibitor, increases muscle mass but weakens bone. Proceedings of the National Academy of Sciences of the United States of America, 117(9), 4910–4920. https://doi.org/10.1073/pnas.1916034117

Szulc, P., Schoppet, M., Goettsch, C., Rauner, M., Dschietzig, T., Chapurlat, R., & Hofbauer, L. C. (2012). Endocrine and clinical correlates of myostatin serum concentration in men--the STRAMBO study. The Journal of clinical endocrinology and metabolism, 97(10), 3700–3708. https://doi.org/10.1210/jc.2012-1273

Tajbakhsh S. (2009). Skeletal muscle stem cells in developmental versus regenerative myogenesis. Journal of internal medicine, 266(4), 372–389. https://doi.org/10.1111/j.1365-2796.2009.02158.x

Takahashi, H., Sato, K., Yamaguchi, T., Miyake, M., Watanabe, H., Nagasawa, Y., Kitagawa, E., Terada, S., Urakawa, M., Rose, M. T., McMahon, C. D., Watanabe, K., Ohwada, S., Gotoh, T., & Aso, H. (2014). Myostatin alters glucose transporter-4 (GLUT4) expression in bovine skeletal muscles and myoblasts isolated from double-muscled (DM) and normal-muscled (NM) Japanese shorthorn cattle. Domestic animal endocrinology, 48, 62–68. https://doi.org/10.1016/j.domaniend.2014.01.007

Thomas D. R. (2007). Loss of skeletal muscle mass in aging: examining the relationship of starvation, sarcopenia and cachexia. Clinical nutrition (Edinburgh, Scotland), 26(4), 389–399. https://doi.org/10.1016/j.clnu.2007.03.008

Trendelenburg, A. U., Meyer, A., Rohner, D., Boyle, J., Hatakeyama, S., & Glass, D. J. (2009). Myostatin reduces Akt/TORC1/p70S6K signaling, inhibiting myoblast differentiation and myotube size. American journal of physiology. Cell physiology, 296(6), C1258–C1270. https://doi.org/10.1152/ajpcell.00105.2009

Tsuchida, K., Nakatani, M., Matsuzaki, T., Yamakawa, N., Liu, Z., Bao, Y., Arai, K. Y., Murakami, T., Takehara, Y., Kurisaki, A., & Sugino, H. (2004). Novel factors in regulation of activin signaling. Molecular and cellular endocrinology, 225(1-2), 1–8. https://doi.org/10.1016/j.mce.2004.02.006

Van Ancum, J. M., Scheerman, K., Jonkman, N. H., Smeenk, H. E., Kruizinga, R. C., Meskers, C. G. M., & Maier, A. B. (2017). Change in muscle strength and muscle mass in older hospitalized patients: A systematic review and meta-analysis. *Experimental gerontology*, *92*, 34–41. https://doi.org/10.1016/j.exger.2017.03.006

Vékony, N., Wolf, S., Boissel, J. P., Gnauert, K., & Closs, E. I. (2001). Human cationic amino acid transporter hCAT-3 is preferentially expressed in peripheral tissues. *Biochemistry*, *40*(41), 12387–12394. https://doi.org/10.1021/bi011345c

Verdijk, L. B., Snijders, T., Holloway, T. M., VAN Kranenburg, J., & VAN Loon, L. J. (2016). Resistance Training Increases Skeletal Muscle Capillarization in Healthy Older Men. Medicine and science in sports and exercise, 48(11), 2157–2164. https://doi.org/10.1249/MSS.0000000000001019

Visser, M., Deeg, D. J., Lips, P., Harris, T. B., & Bouter, L. M. (2000). Skeletal muscle mass and muscle strength in relation to lower-extremity performance in older men and women. Journal of the American Geriatrics Society, 48(4), 381–386. https://doi.org/10.1111/j.1532-5415.2000.tb04694.x

Visser, M., Kritchevsky, S. B., Goodpaster, B. H., Newman, A. B., Nevitt, M., Stamm, E., & Harris, T. B. (2002). Leg muscle mass and composition in relation to lower extremity performance in men and women aged 70 to 79: the health, aging and body composition study. Journal of the American Geriatrics Society, 50(5), 897–904. https://doi.org/10.1046/j.1532-5415.2002.50217.x

Wagner K. R. (2020). The elusive promise of myostatin inhibition for muscular dystrophy. Current opinion in neurology, 33(5), 621–628. https://doi.org/10.1097/WCO.0000000000000853

Wagner, K. R., Fleckenstein, J. L., Amato, A. A., Barohn, R. J., Bushby, K., Escolar, D. M., Flanigan, K. M., Pestronk, A., Tawil, R., Wolfe, G. I., Eagle, M., Florence, J. M., King, W. M., Pandya, S., Straub, V., Juneau, P., Meyers, K., Csimma, C., Araujo, T., Allen, R., … Mendell, J. R. (2008). A phase I/IItrial of MYO-029 in adult subjects with muscular dystrophy. Annals of neurology, 63(5), 561–571. https://doi.org/10.1002/ana.21338

Wagner, K. R., Liu, X., Chang, X., & Allen, R. E. (2005). Muscle regeneration in the prolonged absence of myostatin. Proceedings of the National Academy of Sciences of the United States of America, 102(7), 2519–2524. https://doi.org/10.1073/pnas.0408729102

Walker, R. G., Poggioli, T., Katsimpardi, L., Buchanan, S. M., Oh, J., Wattrus, S., Heidecker, B., Fong, Y. W., Rubin, L. L., Ganz, P., Thompson, T. B., Wagers, A. J., & Lee, R. T. (2016). Biochemistry and Biology of GDF11 and Myostatin: Similarities, Differences, and Questions for Future Investigation. Circulation research, 118(7), 1125–1142. https://doi.org/10.1161/CIRCRESAHA.116.308391

Wang, M., Yu, H., Kim, Y. S., Bidwell, C. A., & Kuang, S. (2012). Myostatin facilitates slow and inhibits fast myosin heavy chain expression during myogenic differentiation. Biochemical and biophysical research communications, 426(1), 83–88. https://doi.org/10.1016/j.bbrc.2012.08.040

Wang, Z. M., Sun, Y. G., & Heymsfield, S. B. (1996). Urinary creatinine-skeletal muscle mass method: a prediction equation based on computerized axial tomography. *Biomedical and environmental sciences : BES*, *9*(2-3), 185–190.

Welle, S., Cardillo, A., Zanche, M., & Tawil, R. (2009). Skeletal muscle gene expression after myostatin knockout in mature mice. Physiological genomics, 38(3), 342–350. https://doi.org/10.1152/physiolgenomics.00054.2009

Wu, I. C., Lin, C. C., Hsiung, C. A., Wang, C. Y., Wu, C. H., Chan, D. C., Li, T. C., Lin, W. Y., Huang, K. C., Chen, C. Y., Hsu, C. C., & Sarcopenia and Translational Aging Research in Taiwan Team (2014). Epidemiology of sarcopenia among community-dwelling older adults in Taiwan: a pooled analysis for a broader adoption of sarcopenia assessments. Geriatrics & gerontology international, 14 Suppl 1, 52–60. https://doi.org/10.1111/ggi.12193

Xing, X. X., Xuan, M. F., Jin, L., Guo, Q., Luo, Z. B., Wang, J. X., Luo, Q. R., Zhang, G. L., Cui, C. D., Cui, Z. Y., Kang, J. D., & Yin, X. J. (2017). Fiber-type distribution and expression of myosin heavy chain isoforms in newborn heterozygous myostatin-knockout pigs. Biotechnology letters, 39(12), 1811–1819. https://doi.org/10.1007/s10529-017-2422-2

Yadin, D., Knaus, P., & Mueller, T. D. (2016). Structural insights into BMP receptors: Specificity, activation and inhibition. Cytokine & growth factor reviews, 27, 13–34. https://doi.org/10.1016/j.cytogfr.2015.11.005

Yang, W. H., Yu, J. H., Gulick, T., Bloch, K. D., & Bloch, D. B. (2006). RNA-associated protein 55 (RAP55) localizes to mRNA processing bodies and stress granules. RNA (New York, N.Y.), 12(4), 547–554. https://doi.org/10.1261/rna.2302706

Yarasheski, K. E., Bhasin, S., Sinha-Hikim, I., Pak-Loduca, J., & Gonzalez-Cadavid, N. F. (2002). Serum myostatin-immunoreactive protein is increased in 60-92 year old women and men with muscle wasting. The journal of nutrition, health & aging, 6(5), 343–348.

Yeung, S., Reijnierse, E. M., Pham, V. K., Trappenburg, M. C., Lim, W. K., Meskers, C., & Maier, A. B. (2019). Sarcopenia and its association with falls and fractures in older adults: A systematic review and meta-analysis. Journal of cachexia, sarcopenia and muscle, 10(3), 485–500. https://doi.org/10.1002/jcsm.12411

Zambrowicz, B. P., Imamoto, A., Fiering, S., Herzenberg, L. A., Kerr, W. G., & Soriano, P. (1997). Disruption of overlapping transcripts in the ROSA beta geo 26 gene trap strain leads to widespread expression of beta-galactosidase in mouse embryos and hematopoietic cells. Proceedings of the National Academy of Sciences of the United States of America, 94(8), 3789–3794. https://doi.org/10.1073/pnas.94.8.3789

Zammit, P. S., Golding, J. P., Nagata, Y., Hudon, V., Partridge, T. A., & Beauchamp, J. R. (2004). Muscle satellite cells adopt divergent fates: a mechanism for self-renewal?. The Journal of cell biology, 166(3), 347–357. https://doi.org/10.1083/jcb.200312007

Zammit, P. S., Heslop, L., Hudon, V., Rosenblatt, J. D., Tajbakhsh, S., Buckingham, M. E., Beauchamp, J. R., & Partridge, T. A. (2002). Kinetics of myoblast proliferation show that resident satellite cells are competent to fully regenerate skeletal muscle fibers. Experimental cell research, 281(1), 39–49. https://doi.org/10.1006/excr.2002.5653

Zammit, P. S., Relaix, F., Nagata, Y., Ruiz, A. P., Collins, C. A., Partridge, T. A., & Beauchamp, J. R. (2006). Pax7 and myogenic progression in skeletal muscle satellite cells. Journal of cell science, 119(Pt 9), 1824–1832. https://doi.org/10.1242/jcs.02908

Zampieri, S., Mosole, S., Löfler, S., Fruhmann, H., Burggraf, S., Cvečka, J., Hamar, D., Sedliak, M., Tirptakova, V., Šarabon, N., Mayr, W., & Kern, H. (2015). Physical Exercise in Aging: Nine Weeks of Leg Press or Electrical Stimulation Training in 70 Years Old Sedentary Elderly People. European journal of translational myology, 25(4), 237–242. https://doi.org/10.4081/ejtm.2015.5374

Zhu, J., Li, Y., Lu, A., Gharaibeh, B., Ma, J., Kobayashi, T., Quintero, A. J., & Huard, J. (2011). Follistatin improves skeletal muscle healing after injury and disease through an interaction with muscle regeneration, angiogenesis, and fibrosis. The American journal of pathology, 179(2), 915–930. https://doi.org/10.1016/j.ajpath.2011.04.008

Zimmers, T. A., Davies, M. V., Koniaris, L. G., Haynes, P., Esquela, A. F., Tomkinson, K. N., McPherron, A. C., Wolfman, N. M., & Lee, S. J. (2002). Induction of cachexia in mice by systemically administered myostatin. Science (New York, N.Y.), 296(5572), 1486–1488. https://doi.org/10.1126/science.1069525

9. Appendix

9.1. Abbreviations

ALK 4	Activin receptor-like kinase 4
ALK 5	Activin receptor-like kinase 5
ACTA1	Human skeletal alpha-actin 1
ACVRII	Activin receptor type II
ACVRIIB	Activin receptor type IIB
AP-1	Activator protein 1
ASM	Appendicular Skeletal Muscle Mass
BIA	Bioelectrical impedance analysis
BSA	Bovine serum albumin
CAG	CMV-early-enhancer/β-actin/ß-globin
CD9	Cluster of differentiation 9
CDK2AP2	Cyclin Dependent Kinase 2 Associated Protein 2
CGREF1	Cell Growth Regulator With EF Hand Domain Protein 1
cMET	Hepatocyte growth factor receptor
Cre	Cyclisation recombinase
CreER^T	tamoxifen-inducible *Cre*
CRP	C-reactive protein
CSA	Cross sectional area
CT	Computed tomography
DAPI	4',6-diamidino-2-phenylindole
DEPC	Diethyl pyrocarbonate
DM	Double muscled
DXA	Dual X-ray absorptiometry
ECM	Extracellular matrix
eGFP	Enhanced green fluorescent protein
ELISA	Enzyme-linked immunosorbent assay
ERK	Extracellular signal-regulated kinases
ESC	Embryonic stem cell
EWGSOP	European Working Group on Sarcopenia in Older People

FES	Functional electrical stimulation
FIJI	FIJI is just imageJ
FOV	Field of view
FST	Follistatin
FSTL3	Follistatin related protein 3
FT	Fast twitching
GASP1/2	Growth and differentiation factor-associated serum proteins 1/2
GDF8	Growth and differentiation factor 8
GDF11	Growth and differentiation factor 11
GLUT4	Glucose transporter type 4
GPDH	Glycerol-3-phosphate dehydrogenase
HGF	Hepatocyte growth factor
IGF-1	Insulin-like growth factor 1
IHC	Immunohistochemistry
IL-6	Interleukin-6
***IRES*-e^{GFP}**	internal ribosomal entry sites - enhanced green fluorescence protein
ITGB1	Integrin-beta1
JNK	c-Jun N-terminal kinases
KO	Knockout
LBX1	Ladybird homeobox 1
loxP	Locus of X-over P1
LSM 14	LSM14A MRNA Processing Body Assembly Factor
MAPK	Mitogen-activated protein kinase
mATPase	Myosin adenylpyrophosphatase
MCK	Muscle creatine kinase
MCK-3E	Mutated muscle creatine kinase
MPC	Muscle precursor cell
MRI	Magnetic resonance imaging
MSTN	Myostatin
mTOR	Mammalian target of rapamycin
Myf5	Myogenic factor 5
Myh	Myosin heavy chain
MYOD1	Myoblast determination factor 1

NFKBIL1	Nuclear Factor Of Kappa Light Polypeptide Gene Enhancer In B-Cells Inhibitor-Like 1
NGS	Next generation sequencing
NM	Normal muscled
Pax3	Paired box protein 3
Pax7	Paired box protein 7
PBS	Phosphate buffered saline
QF	Quadriceps femoris muscle
REE/FFM	Resting energy expenditure/ fat-free-mass
RhoA	Ras homolog family member A
RhoE	Ras homolog family member E
Rosa26	Reverse orientation splice acceptor 26
SC	Satellite cells
Sdc4	Syndecan 4
SDH	Succinate dehydrogenase
SER	Smooth endoplasmatic reticulum
SERCA	Sarco/endoplasmic reticulum Ca^{2+}-ATPase
SF	Slow fibre
Shh	Sonic hedgehog
SLC7A3	Solute Carrier Family 7 Member 3
SMAD	Small Mothers Against Decapentaplegic
SMM	Skeletal Muscle Mass
ST	Slow-twitching
TA	Tibialis anterior muscle
TGF	Transforming growth factor
TIFF	Tagged Image File Format
TNF-α	Tumor necrosis factor alpha
TS	Triceps surae muscle
TUG	Timed-up and Go test
WNT	Wingless type family member 1
WT	Wildtype

9.2. List of Figures

Figure references:

1. Druet, T., Ahariz, N., Cambisano, N., Tamma, N., Michaux, C., Coppieters, W., Charlier, C., & Georges, M. (2014). Selection in action: dissecting the molecular underpinnings of the increasing muscle mass of Belgian Blue Cattle. *BMC genomics*, *15*(1), 796. https://doi.org/10.1186/1471-2164-15-796
2. Walker, R. G., Poggioli, T., Katsimpardi, L., Buchanan, S. M., Oh, J., Wattrus, S., Heidecker, B., Fong, Y. W., Rubin, L. L., Ganz, P., Thompson, T. B., Wagers, A. J., & Lee, R. T. (2016). Biochemistry and Biology of GDF11 and Myostatin: Similarities, Differences, and Questions for Future Investigation. *Circulation research*, *118*(7), 1125–1142. https://doi.org/10.1161/CIRCRESAHA.116.308391
3. Encyclopædia Britannica® - https://www.britannica.com/science/skeletal-muscle (last access: 7 December 2022).
4. Blausen.com staff (2014). "Medical gallery of Blausen Medical 2014". WikiJournal of Medicine (last access: 7 December 2022).

9.5. List of Tables

Acknowledgments

Lastly, I would like to express my appreciation to the following people, who supported me in various ways during the realisation of this thesis:

Maximilian Saller, for your respectful and professional supervision of my experiments and the beneficial feedback. During my experimental work, as well as writing the thesis you have always been extraordinarily supportive. I am thankful for the opportunity to learn good scientific practice, from which I profit in my clinical and scientific work everyday.

Attila Aszodi, for your constructive criticism in the weekly meetings that helped my experiments to improve and my thesis to progress.

Paolo Alberton, for your good sense of humor that helped to cope with quite some stressful times. Also, I am thankful for your professional support during my experimental work.

Martina Burggraf, Zsuzsanna Farkas and **Heidrun Grondinger**, for your kind and helpful introduction into basic and more advanced laboratory skills.

Julian Kruse, Philipp Zeimet, Sebastian Reiprich, **Hans Dugonitsch, Celine Kohll, Lucas Heilmeier and Sara Taha**, last but not least I want to thank you all, for the superb companionship that we all could experience in the laboratory. It was a pleasure to share this exciting time with you.

Declaration

Ich erkläre hiermit an Eides statt,

dass ich die vorliegende Dissertation mit dem Thema:

"Characterisation of a skeletal muscle-specific myostatin over-expressing mouse model"

selbstständig verfasst, mich außer der angegeben keiner weiteren Hilfsmittel bedient und alle Erkenntnisse, die aus dem Schrifttum ganz oder annähernd übernommen sind, als solche kenntlich gemacht und nach ihrer Herkunft unter Bezeichnung der Fundstelle einzeln nachgewiesen habe.

Ich erkläre des Weiteren, dass die hier vorgelegte Dissertation nicht in gleicher oder ähnlicher Form bei einer anderen Stelle zur Erlangung eines akademischen Grades eingereicht wurde.

München, den 23.10.2024

Maximilian Strenzke